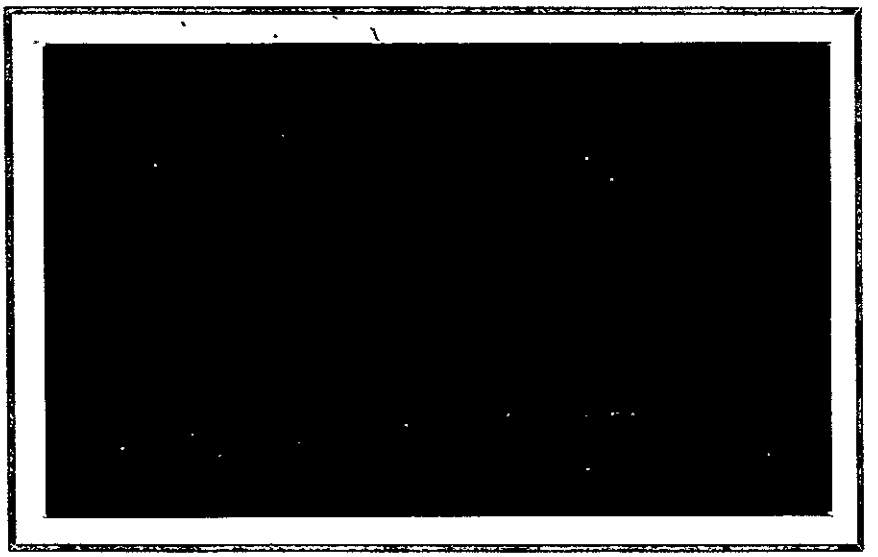

DEPARTMENT OF MECHANICAL ENGINEERING

UNIVERSITY OF UTAH

SALT LAKE CITY, UTAH 84112

N70-36980
(ACCESSION NUMBER)

91
(PAGES)

CR-112778
(NASA CR OR TMX OR AD NUMBER)

FACILITY FORM 602

(THRU)
1
(CODE)
30
(CATEGORY)

NASA SCIENTIFIC AND TECHNICAL INFORMATION FACILITY

OPERATED BY INFORMATICS TISCO, INC.

POST OFFICE BOX 33 COLLEGE PARK, MARYLAND 20740 TELEPHONE (301) 779-2121

SUBJECT: Completion of Document Release Form No. 70-01506

Gentlemen:

The report referenced on the attached Document Release Form was recently received by the NASA Scientific and Technical Information Facility.

In accordance with NASA policy each NASA and NASA supported document requires a written release from the responsible NASA Program Office or its designee before it can be processed into the NASA Information System.

We would appreciate your cooperation in completing the attached form. Your instructions will provide us with the necessary guidelines for entering the document into the NASA Information Holdings in one of the accession series described below:

Announcement Series: Reports evaluated for announcement in STAR or CSTAR are cataloged, abstracted, indexed and generally microfiched. They are available on specific request and on automatic distribution to qualified NASA users. If the document is unclassified and publicly available, it is announced in STAR in the N10K accession series. Documents that bear a security classification and/or an availability limitation are announced in CSTAR in the X10K accession series.

Index Series: Research and development reports that are too old for STAR or CSTAR announcement and current reports that do not meet the content or reproducibility criteria for announcement are assigned to the N80K or X80K accession series. These reports are cataloged and indexed, retrievable through bibliographic searches and available only on specific request.

Record Card Series: Reports assigned to this series contain administrative (financial or scheduling) information only. They are accessioned into the N90K or X90K series depending on security classification and/or availability limitations. They are cataloged; they are not included in routine bibliographic searches and are available on specific request only.

Should you require further information, please consult NASA Publication SP-7034 R & D Reporting Guidance for Technical Monitoring of NASA Contracts. Copies of this publication are available from your NASA Librarian or may be obtained by direct request to this office.

Thank you for your cooperation.

Sincerely yours,

Sylvaine L. Kenyon, Manager
Acquisitions and Input Branch

UTEC ME 70-033
JUN 1970

SOLAR ELECTRIC GRAND TOUR MISSIONS TO THE OUTER PLANETS

by

G. A. Flandro
Associate Professor

to

National Aeronautics and Space Administration
Washington, D.C. 20546

FINAL REPORT:
NASA Grant No. NGR 45-003-050

University of Utah
Department of Mechanical Engineering
Salt Lake City, Utah 84112

ACKNOWLEDGMENTS

The writer gratefully acknowledges the assistance offered by members of the technical staff of the Jet Propulsion Laboratory, California Institute of Technology. Particular appreciation is due Thomas A. Barber for numerous suggestions and to Carl G. Sauer for assistance in generating the low thrust trajectory data so essential to this research. Special thanks are due Alva Joseph and Jeannyne Gunkel also of JPL for their aid in securing multiplanet ballistic trajectories. Robert K. Wilson, a graduate assistant at the University of Utah during the course of this research, must also be mentioned in this regard.

The author wishes to express his sincere appreciation to the National Aeronautics and Space Administration for financial support in the form of Grant No. NGR 45-003-050 which made this work possible.

SOLAR ELECTRIC GRAND TOUR MISSIONS TO THE OUTER PLANETS

G. A. Flandro
University of Utah

SUMMARY

Practical unmanned exploration of the distant outer planets of the solar systems requires application of advanced mission techniques. To achieve both reasonable mission duration and payload mass, energy sources in addition to that represented by the launch vehicle system itself must be employed. In this study a combination of optimized solar electric low thrust propulsion and gravitational boost from intermediate planet hyperbolic encounters was applied to this purpose.

The period 1975-1980 abounds in multi-planet mission opportunities. Earth-Jupiter-Saturn-Pluto and Earth-Jupiter-Uranus-Neptune "grand tour" missions would enable a complete preliminary exploration of all of the outer planets by a pair of spacecraft launched by booster vehicle systems already in advanced stages of development. Optimum launch dates and performance parameters for these missions were obtained for Titan/Centaur and Atlas/Centaur launch systems with optimized solar-electric final propulsive staging. Payload is increased over purely ballistic trajectories by more than three times. Use of the Titan 3X (1205)/Centaur permits two spacecraft of over 1000 Kg (2200 lb) payload each to reach all planets of the outer solar system within a seven-year period.

TABLE OF CONTENTS

LIST OF FIGURES

INTRODUCTION

The gain in heliocentric total energy available from close passage of the massive planet Jupiter can greatly decrease required trip time to the outer planets of the solar system (1,2,3). Although required launch energy is also reduced somewhat, rather large launch vehicles are still required to accommodate payloads of useful size. Other studies (4,5) have shown that the application of low thrust electric propulsion in Jupiter flyby missions can significantly increase payload, and solar electric systems appear to be developing at a rate which should make them available for flight in the 1970 decade. It is thus natural to consider application of solar electric propulsion to make the Jupiter swingby missions possible without the need for large launch vehicles. This approach was investigated by Flandro (6) in a preliminary way for a single class of boost vehicles. This report extends that analysis to other vehicles and to a new set of "grand tour" mission profiles. Of particular interest are the Earth-Jupiter-Saturn-Pluto and Earth-Jupiter-Uranus-Neptune missions which by use of optimum solar electric Earth-Jupiter trajectory legs open the entire outer solar system to automatic unmanned scientific exploration utilizing launch vehicles already in advanced stages of development.

The mission designs presented here offer advantages in performance and simplicity over other proposed techniques such as staged space propulsion systems (7). A possible disadvantage appears in the form of increased guidance complexity, but preliminary studies (8) have indicated that standard techniques are entirely sufficient for unmanned precursor probes of the type

considered here. The trajectory optimization method used in what follows is based on maximization of payload delivered at the intermediate planet Jupiter for a given time of flight. Continuation ballistic trajectories to the secondary target planets Saturn-Pluto and Neptune-Uranus are optimized by selection of best possible Jupiter arrival date for a given low-thrust Earth-Jupiter flight duration and thus arrival hyperbolic approach speed. This method yields results representing very closely the optimum mission profiles. Complete optimization computer programs are under development (9) but are not yet in a form suitable for mission analysis. Because of the complexity introduced into the mission analysis process by incorporation of low thrust propulsion (5), only three potential launch vehicles were selected for detailed evaluation: (1) Atlas SLV-3C/Centaur, (2) Atlas SLV-3X/Centaur, and (3) Titan 3X (1205)/Centaur. This results mainly from the inseparability of the escape and interplanetary phases of powered flight in low thrust analyses. The spacecraft itself must be regarded as part of the launch vehicle and the propulsion system must be optimized over the entire trajectory rather than only in the vicinity of the earth. The performance results given in this report are based on current electric propulsion state-of-the-art (powerplant specific mass of 30 kg/kw).

Earth-Jupiter-Saturn-Pluto and earth-Jupiter-Uranus-Neptune missions were chosen for detailed analysis in this study. A pair of such "Grand Tour" missions would enable closeup study of all planets of the outer solar system; this scheme avoids the Saturn ring constraint problem which arose in previous "Grand Tour" profiles such as the earth-Jupiter-Saturn-Uranus-Neptune mission proposed in References 1 and 6. For reasonable trip times, the previous mission designs required passage of the spacecraft between Saturn's surface and its inner

ring structure. This is a doubtful approach since the guidance accuracy requirements would be extreme and, in fact, material associated with the ring system appears to extend much closer to the planet than formerly believed. Optimum launch dates for each of the grand tour missions are established for the three launch vehicle combinations. Performance is summarized in terms of the tradeoff between payload and time of flight to the target planets.

MISSION ANALYSIS PROCEDURES

Developed in this section are the mission analysis procedures required for combined use of the intermediate planet swingby technique and optimized solar electric low thrust propulsion in the design of multiplanet trajectories.

APPLICATION OF ENERGY GAINED IN INTERMEDIATE PLANET ENCOUNTERS

Modification of interplanetary trajectories by the gravitational perturbation of an intermediate planet is not a new concept; Hohmann studied ballistic round trip trajectories to Mars and Venus in 1925 (10). More recently investigators (c.f. References 1 and 3) have realized that a significant change in spacecraft heliocentric energy results from a midcourse planetary encounter. Under favorable geometrical conditions this energy can be utilized in reducing the required launch vehicle size required to fly a given payload to the final target planet. In the case of missions to the outer solar system, the most important application of the energy gained in a close passage of the planet Jupiter is in reducing the total trip time to the final target planets. For example, as compared to a direct ballistic flight, travel time to the vicinity of Neptune can be reduced by a factor of four by first passing Jupiter (1).

The mechanism by which the heliocentric energy of the space vehicle is changed by the gravitational perturbation during passage of an intermediate planet is readily demonstrated in terms of basic principles. To the spacecraft, the planet represents a force field moving relative to an inertial heliocentric coordinate system. The work done by this moving force alters

the heliocentric kinetic energy.

Let the heliocentric position of the planet and the probe be designated by $\bar{\rho}$ and $\bar{R}$, respectively, and the position of the probe relative to the planet by $\bar{r}$ (see Figure 1). Thus

$$\bar{R} = \bar{\rho} + \bar{r} \tag{1}$$

and the total work done on the spacecraft by the planetary gravitational force is

$$U = \int_i^o \bar{F}_p \cdot d\bar{R} = \int_i^o \bar{F}_p \cdot (d\bar{\rho} + d\bar{r}) \tag{2}$$

Limits i and o refer to incoming and outgoing points on the sphere of influence of the planet. The perturbing force is

$$\bar{F}_p = -\frac{GM\bar{r}}{r^3} \tag{3}$$

where GM is the gravitational parameter of the planet and r is the planet-to-spacecraft radial distance. The part of the work integral due to relative motion, $\int_i^o \bar{F}_p \cdot d\bar{r}$, is zero if it is assumed that there is no sensible influence on the planet's orbit due to passage of the probe. Introducing an angular position coordinate θ as shown in Figure 1 and writing

$$d\bar{\rho} = \left(\frac{d\bar{\rho}}{dt}\right)dt = \bar{v}_p \left(\frac{d\theta}{dt}\right)^{-1} d\theta \tag{4}$$

where θ is measured from the axis of the encounter hyperbola and $\bar{v}_p$ is velocity vector of the planet

$$\bar{v}_p = v_p \hat{P} \tag{5}$$

$\hat{P}$ is a unit vector in the direction of motion. Remembering that

$$\frac{d\theta}{dt} = \frac{[GMa(e-1)]^{\frac{1}{2}}}{r^2} \tag{6}$$

for a hyperbolic trajectory where a is the semimajor axis and e the eccentricity,

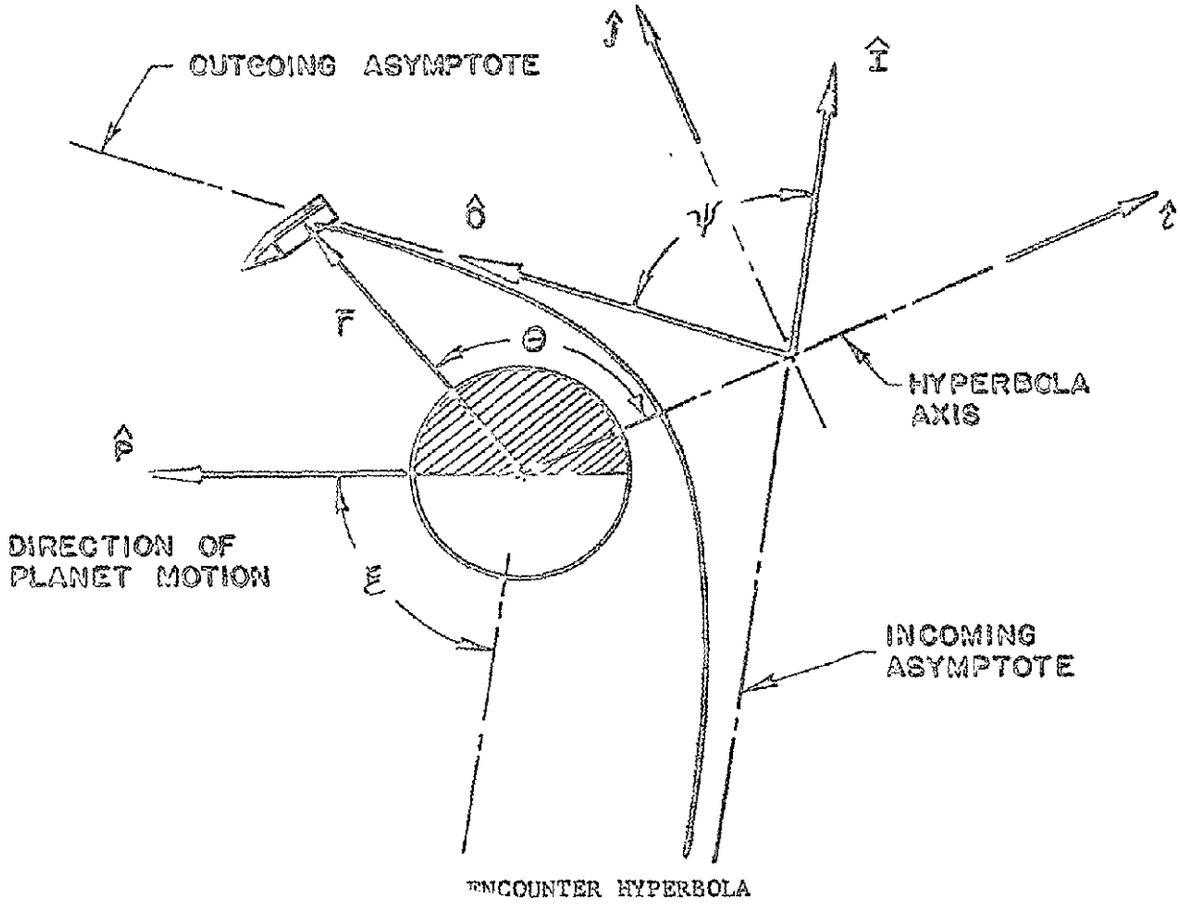
OUTGOING ASYMPTOTE
$\hat{J}$
$\hat{I}$
$\hat{O}$
$\hat{\psi}$
$\hat{i}$
$\hat{r}$
θ
HYPERBOLA AXIS
$\hat{P}$
DIRECTION OF PLANET MOTION
ξ
INCOMING ASYMPTOTE
ENCOUNTER HYPERBOLA

the angular rate can be written in terms of the hyperbolic excess speed v_h since $a = GM/v_h^2$. Also, the eccentricity may be written in terms of the deflection angle between the incoming asymptote $\hat{I}$ and the outgoing asymptote $\hat{O}$ as $e = \csc \psi/2$. Finally

$$\frac{d\theta}{dt} = \frac{GM \cot(\psi/2)}{r^2 v_h} \tag{7}$$

where $\psi = \cos^{-1}(\hat{I} \cdot \hat{O})$ and $\hat{I}$ and $\hat{O}$ are unit vectors pointing along the incoming and outgoing asymptotes as shown in Figure 1. Choosing a coordinate system aligned with the axis of the encounter hyperbola, one may write the unit vectors $\hat{i}$ and $\hat{j}$ defining a right-handed set in terms of $\hat{I}$ and $\hat{O}$ as follows

$$\hat{i} = \frac{\hat{I} - \hat{O}}{\sqrt{2(1-\cos\psi)}}, \quad \hat{j} = \frac{\hat{I} + \hat{O}}{\sqrt{2(1+\cos\psi)}}$$

In this system, the probe position is $\bar{r} = (r \cos\theta)\hat{i} + (r \sin\theta)\hat{j}$ and the work integral becomes

$$U = \int_{\frac{\psi+\pi}{2}}^{\frac{\psi+\pi}{2}} \left[-v_h v_p \tan\psi/2\right] \hat{P} \cdot \left[\frac{\cos\theta(\hat{I}-\hat{O})}{\sqrt{2(1-\cos\psi)}} + \frac{\sin\theta(\hat{I}+\hat{O})}{\sqrt{2(1+\cos\psi)}}\right] d\theta$$

Integrating

$$U = v_p v_h \hat{P} \cdot (\hat{O} - \hat{I}) \tag{8}$$

and if one neglects the change in $|\bar{r}|$ during passage through the sphere of influence as compared to the change in $|\bar{\rho}|$, the increment of vehicle heliocentric total energy is equal to the work done by the moving gravitational perturbation. Thus

$$\Delta E = U = v_p v_h \hat{P} \cdot (\hat{O} - \hat{I}) \tag{9}$$

which is the most useful form for swingby performance calculations.

It is convenient to define a characteristic energy

$$E^* \equiv 2v_p v_h \tag{10}$$

which represents the largest theoretically possible energy increment; this corresponds to a point mass planet with vehicle passage at the center point and $\psi = 180^o$. All geometrical aspects of the encounter are encompassed in an energy change index f such that the actual energy increment is

$$\Delta E = f\, E^* \tag{11}$$

f is a number between -1 and 1 given by

$$f = \tfrac{1}{2}\, \hat{P} \cdot (\hat{O} - \hat{I}) \tag{12}$$

For a point mass approximation for the planet f = 1 if the probe approaches in the direction of the planet, passes through the center, and executes a 180^o deflection. Of course $|f|<1$ always due to the finite size of the planet so E^* can never be achieved in practice. The actual value of f depends on the direction of the approach asymptote and the total deflection angle ψ at the planet. The latter depends on the gravitational parameter GM and on the distance of closest approach to the surface d:

$$\psi = 2 \sin^{-1}\left[1 + \frac{v_h^2}{GM} (d + r_p)\right]^{-1} \tag{13}$$

where r_p = radius of planet at point of closest approach. The geometry represented in Equation 12 is illustrated in Figure 2. The vector $\hat{I}$ along the approach asymptote and $\hat{P}$ in the direction of the planet's heliocentric motion are fixed by the incoming trajectory and the arrival date. A convenient reference angle between these two vectors is the approach angle ξ defined by

$$\xi = \cos^{-1} (-\hat{P} \cdot \hat{I}) \tag{14}$$

For a given $\hat{I}$ and $\hat{P}$, the value of f and the departure asymptote are set by $\hat{O}$. The outgoing asymptote may be anywhere in a cone with semi-vertex angle equal

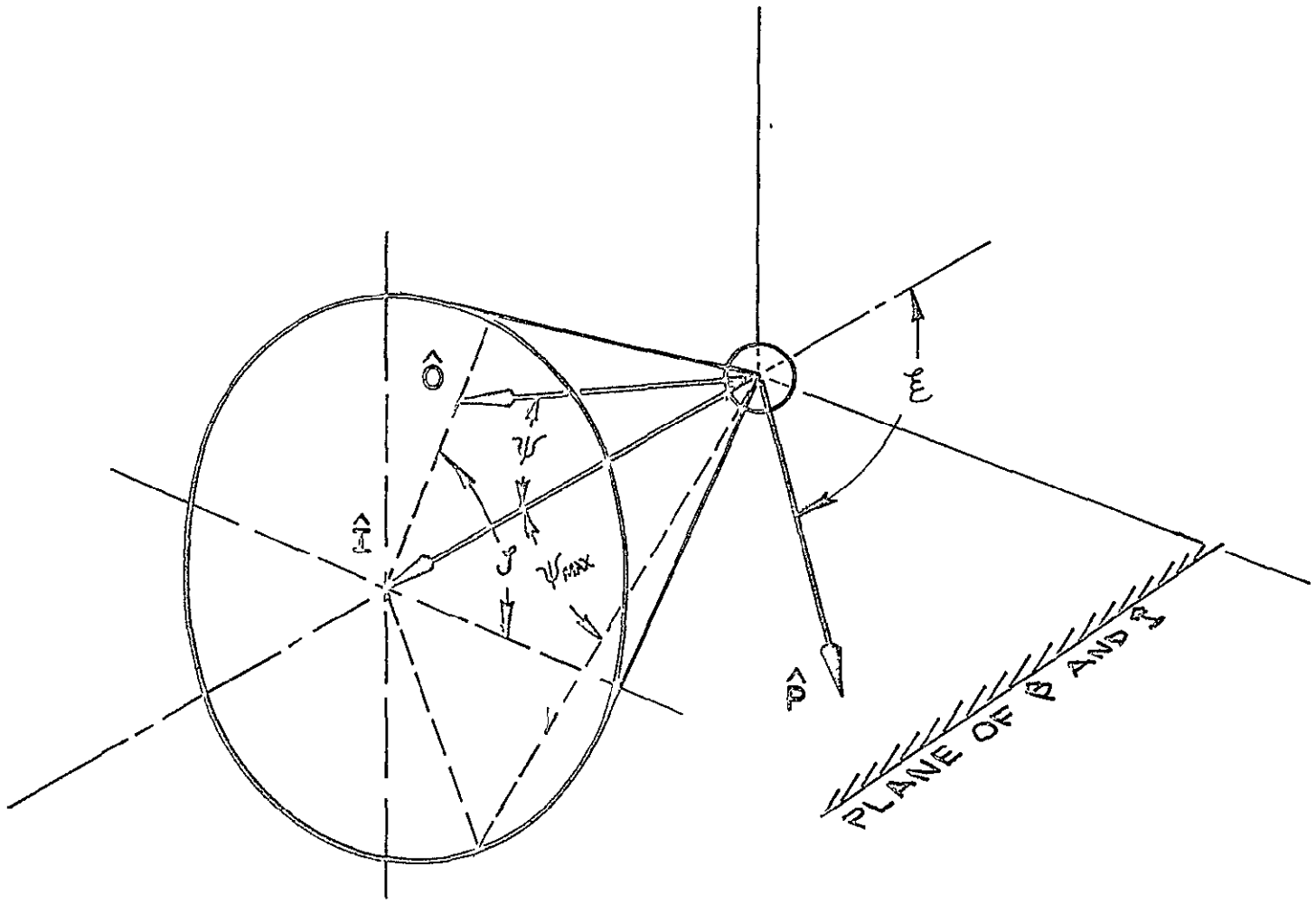

FIG. 2 - CONE OF ALLOWABLE OUTGOING ASYMPTOTES

to the maximum deflection angle ψ_{max} given by Equation 13 with d set equal to a minimum allowable passage distance (see Figure 2). $\hat{0}$ is determined for a given target planet by the hyperbolic speed v_h and the arrival date at the intermediate planet. Figure 3 shows maximum obtainable energy increments for all planets of the solar system with known mass and radius. The increment may be either a gain or an energy loss depending on whether the probe passes in front of or behind the intermediate planet as shown in Figure 4.

Trajectory optimization for a given arrival hyperbolic speed is accomplished by varying the arrival date at the intermediate planet. There will in general be four possible continuation trajectories to the target planet but of these only the type I, class I (c.f. Reference 3) are of interest in outer planet missions. For ballistic vehicles, f and E* are set by the launch date and launch energy. Trajectory optimization consists simply of finding launch dates that minimize the flight duration for a given launch energy. Optimization is more involved when low thrust propulsion is employed anywhere in the trajectory. This problem will be discussed in the following section.

SWINGBY TRAJECTORY OPTIMIZATION WITH LOW THRUST PROPULSION

Equation 9 shows that to achieve a large energy gain with an accompanying decrease in flight time to the target planet, the geometry of the midcourse encounter must be optimized to produce the maximum possible energy gain index f and v_h must be as large as possible. For ballistic vehicles, f and E* are set by the launch date and launch energy. Trajectory optimization then consists simply of finding launch dates that minimize the flight duration for a given launch energy. The optimization problem is much more complex when low-thrust

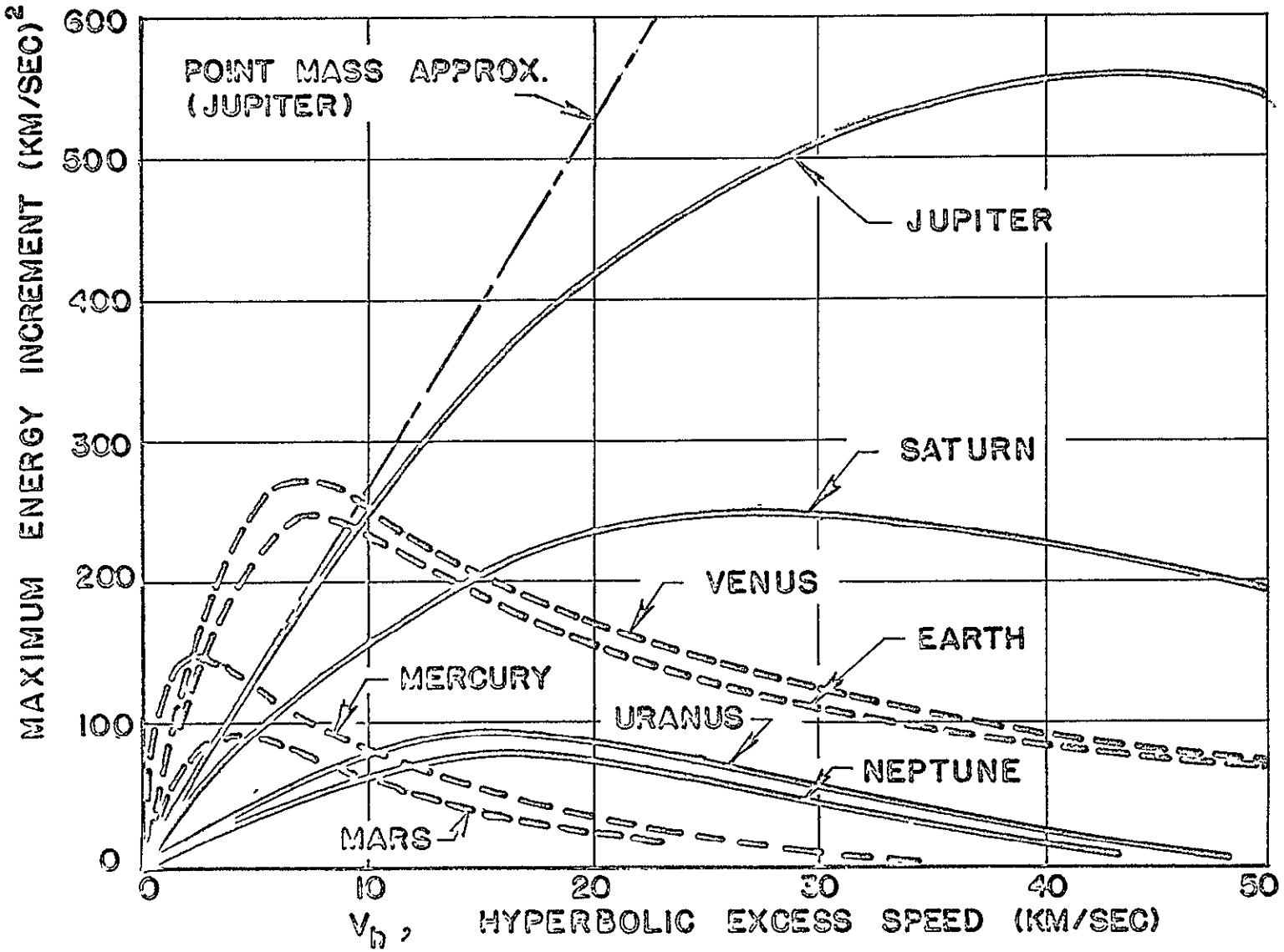

FIG. 3 - MAXIMUM ENERGY INCREMENT VS. HYPERBOLIC EXCESS SPEED

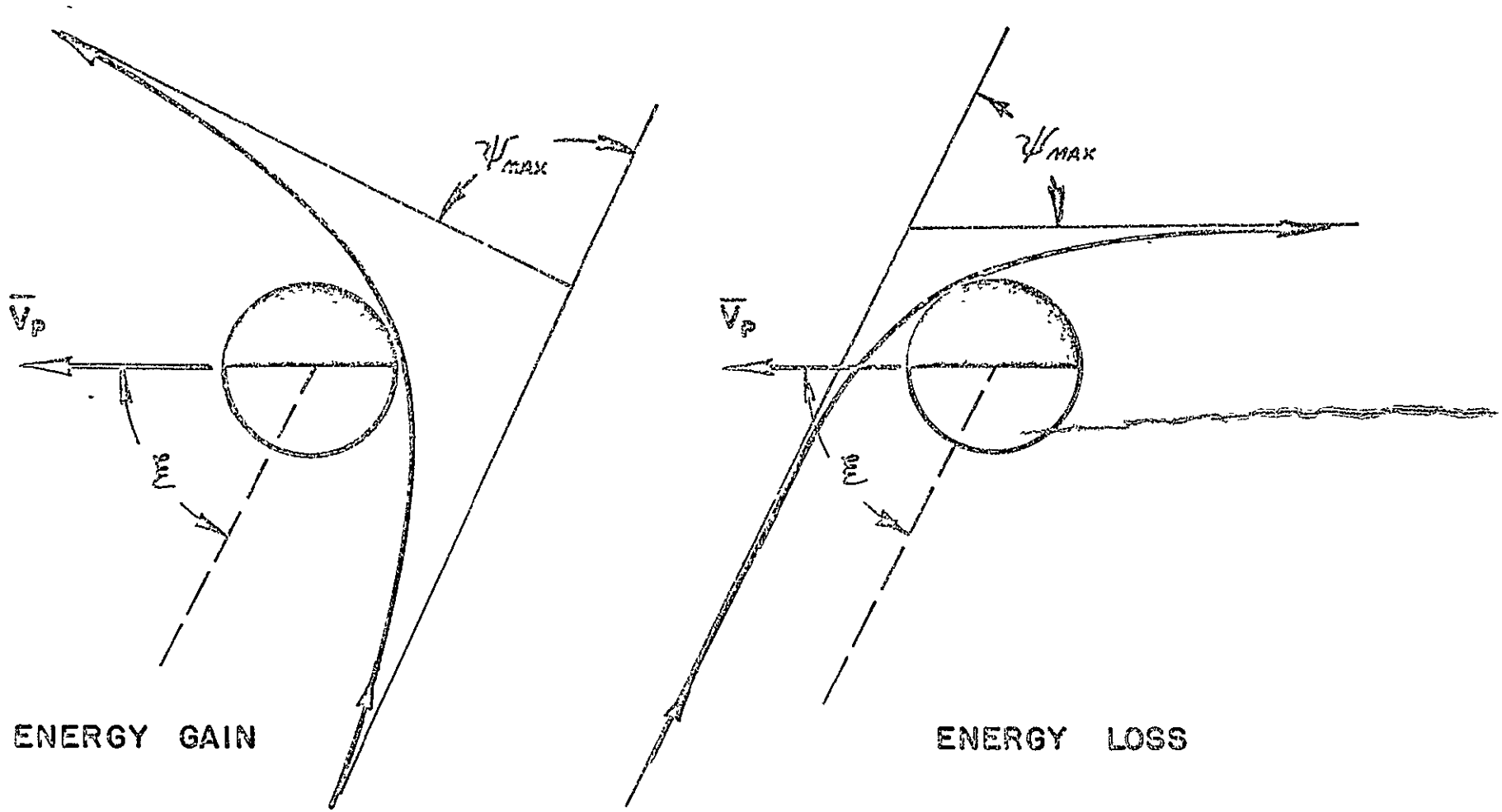

FIG. 4 - OPTIMUM ENERGY CHANGE FOR A GIVEN APPROACH ANGLE

propulsion is utilized, especially if the propulsion system operates beyond the encounter with the intermediate planet. In addition to the complexities introduced by the necessity to consider the spacecraft itself as part of the launch vehicle, one must consider optimization of parameter f. Thus, constraints in addition to the usual set encountered in low thrust flyby trajectory optimization must be included in general. The low thrust steering program must be optimized to produce the best possible approach geometry. The problem reduces to one of a tradeoff between payload delivered and travel time to the target planet.

In the present case in which Jupiter is considered as the intermediate planet and solar electric propulsion is used, several simplifications are possible. First, all optimum trajectory modes to Jupiter with solar electric propulsive staging are characterized by shut-down of the propulsion system long before Jupiter encounter. This eliminates a complicated optimization phase which would be required if the propulsion system functioned within Jupiter's sphere of influence. Second, for the launch vehicles considered in this report, low thrust trajectories which optimize the payload delivered at Jupiter can be found which also coincide very closely with optimum continuation trajectories to the secondary target planets. This is possible because the time of flight to the secondary planets changes quite slowly with variations in arrival date at Jupiter near the optimum encounter dates. This effect is illustrated in Figure 5 for earth-Jupiter-Saturn missions. Shown are plots of time of flight from Jupiter to Saturn versus Jupiter arrival date with hyperbolic excess speed as parameter. Superimposed are plots of optimized solar electric trajectory data which match the hyperbolic excess

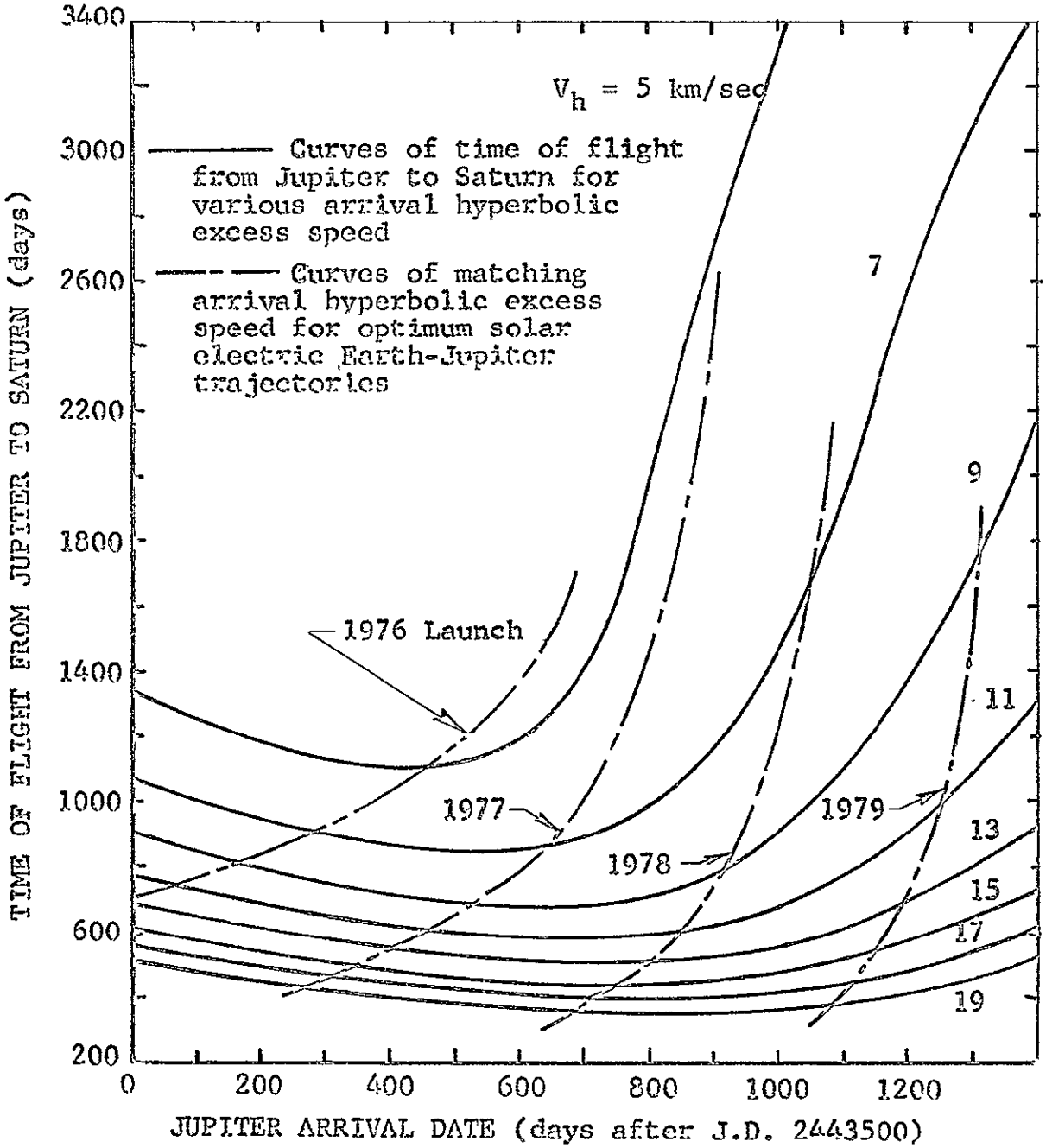

FIG. 5 - MATCHING OF OPTIMIZED LOW THRUST EARTH-JUPITER TRAJECTORIES WITH BALLISTIC CONTINUATION ORBITS TO SATURN

speeds on the optimum first leg arrival dates. Note that vehicles launched in 1976 give nearly optimum continuation trajectories for $v_h \approx 5$ km/sec. Similarly 1977 launch dates are optimum for $v_h \approx 8$ km/sec and 1978 gives optimum results for $v_h \approx 15$ km/sec. The low thrust data shown are for Titan/Centaur type I (direct mode) solar electric trajectories. The data will be discussed in detail later in the report. To summarize, combined low-thrust Jupiter swingby trajectories can be found (which are very nearly optimum to within a few days of flight duration) by systematically varying the launch year. On the basis of these observations, the optimum trajectories for the purposes of this study are those which deliver the largest payload to the intermediate planet for a given hyperbolic excess speed at encounter.

Techniques for generating optimized low thrust trajectory data are treated thoroughly in the literature (c.f. References 4 and 9) and will not be discussed here. A complete set of low thrust trajectory data for solar electric earth-Jupiter flights is given in Reference 4 for the standard Atlas SLV-3C/Centaur launch vehicle.* Appendix 1 summarizes the optimized solar electric data for the Titan 3X (1205)/Centaur (referred to in what follows as Titan/Centaur) launch vehicle. Shown in Figures A-1 through A-10 are gross payload, hyperbolic excess speed at Jupiter encounter, initial spacecraft mass, propulsion time, optimum thruster input power at launch, propellant mass, heliocentric transfer angle, optimum injection energy, sun-planet-probe angle at

*The proposed SLV-3X/Centaur combination has very nearly the same basic trajectory characteristics but about twice the payload capacity. Thus, SLV-3X performance may be estimated conveniently by doubling SLV-3C payload data. SLV-3X data presented in this report was secured in this manner.

Jupiter arrival, and optimum thruster exhaust velocity as functions of flight time to Jupiter. Similar data are given in Reference 4 for the Atlas boost vehicle. Figure 6 shows the variation of gross payload delivered to Jupiter with launch date with earth-Jupiter trip time (T_f) as parameter. Data are given for the entire earth-Jupiter synodic period of 1975. Later launch years may be represented by adding appropriate multiples of the synodic period (about 398 days) to the dates shown. Note that solar electric Jupiter missions may be flown at any time during the synodic period. However, two sub-regions exhibit maxima in payload delivery and these are set off by dashed lines. Submap 1 with the largest payload for a given trip time involves use of the indirect trajectory mode (4,5) which requires an inward loop toward the sun to make optimum use of the solar energy flux and a heliocentric transfer angle of greater than 360^{0} degrees. Figure 7 illustrates a typical indirect mode flight path. Submap 2 encompasses trajectories with lower performance in terms of payload delivered. These trajectories will be referred to as "direct mode" trajectories since they do not involve the solar loop. In addition to the greater payload delivery, the trajectories of Submap 1 result in considerably higher hyperbolic excess speed at Jupiter as shown in Figure 8. These two characteristics couple to make the indirect trajectory performance for swingby continuation to the secondary target planets significantly better than that which can be achieved with the direct mode. However, this performance comes at the considerable expense of greatly increased spacecraft mechanical complexity resulting from the following: (1) temperature control problems due to rather close passage of the sun (typically 0.6 a.u.) and (2) requirement for wide variation in thrust vector pointing direction required for

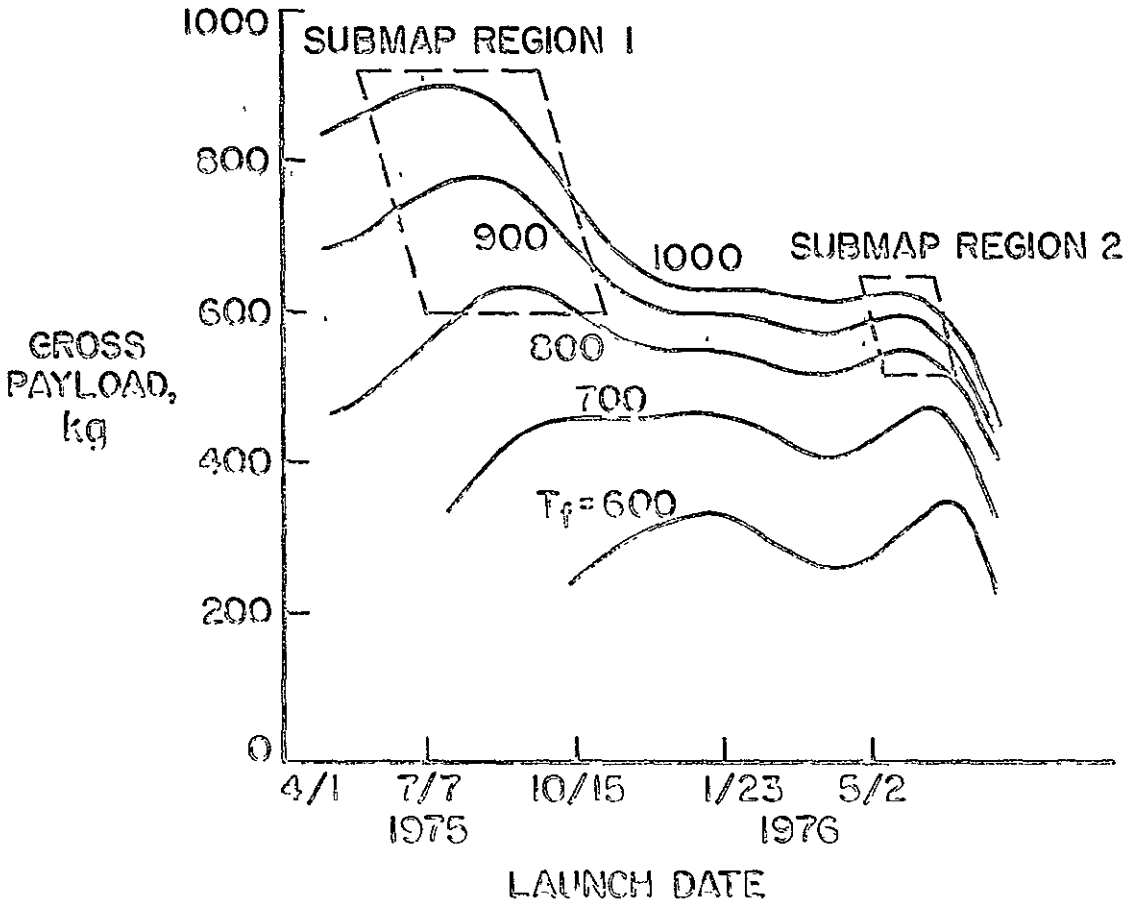

FIG. 6 - GROSS PAYLOAD AT JUPITER VS. LAUNCH DATE FOR 1975 SYNODIC PERIOD. ATLAS SLV-3X/CENTAUR.

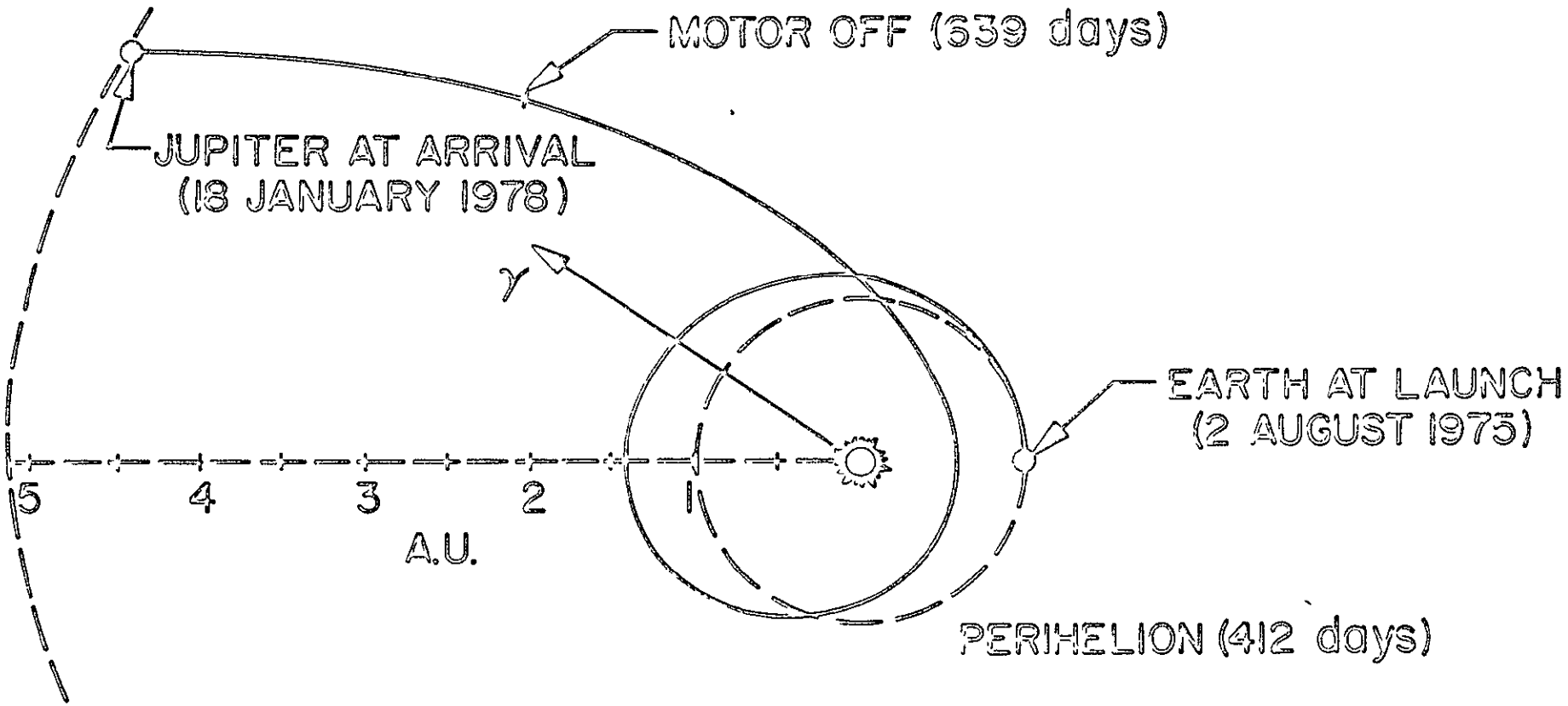

FIG. 7 - TYPICAL OPTIMUM EARTH-JUPITER SOLAR ELECTRIC FLIGHT PATH - INDIRECT MODE

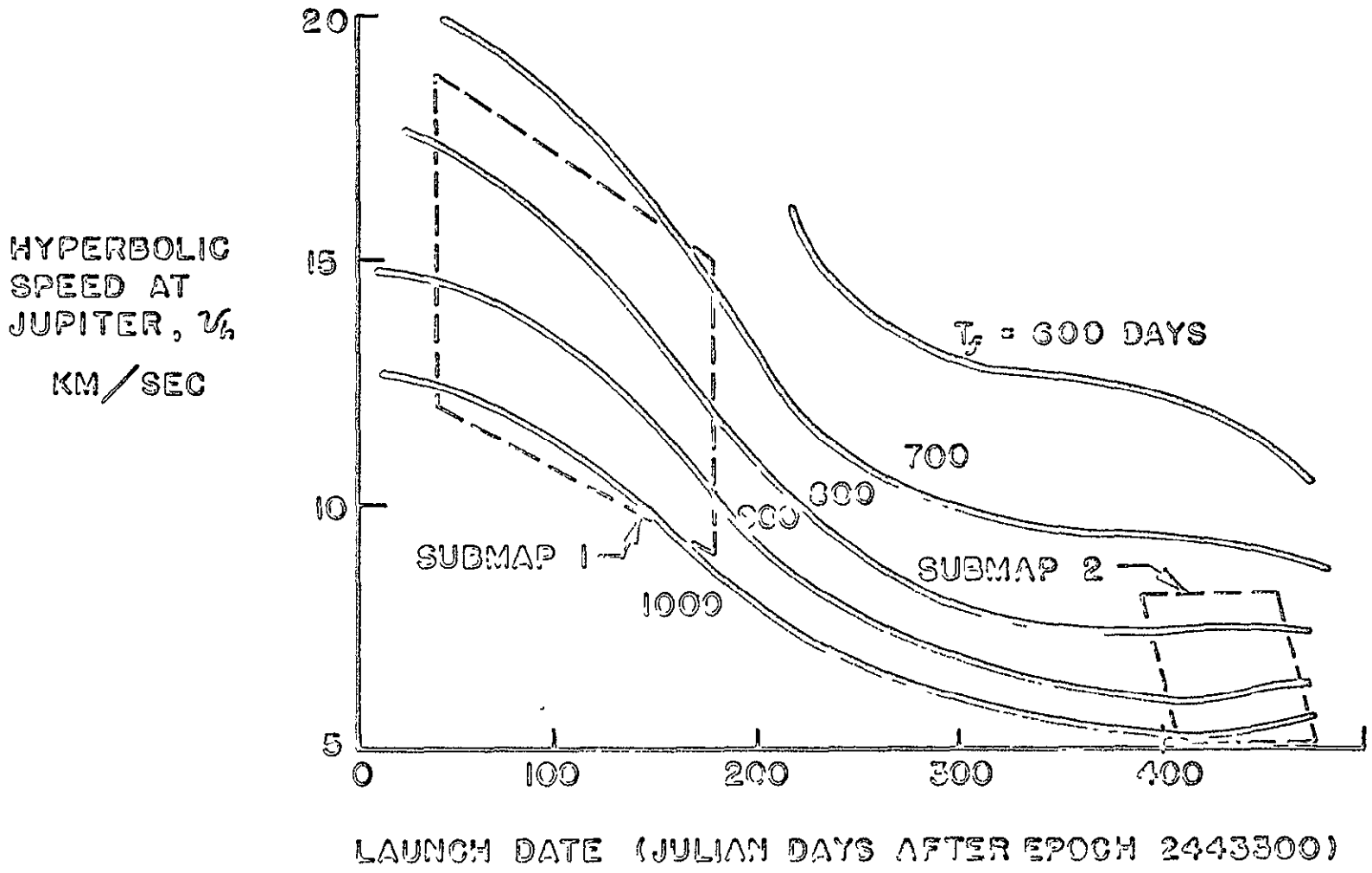

FIG. 8 - HYPERBOLIC APPROACH SPEED AT JUPITER VS. LAUNCH DATE FOR 1977 SYNODIC PERIOD.

generating the optimum indirect mode flight path. The latter effect is illustrated in Figure 9. Note that the spacecraft must provide for a swing of more than 360^{o} in the thruster alignment relative to the spacecraft-sun line while maintaining the solar panel array in normal attitude with respect to the sun. Spacecraft designs which accomplish this have been proposed (11) but much of the potential payload advantage resulting from the indirect mode approach is lost in solving the mechanization problems. Additional problems relating to spacecraft reliability and guidance considerations also arise; these are difficult to assess quantitatively in terms of overall performance but the present interpretation is that use of the direct mode is more desirable in an overall sense. Both direct and indirect mode performance data will be discussed below for the Atlas/Centaur launch vehicles; Titan/Centaur payload performance is given only for the direct mode on the basis of the above observations.

Methods for presentation of low thrust trajectory data are still evolving. Several forms of presentation are employed in what follows. A particularly graphic representation of a given mission opportunity is provided in plots of time of flight versus launch date.* In ballistic studies, the launch energy or hyperbolic excess speed provides a convenient parameter for these curves; payload for a given mission point is then determined for a launch vehicle of interest by utilizing the launch energy versus payload curves

---

*This is preferable to the standard arrival date versus launch date plots in outer planet studies since flight times are so long that data resolution is lost if dates rather than time of flight are used.

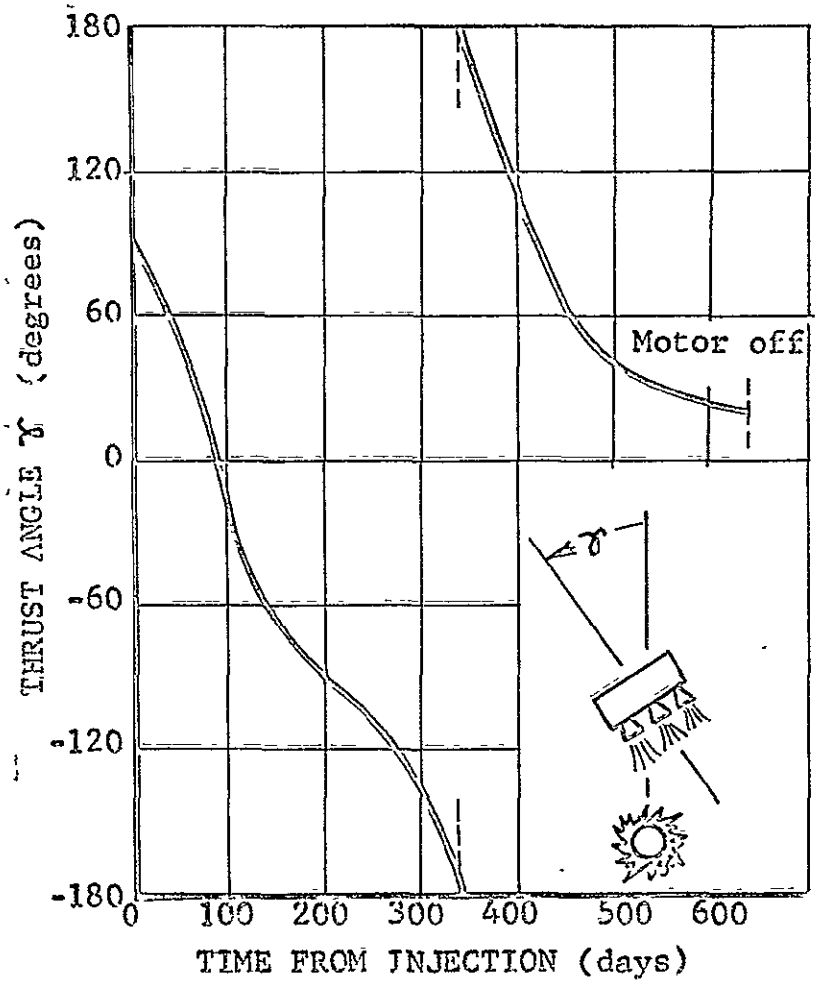

FIG. 9 - THRUST ANGLE VS TIME FOR OPTIMUM 900-DAY JUPITER FLYBY MISSION (INDIRECT MODE).

for that booster. As already pointed out, this simple procedure cannot be used in low thrust studies since the spacecraft must be considered as part of the launch vehicle system. Thus, separate performance curves are required for each boost vehicle and a convenient form for data presentation is the use of payload mass as parameter replacing the launch energy or hyperbolic excess speed used in the corresponding ballistic plots. All trajectory data of importance can be presented in this way--the mission designer can then tell at a glance, by use of overlays of this data, where the best combination of desired mission characteristics lies within the spectrum of launch dates. Comparison of different launch vehicles and trajectory modes is most conveniently made in terms of plots of payload versus mission duration for optimal conditions. This method will be used later for assessing the capabilities of the boost vehicles selected for the present study in low thrust swingby missions to the outer planets.

All low thrust earth-Jupiter trajectories utilized in what follows are based on current state-of-the-art with powerplant specific mass of 30 kg/kw. N-P solar cells are assumed and the solar constant is taken as 140 milliwatts/cm^2. Solar power variation with radial distance is based on current Jet Propulsion Laboratory N-P solar cell estimates. Ballistic continuation trajectories were generated with a three-dimensional conic trajectory programs.*

---

*Space Research Conic Program Phase III, Jet Propulsion Laboratory Report 900-130, April 1968.

EARTH-JUPITER-SATURN MISSIONS WITH SOLAR ELECTRIC PROPULSION

The several possible launch years for flights to Saturn utilizing the Jupiter encounter maneuver were established by superimposing plots of hyperbolic excess speed at Jupiter versus Jupiter arrival date for optimal low thrust trajectories on plots of hyperbolic excess speed at Jupiter required for continuation to Saturn. These plots are related to those already discussed in Figure 5. Optimum launch year depends on the desired payload for a given launch vehicle as will be shown. Acceptable launch dates for this mission fall between the summer of 1976 and the winter of 1978. Constraints which prohibit launch dates in earlier or later years will be discussed presently. Three-year launch opportunities recur with a period of about twenty years; thus, if the 1976-78 opportunity is missed, 1996 would represent the next acceptable launch year.*

Figure 10 illustrates a typical Earth-Jupiter-Saturn flight path utilizing the indirect solar electric mode. The characteristic inward loop toward the sun is evident. Motor operation time is quite long--typically 600 days for the indirect mode. Direct mode trajectories are almost ballistic in appearance and motor operation time is much shorter--usually less than 400 days for trajectories of interest (c.f. Figure A.4). This again represents a reliability consideration in flight mode selection.

---

*These observations hold for ballistic as well as for solar-electric earth-Jupiter-Saturn missions.

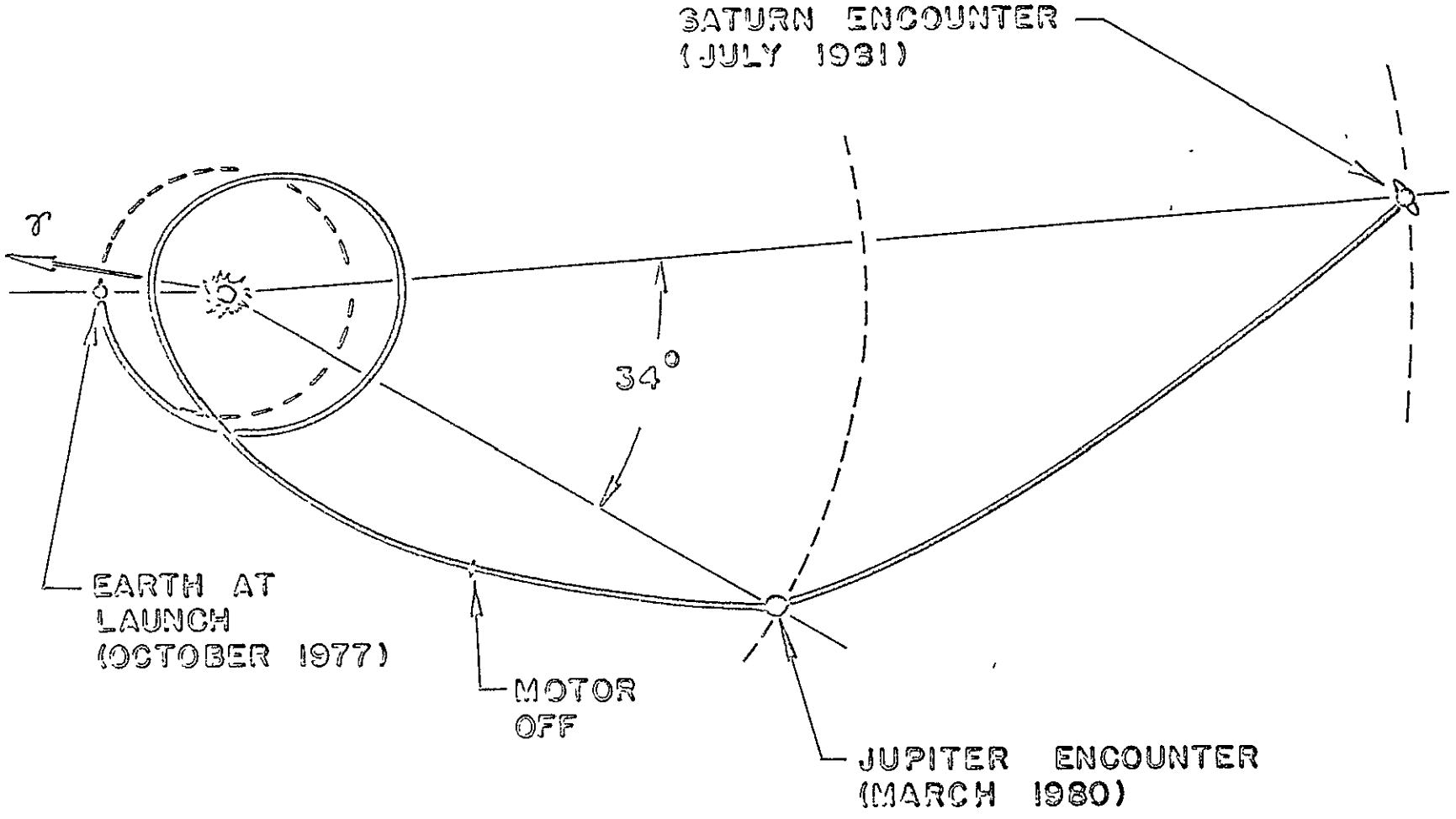

FIG. 10 - TYPICAL INDIRECT MODE EARTH-JUPITER-SATURN FLIGHT PATH

Figures 11, 12, and 13 are plots of total flight time to Saturn versus launch date with payload as parameter for the Atlas SLV-3X/Centaur booster for the 1976, 1977, and 1978 launch opportunities, respectively. These plots are are for the indirect low-thrust mode. Launches in 1977 provide the best performance in terms of payload delivered for trip times less than four years; 1976 is the superior launch year for trip times greater than four years.

Figures 14, 15, and 16 show plots of flight duration versus launch date for direct mode solar electric earth-Jupiter-Saturn missions utilizing the Atlas SLV-3X/Centaur launch vehicle. Notice that for shorter flight times (less than 3.5 years) and lower payloads (less than 400 kg), 1978 represents the optimal launch year; for larger payloads (and flight time), 1977 is the best launch year.

Figures 17, 18, and 19 are plots of the optimum launch dates versus payload mass for 1976, 1977, and 1978 for direct mode trajectories utilizing the Titan/Centaur boost vehicle. Figure 20 shows the corresponding passage distances at Jupiter required to enter the Jupiter-to-Saturn continuation orbits. Notice that short flight-time trajectories in 1976 are limited by the deflection angle constraint; to achieve continuation with total flight time less than 3.2 years would require a propulsive maneuver near Jupiter. It must be pointed out that in addition to the payload-flight duration tradeoff already discussed, the mission planner must take account of intermediate planet passage distance in terms of desired scientific data return. The instrumentation requirements play a part in launch year selection; 1976 trajectories yield very close passage distance while 1978 launches pass far from Jupiter's surface since the required continuation bend angle is much smaller. Payload performance for the three available launch years is summarized in Figure 21 for the Titan/Centaur

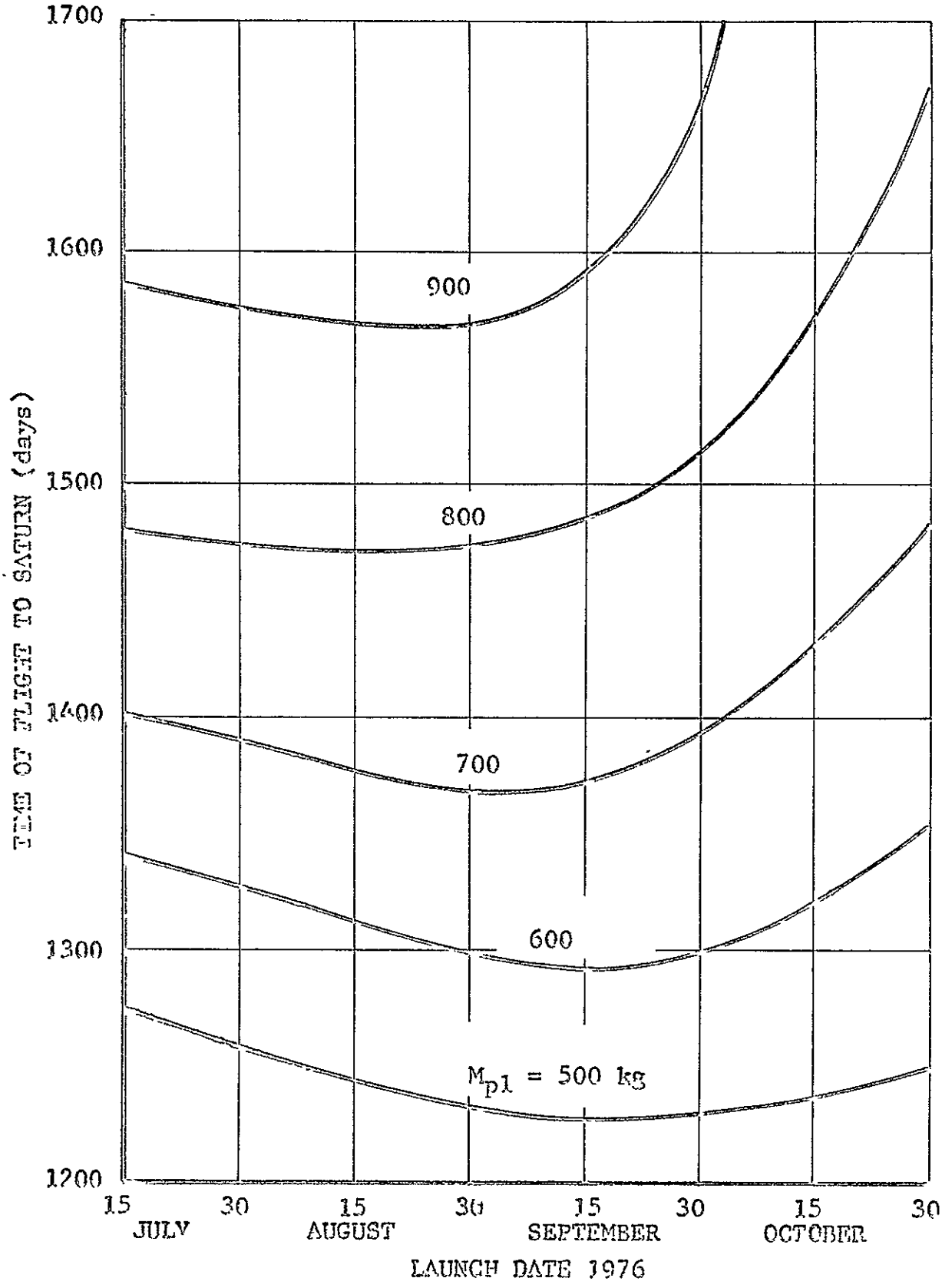

FIG. 11 - FLIGHT DURATION VS LAUNCH DATE FOR 1976 EARTH-JUPITER-SATURN MISSION SLV-3X/Centaur INDIRECT MODE

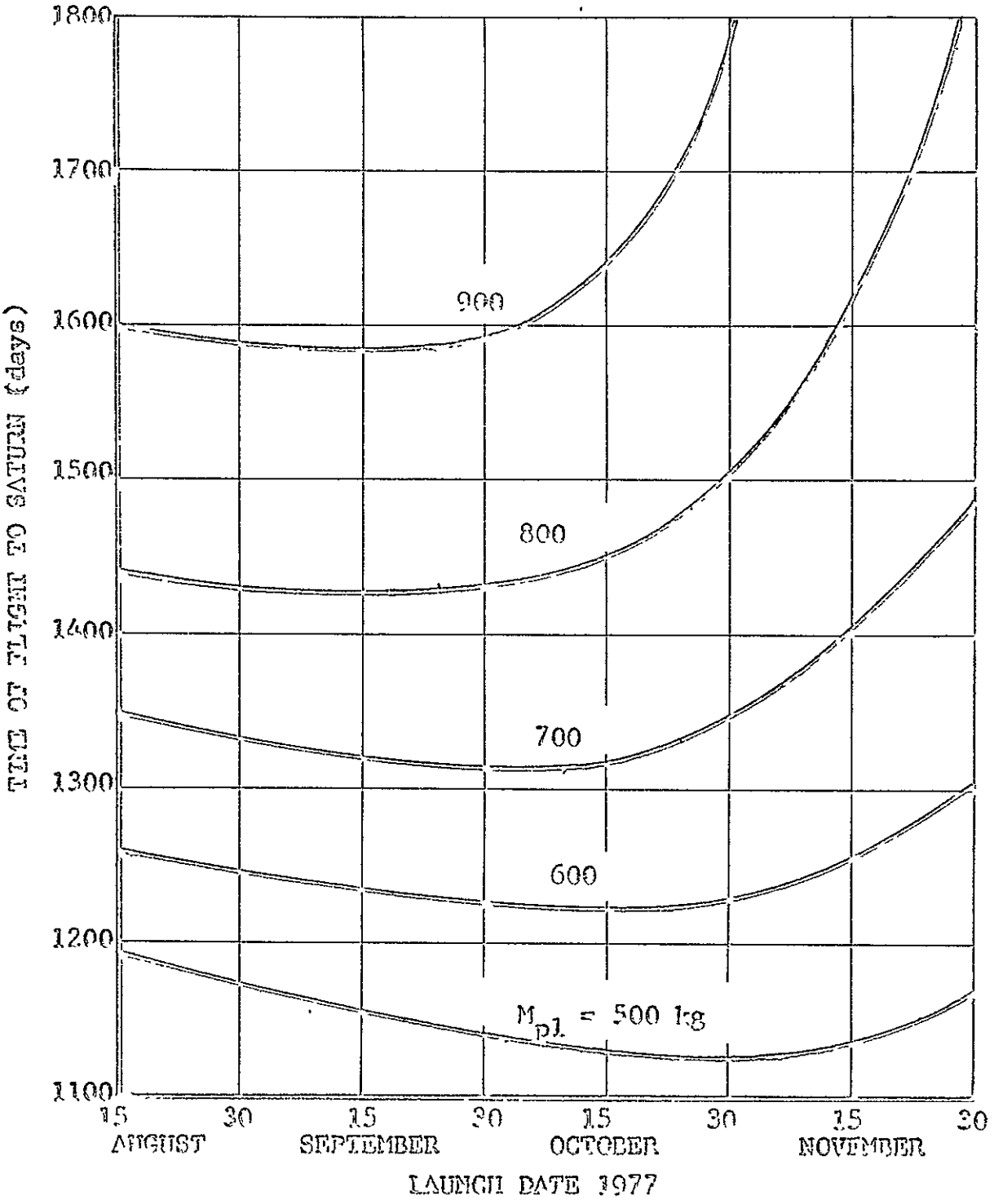

FIG. 12 - FLIGHT DURATION VS LAUNCH DATE FOR 1977 EARTH-JUPITER-SATURN MISSION SLV-3X/CENTAUR INDIRECT MODE

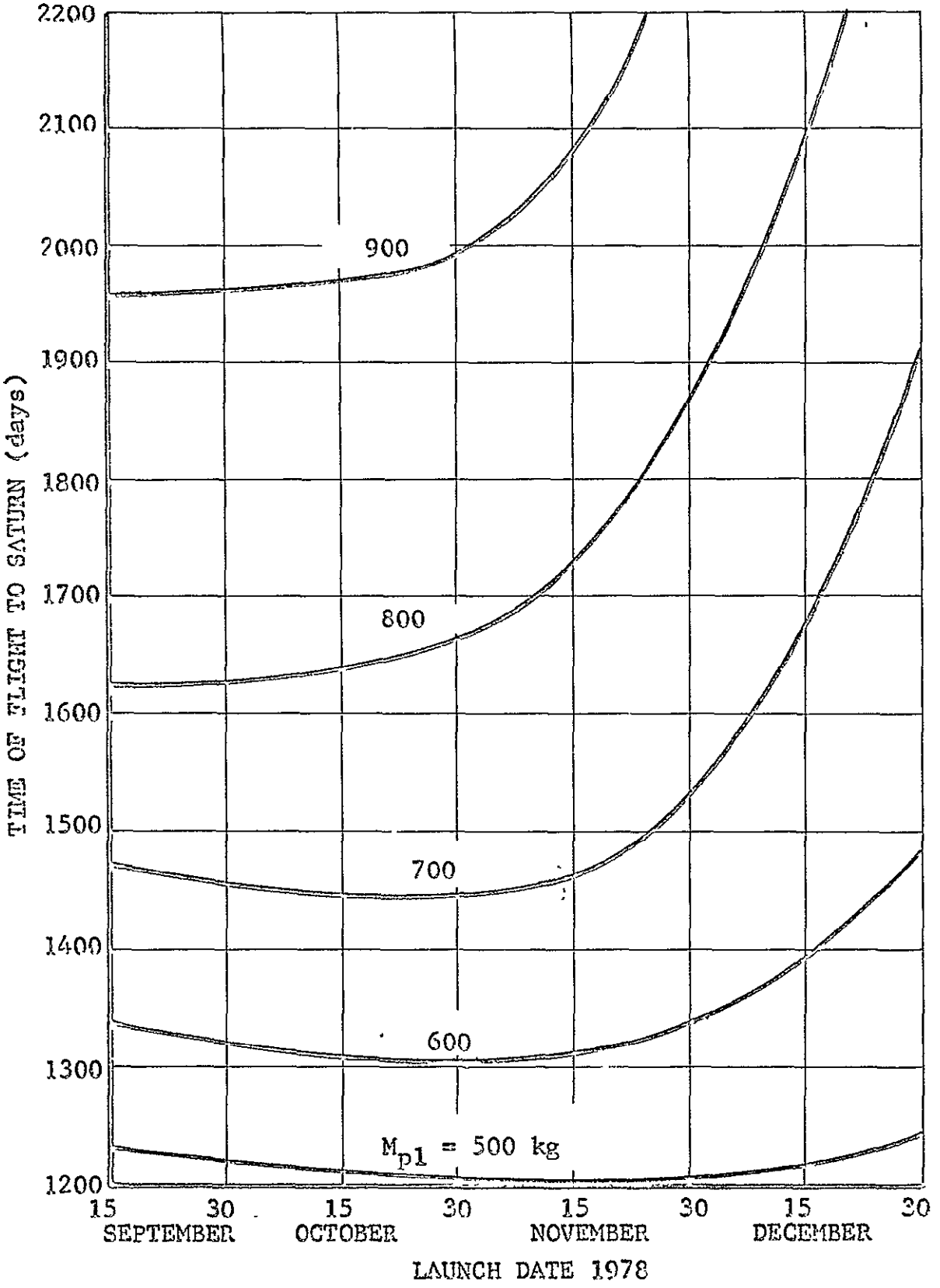

FIG. 13 - FLIGHT DURATION VS LAUNCH DATE FOR 1978 EARTH-JUPITER-SATURN MISSION SLV-3X/CENTAUR INDIRECT MODE

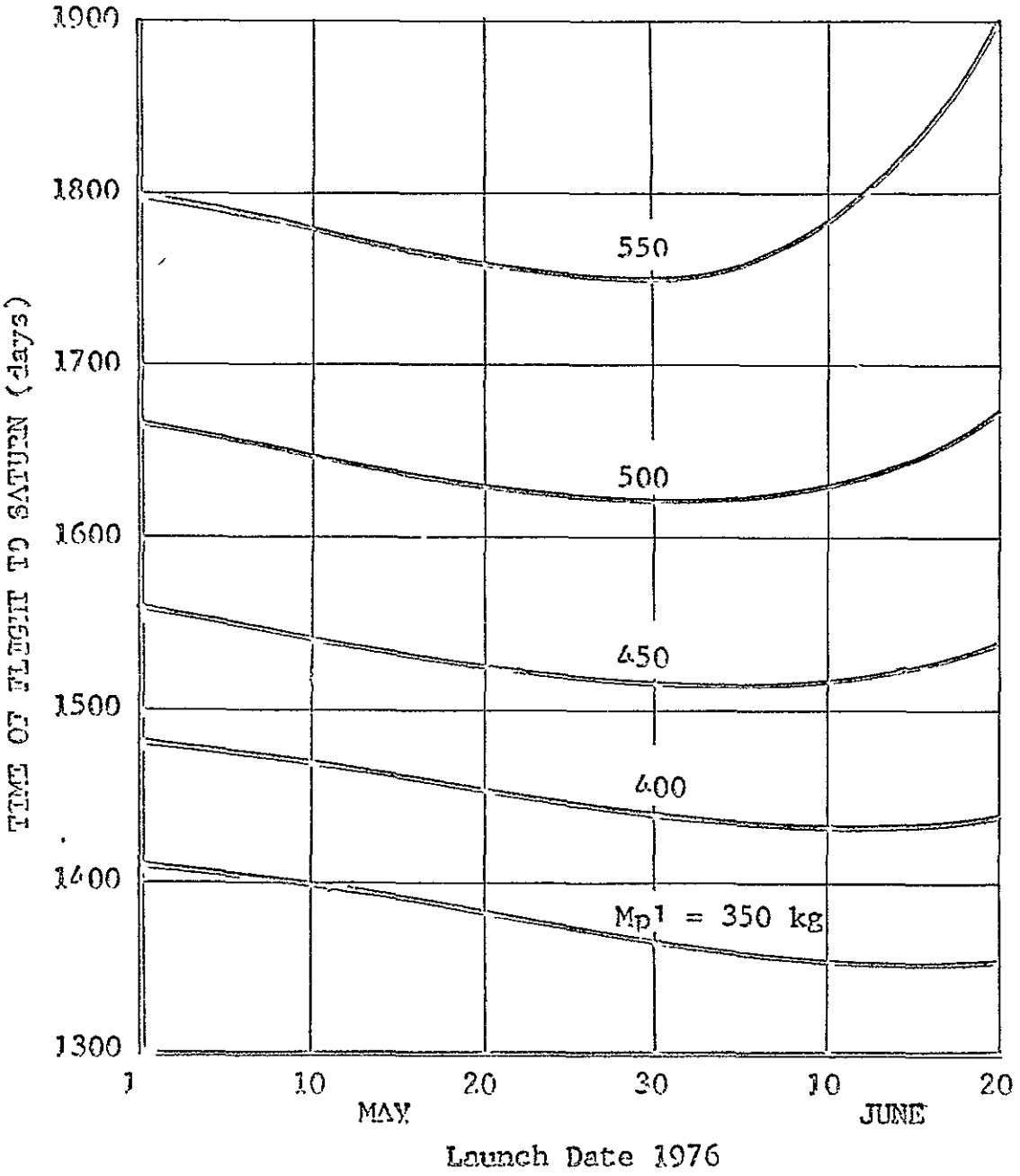

FIG. 14 - FLIGHT DURATION VS LAUNCH DATE FOR 1976 EARTH-JUPITER-SATURN MISSION. SLV-2Y/CENTAUR DIRECT MODE.

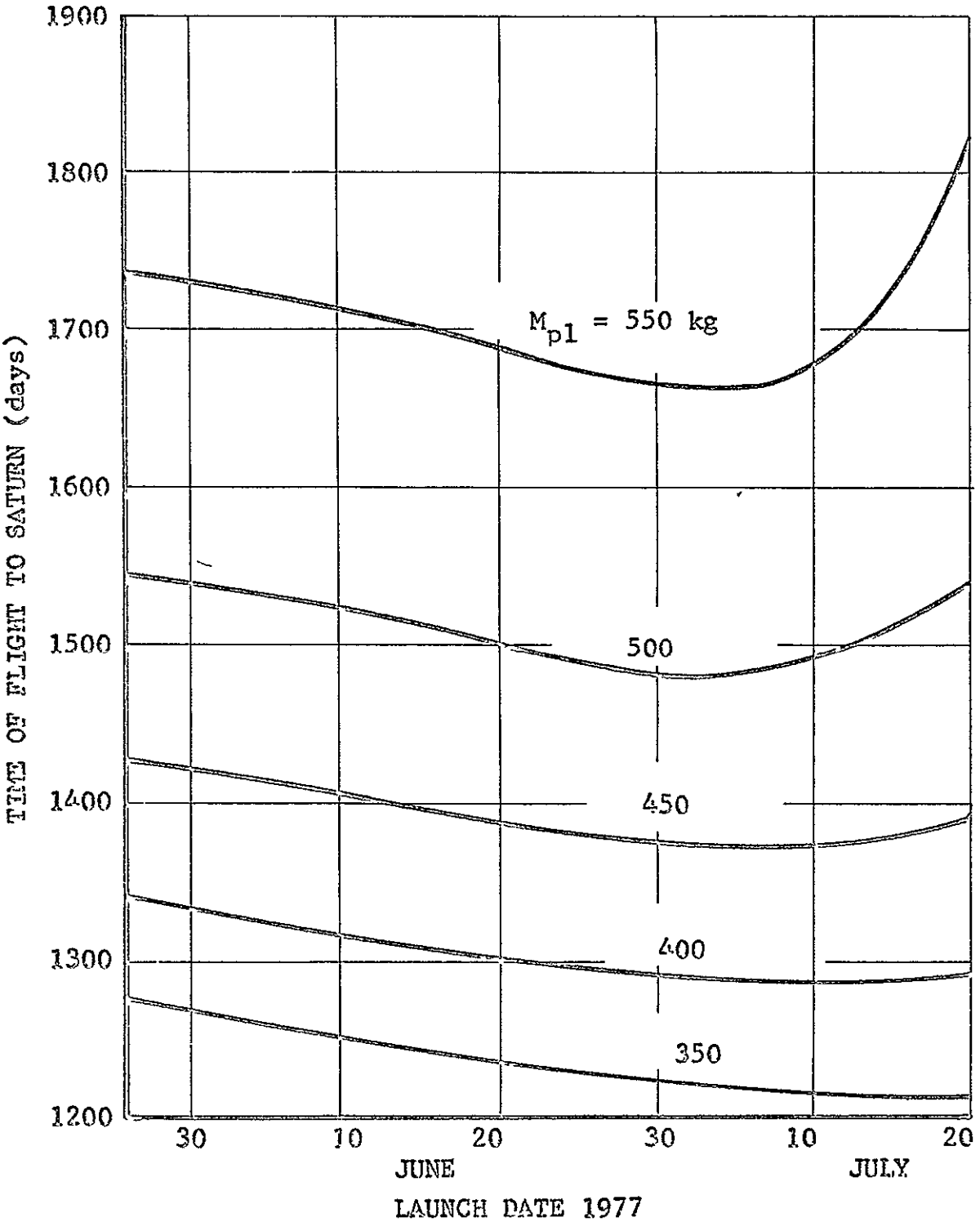

FIG. 15 - FLIGHT DURATION VS LAUNCH DATE FOR 1977 EARTH-JUPITER-SATURN MISSION. SLV-3X/CENTAUR DIRECT MODE.

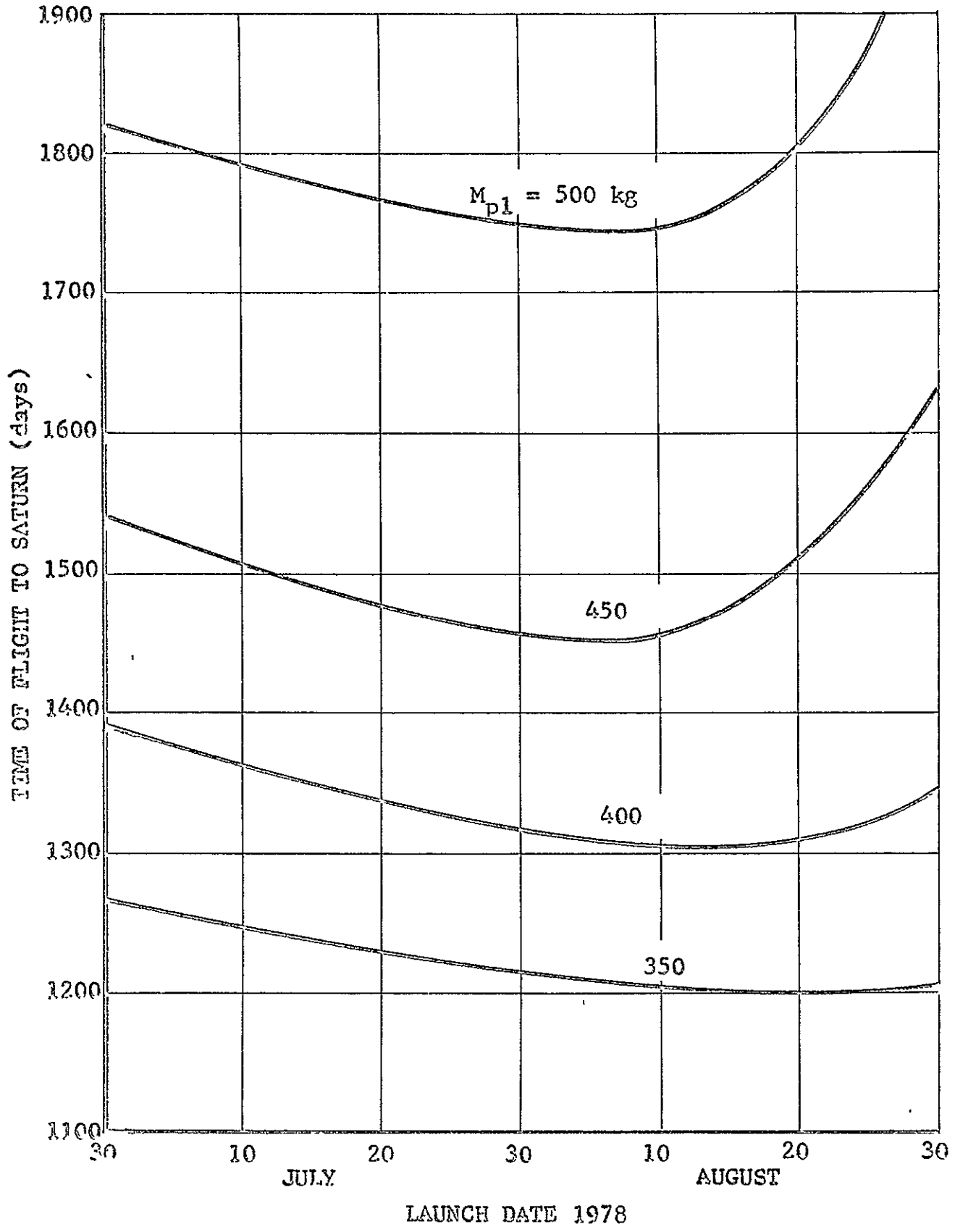

FIG. 16 - FLIGHT DURATION VS LAUNCH DATE FOR 1978 EARTH-JUPITER-SATURN MISSION. SLV-3X/CENTAUR DIRECT MODE.

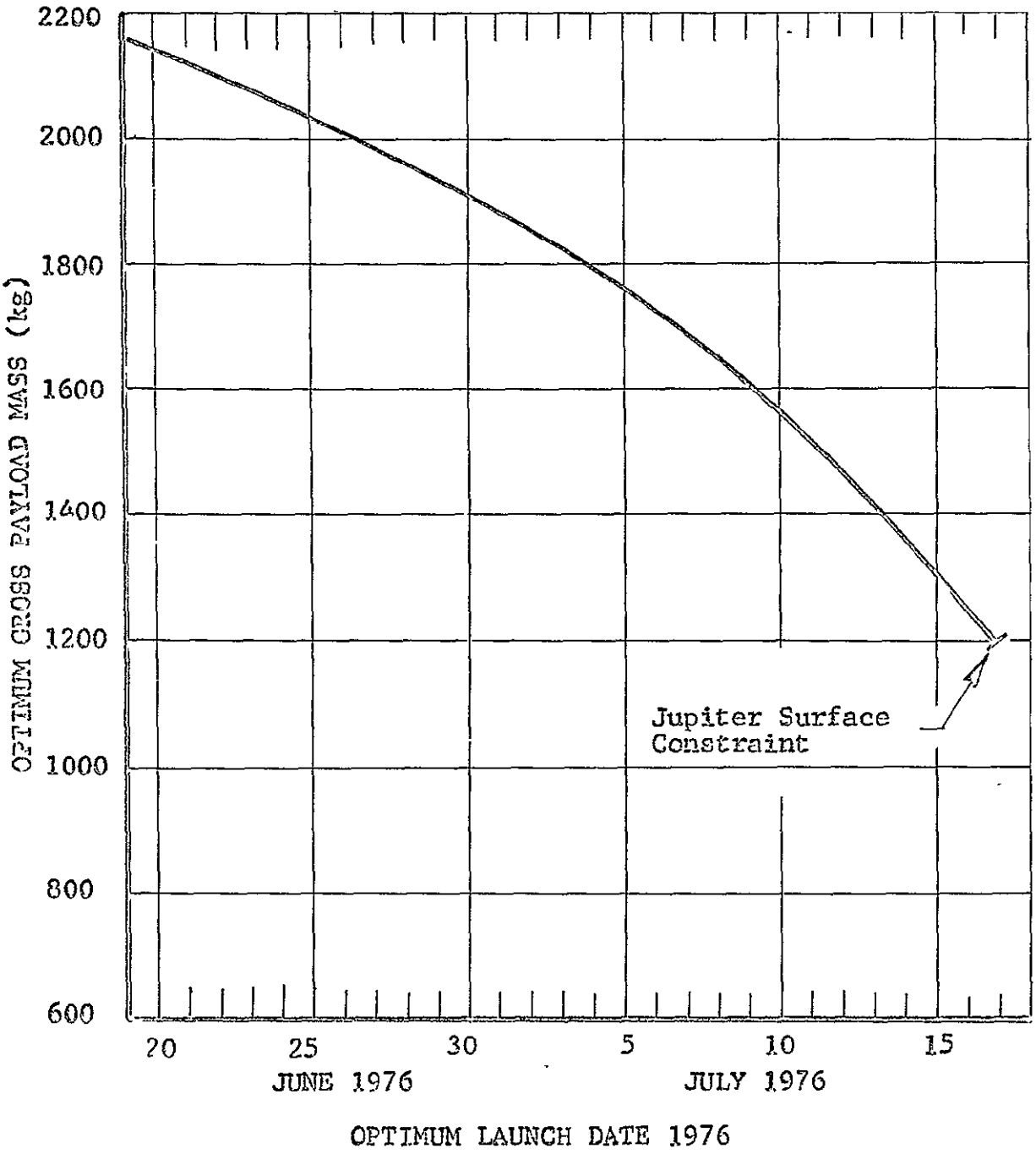

FIG. 17 - OPTIMUM LAUNCH DATE VS PAYLOAD MASS FOR 1976 EARTH JUPITER-SATURN MISSION. DIRECT MODE TITAN 3X(1205)/CENTAUR LAUNCH VEHICLE.

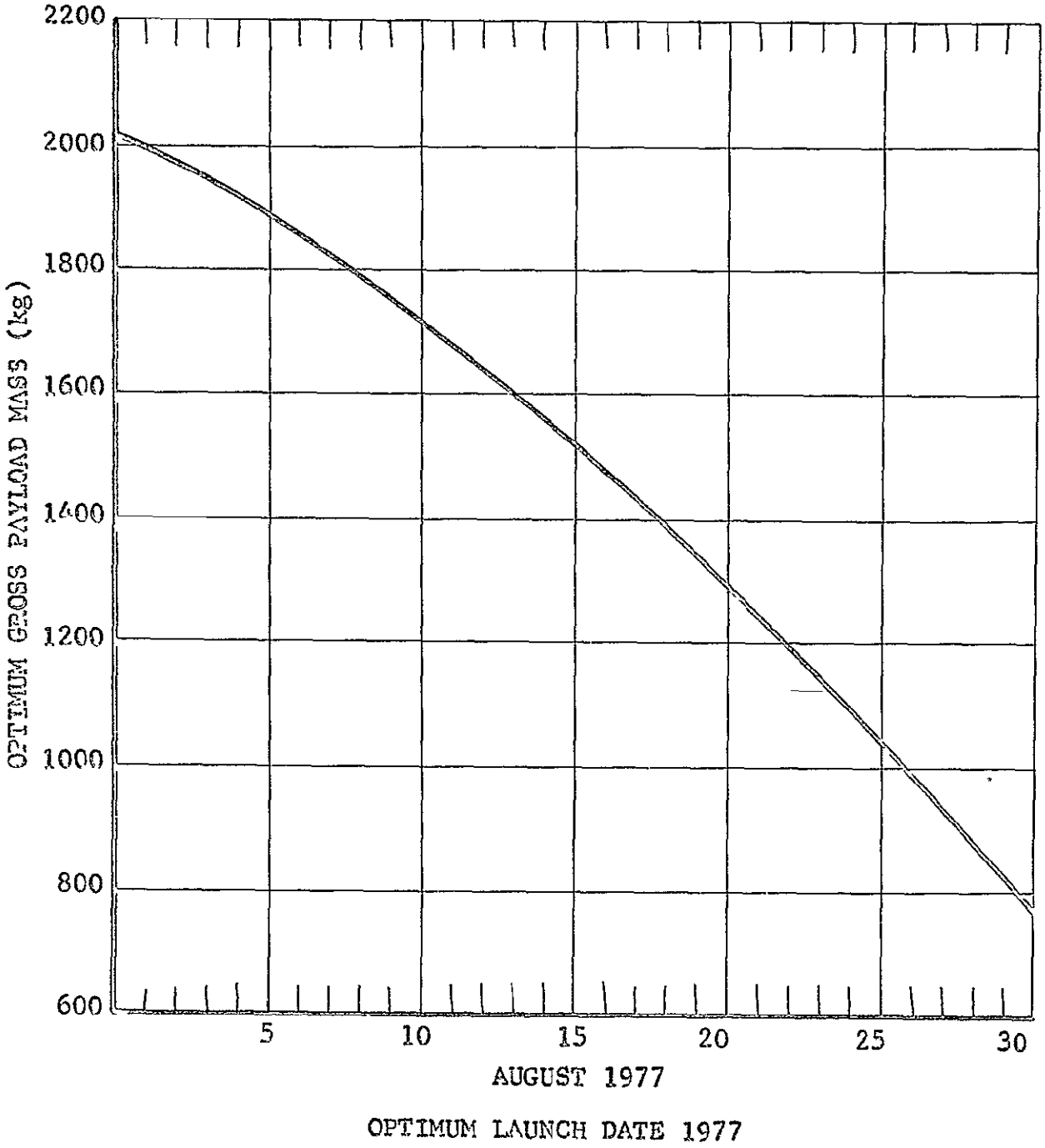

FIG. 18 - OPTIMUM LAUNCH DATE VS PAYLOAD FOR 1977 EARTH-JUPITER-SATURN MISSION. DIRECT MODE TITAN 3X/CENTAUR BOOSTER.

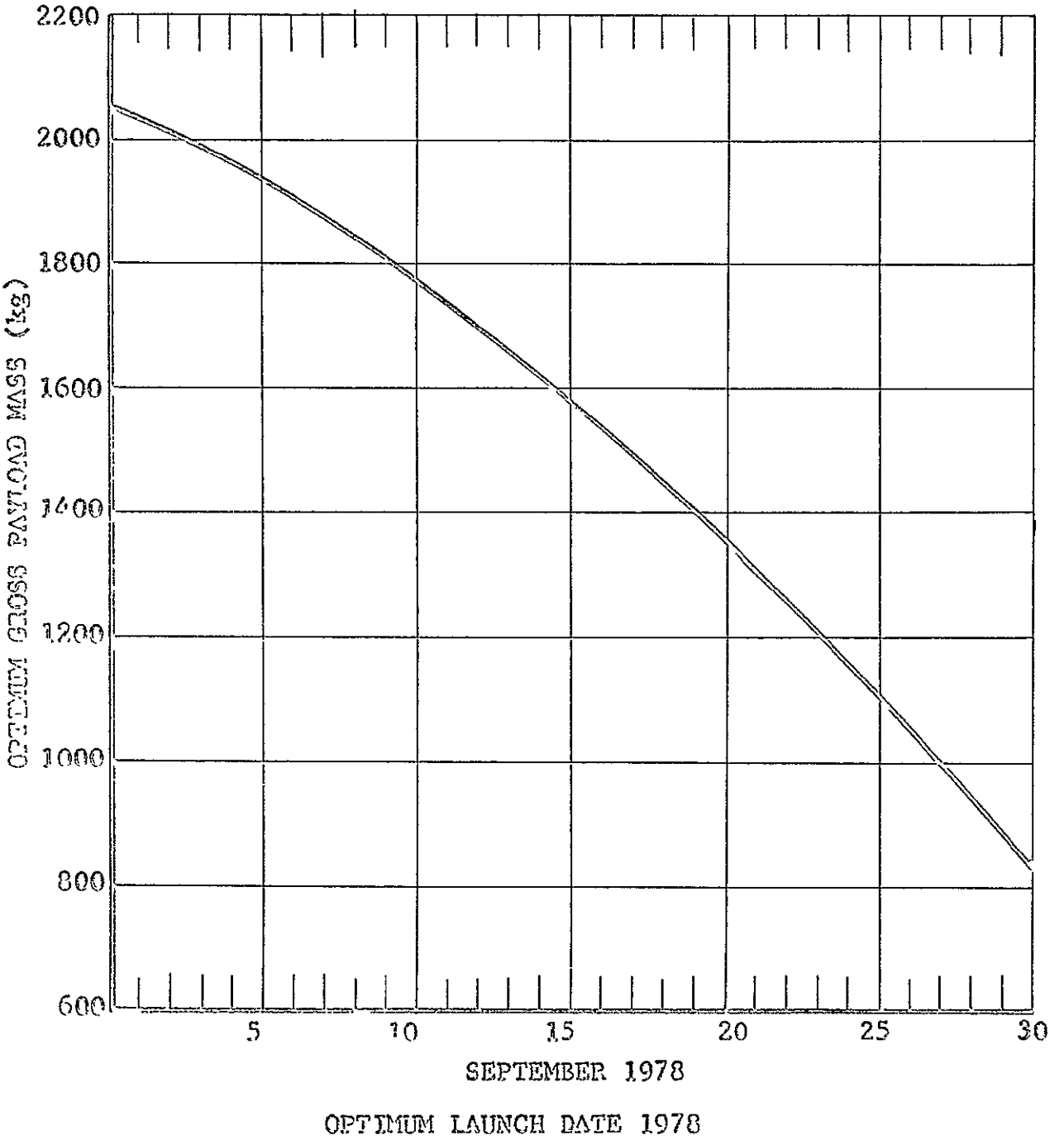

FIG. 19 - OPTIMUM LAUNCH DATE VS PAYLOAD FOR 1978 EARTH-JUPITER-SATURN MISSION. DIRECT MODE TITAN 3X/CENTAUR BOOSTER.

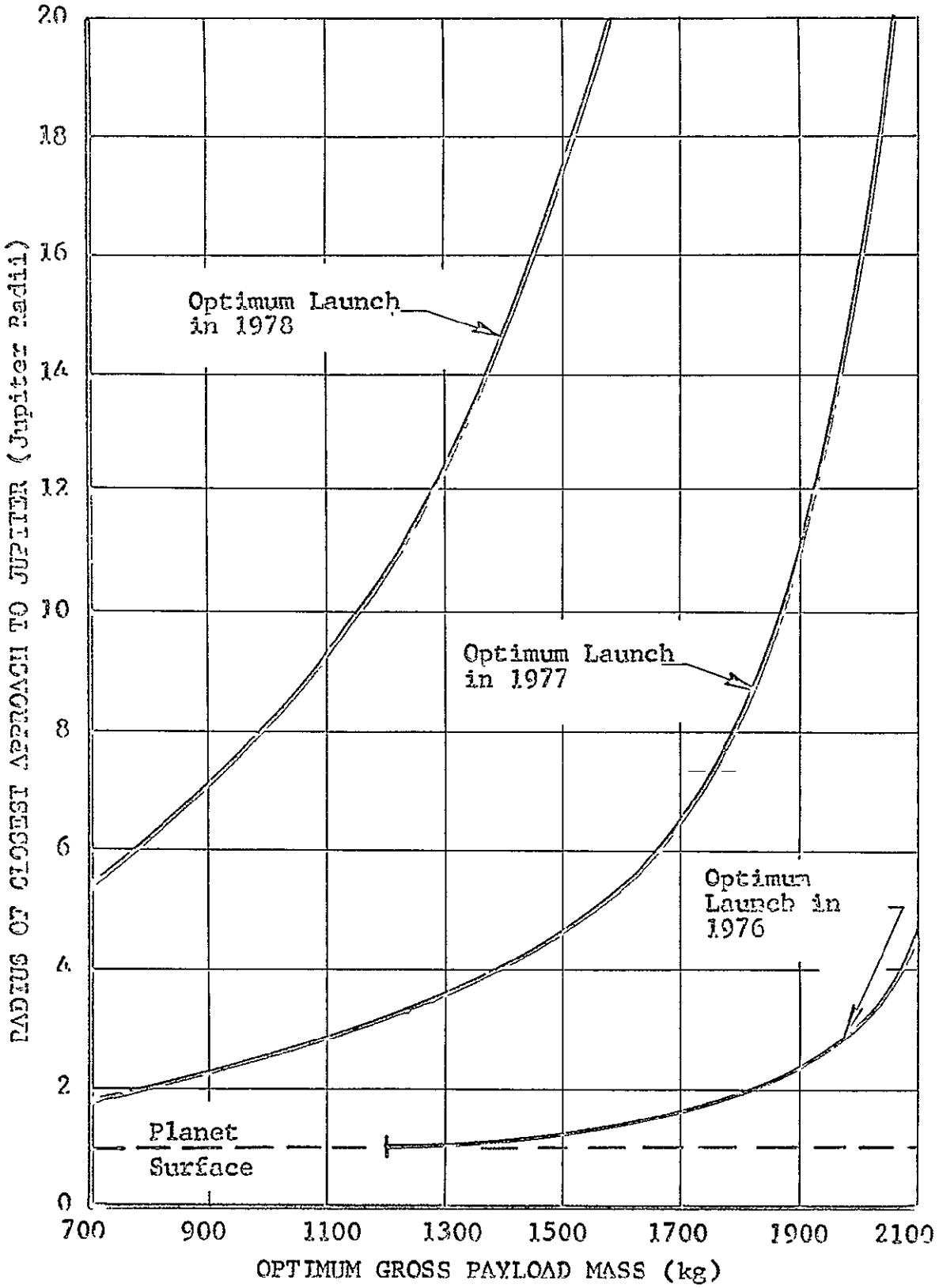

FIG. 20 - RADIUS OF CLOSEST APPROACH TO JUPITER VS OPTIMUM GROSS PAYLOAD FOR EARTH-JUPITER-SATURN MISSION. TITAN 3X(1205)/CENTAUR LAUNCH VEHICLE, DIRECT MODE.

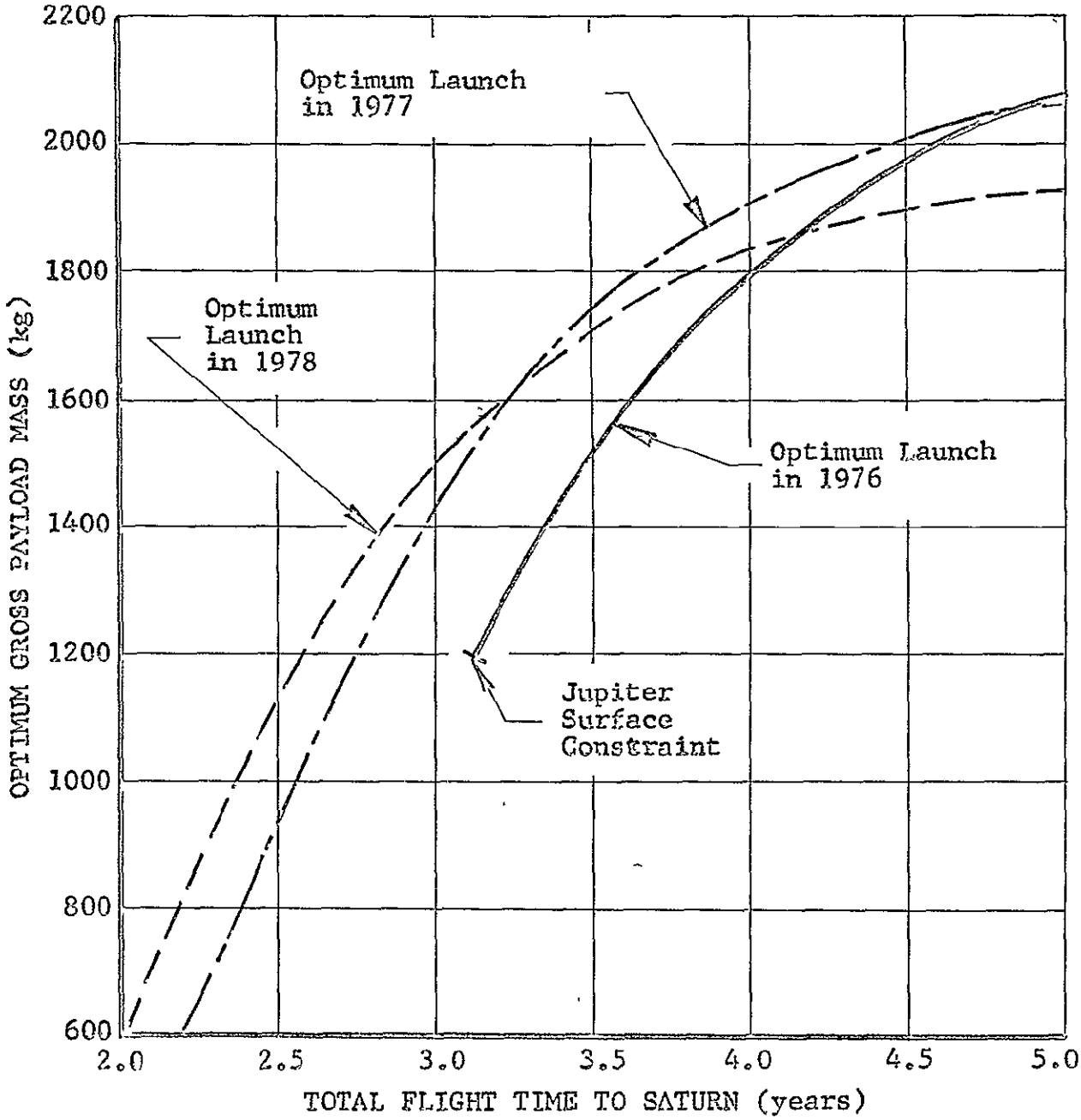

FIG. 21 - FLIGHT DURATION - PAYLOAD TRADEOFF FOR EARTH-JUPITER-SATURN MISSION. TITAN 3X/CENTAUR DIRECT MODE.

booster. Note that 1978 produces the best trajectories for flight times less than 3.2 years, 1977 is best for flights between 3.2 and 4.8 years duration, and 1976 is best for mission times greater than 4.8 years.

SOLAR ELECTRIC SWINGBY MISSIONS TO URANUS, NEPTUNE, AND PLUTO

The techniques discussed previously were used to investigate Jupiter swingby missions to Uranus, Neptune, and Pluto with optimum low thrust propulsion. Since Neptune and Pluto may be reached by continuation trajectories from Uranus and Saturn, respectively, to be discussed in the next section, detailed data is not given here for those mission possibilities. Reference 6 gives some results for earth-Jupiter-Neptune and earth-Jupiter-Pluto missions.

Figures 22 and 23 are plots of flight duration to Uranus versus launch date for Atlas SLV-3X/Centaur indirect mode optimum solar electric trajectories; Figures 24 and 25 give the same results for direct mode trajectories utilizing the Atlas/Centaur and launches in 1978 and 1979. Indirect mode trajectories are best launched in 1978; direct mode flights of less than 6.5 years duration should be initiated in 1979. Direct mode flights of duration longer than 6.5 years are best launched in 1978.

Figures 26, 27, and 28 show optimum launch dates in the years 1978, 1979, and 1980, respectively, for direct mode earth-Jupiter-Uranus flights utilizing the Titan/Centaur boost vehicle. Figure 29 illustrates the closest approach distance corresponding to the above trajectories. The Uranus surface constraint called out in Figure 29 refers to continuation trajectories to Neptune to be discussed later. Figure 30 summarizes the Titan/Centaur data in terms of a trip time-payload tradeoff for the three potential launch years. 1980 is an acceptable launch year only for very high energy (low payload)

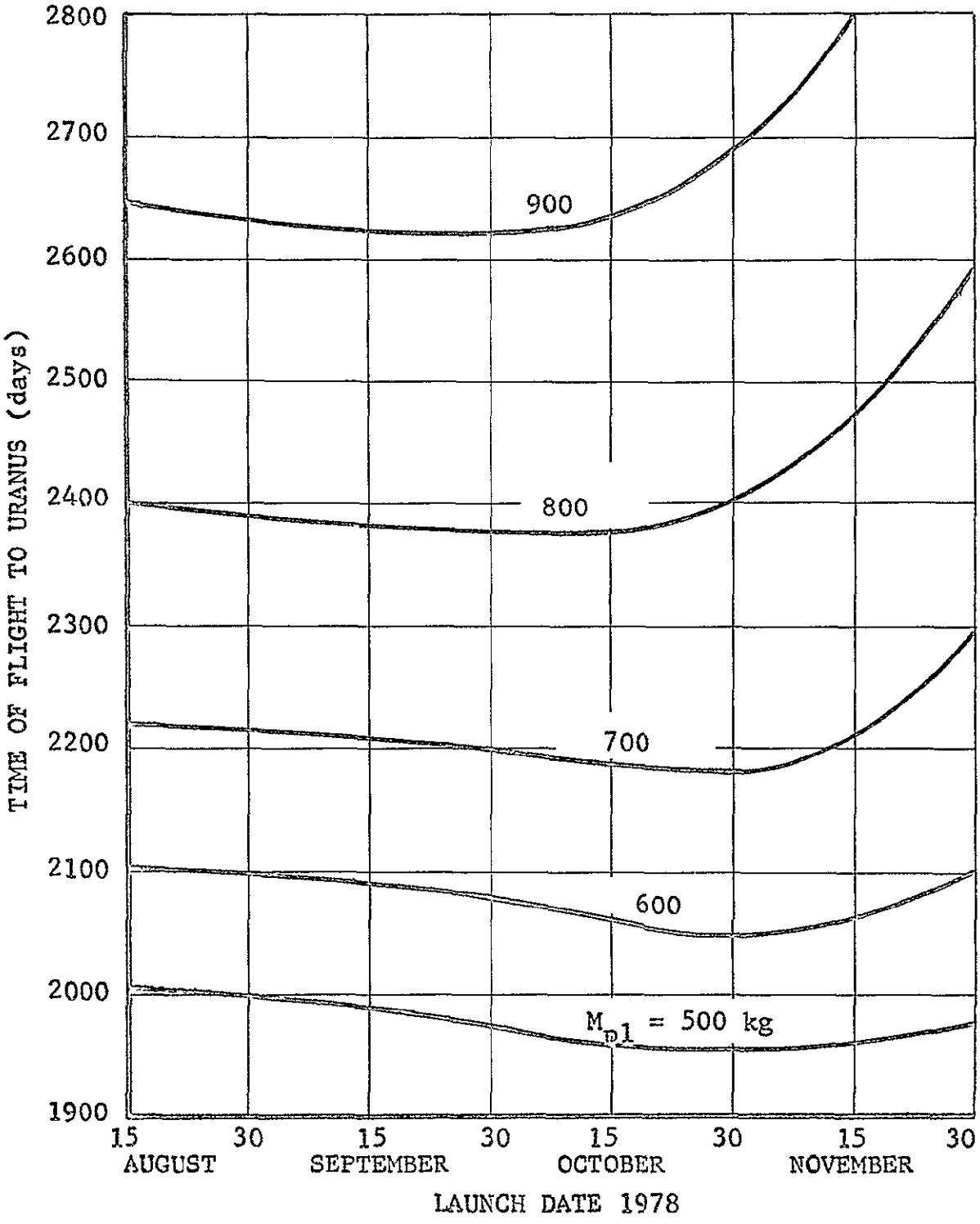

FIG. 22 - FLIGHT DURATION VS LAUNCH DATE FOR 1978 EARTH-JUPITER-URANUS MISSION. SLV-3X/CENTAUR INDIRECT MODE.

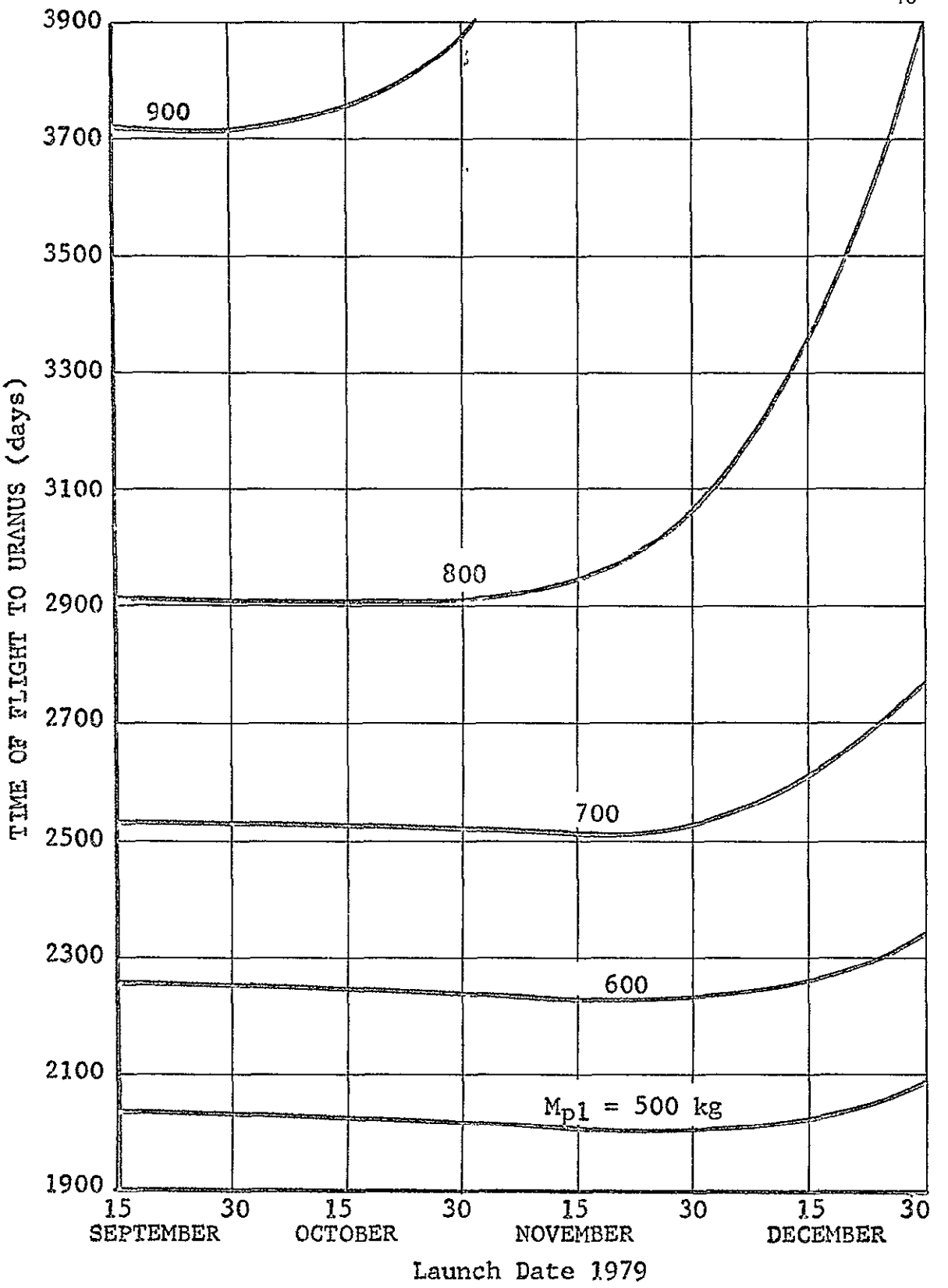

FIG. 23 - FLIGHT DURATION VS LAUNCH DATE FOR 1979 EARTH-JUPITER-URANUS MISSION. SLV-3X/CENTAUR INDIRECT MODE.

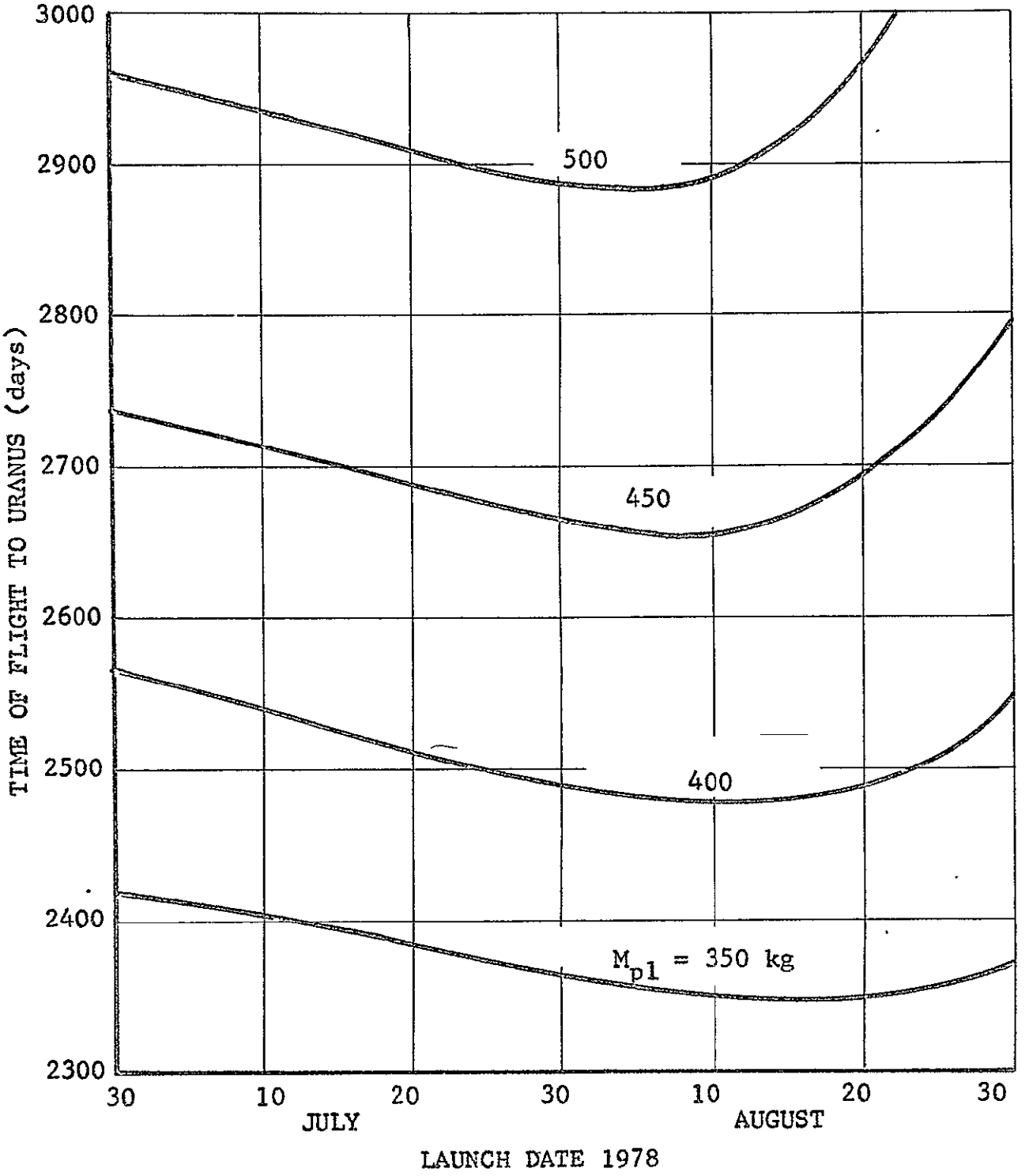

FIG. 24 - FLIGHT DURATION VS LAUNCH DATE FOR 1978 EARTH-JUPITER-URANUS MISSION. SLV-3X/CENTAUR DIRECT MODE.

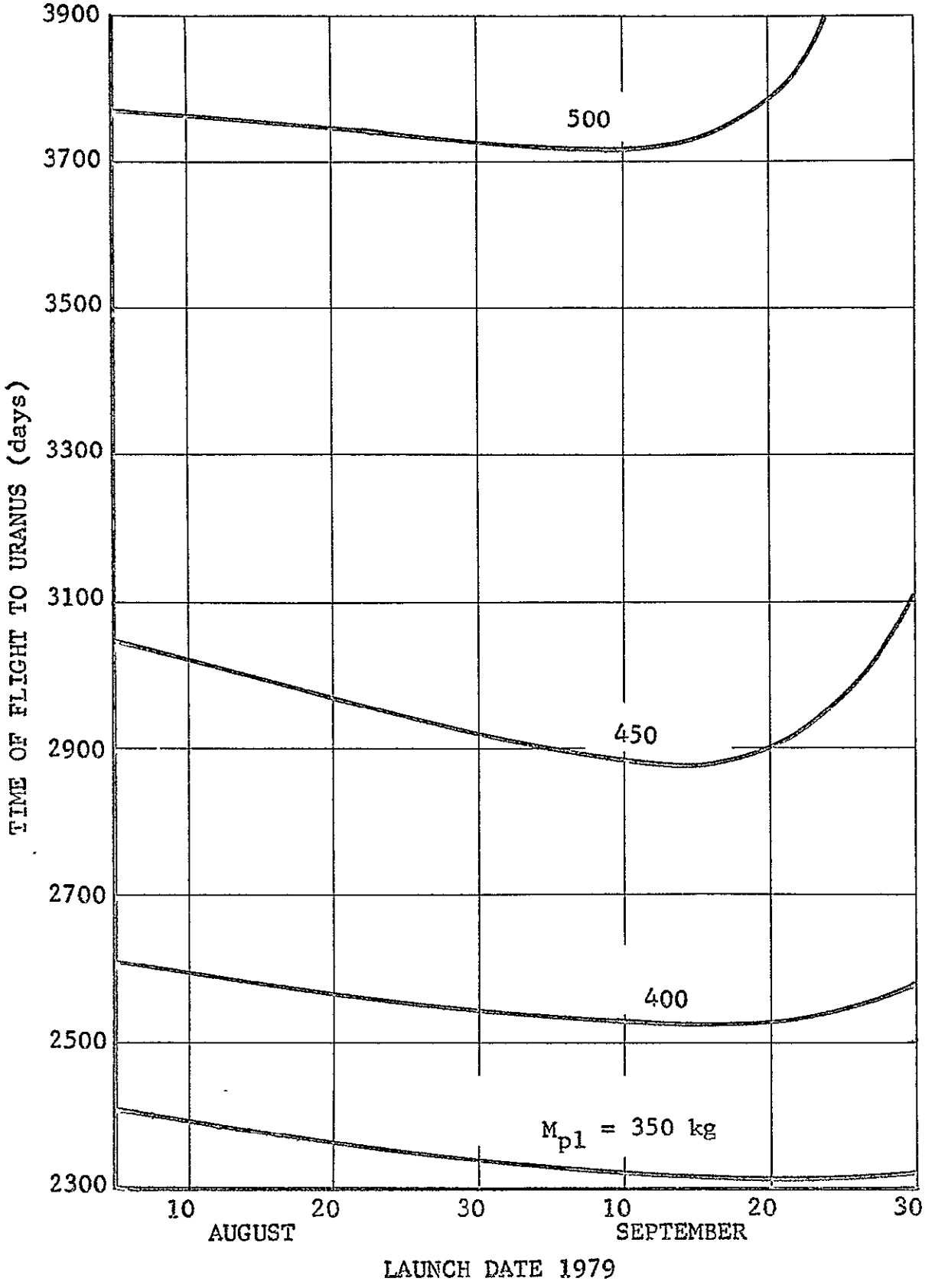

FIG. 25 - FLIGHT DURATION VS LAUNCH DATE FOR 1979 EARTH-JUPITER-URANUS MISSION. SLV-3X/CENTAUR DIRECT MODE.

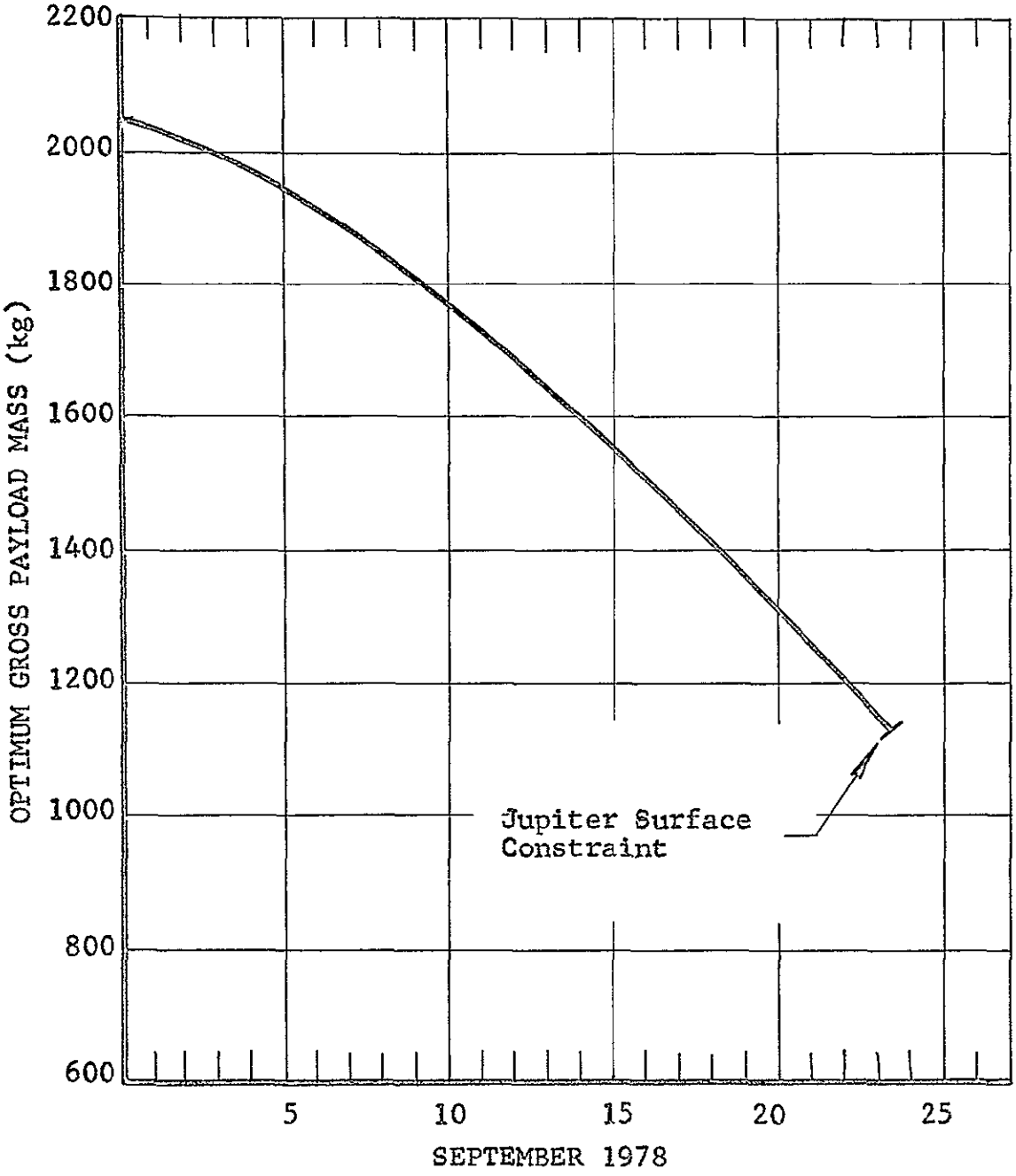

FIG. 26 - OPTIMUM LAUNCH DATE VS PAYLOAD MASS FOR 1978 EARTH-JUPITER-URANUS MISSION. DIRECT MODE TITAN 3X(1205)/CENTAUR LAUNCH VEHICLE.

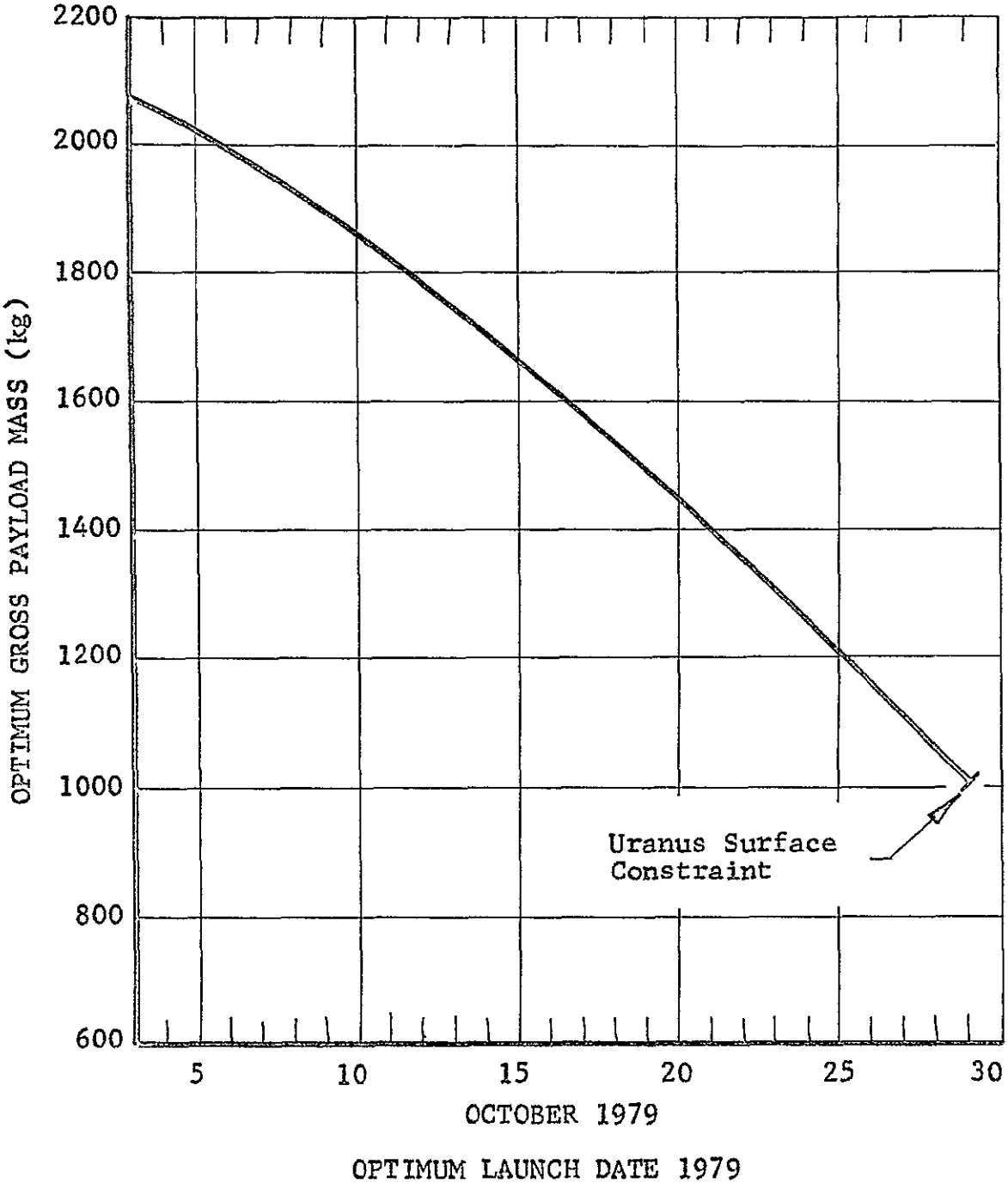

FIG. 27 - OPTIMUM LAUNCH DATE VS PAYLOAD MASS FOR 1979 EARTH-JUPITER-URANUS MISSION. DIRECT MODE TITAN 3X(1205)/CENTAUR LAUNCH VEHICLE.

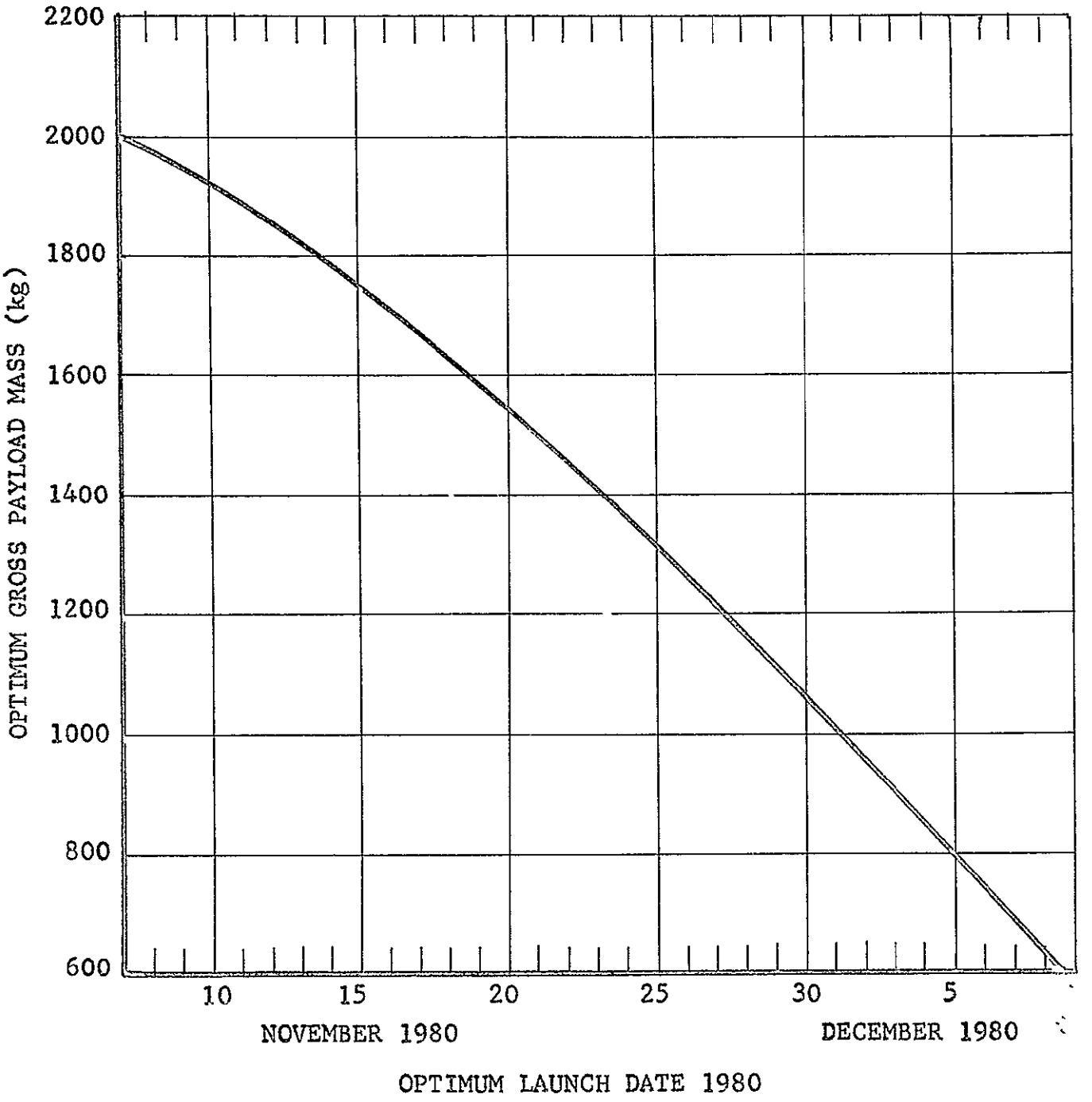

FIG. 28 - OPTIMUM LAUNCH DATE VS PAYLOAD MASS FOR 1980 EARTH-JUPITER-URANUS MISSION. DIRECT MODE TITAN 3X(1205)/CENTAUR LAUNCH VEHICLE.

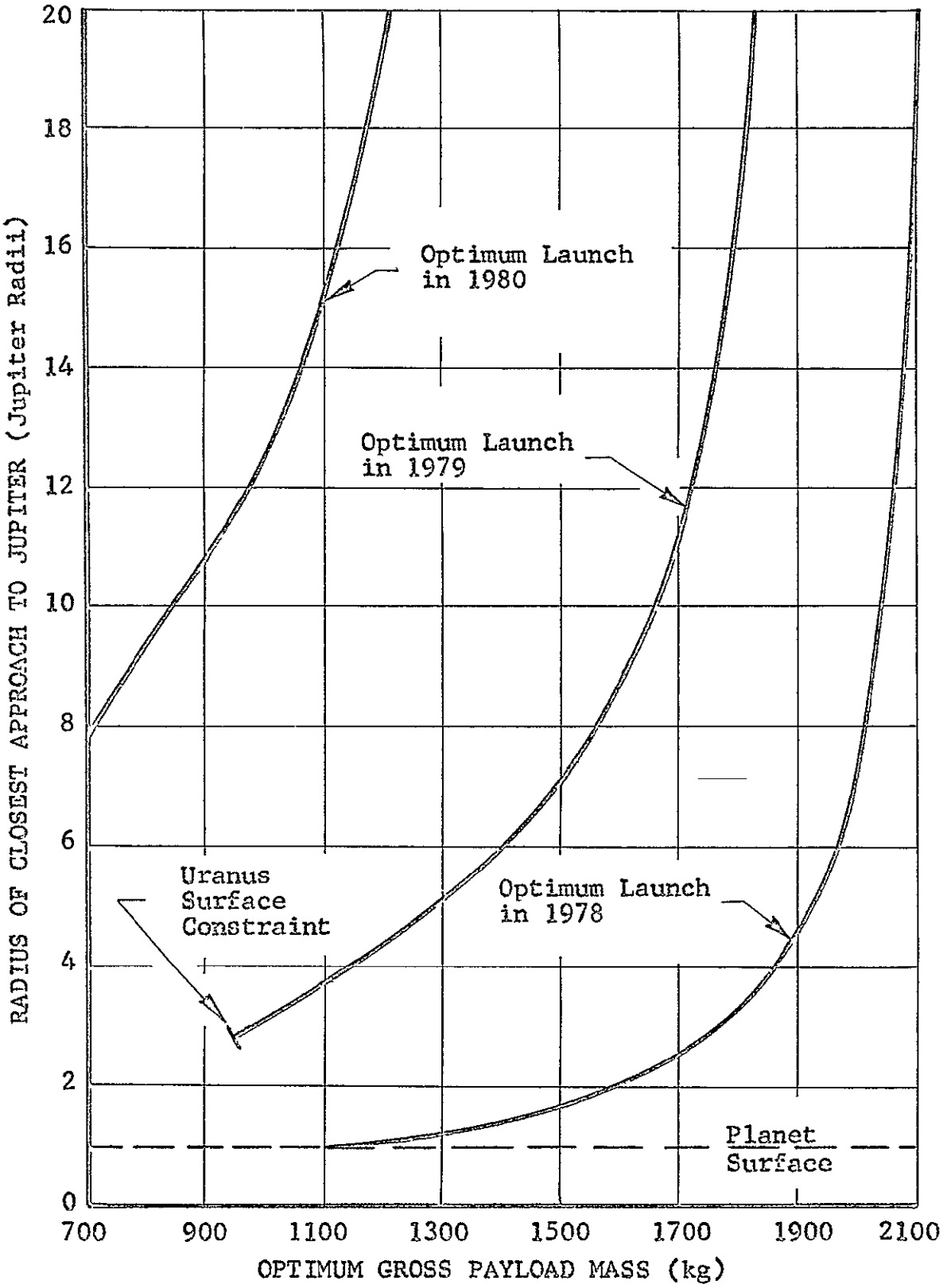

FIG. 29 - RADIUS OF CLOSEST APPROACH TO JUPITER VS OPTIMUM GROSS PAYLOAD FOR EARTH-JUPITER-URANUS MISSION TITAN 3X/CENTAUR LAUNCH VEHICLE, DIRECT MODE.

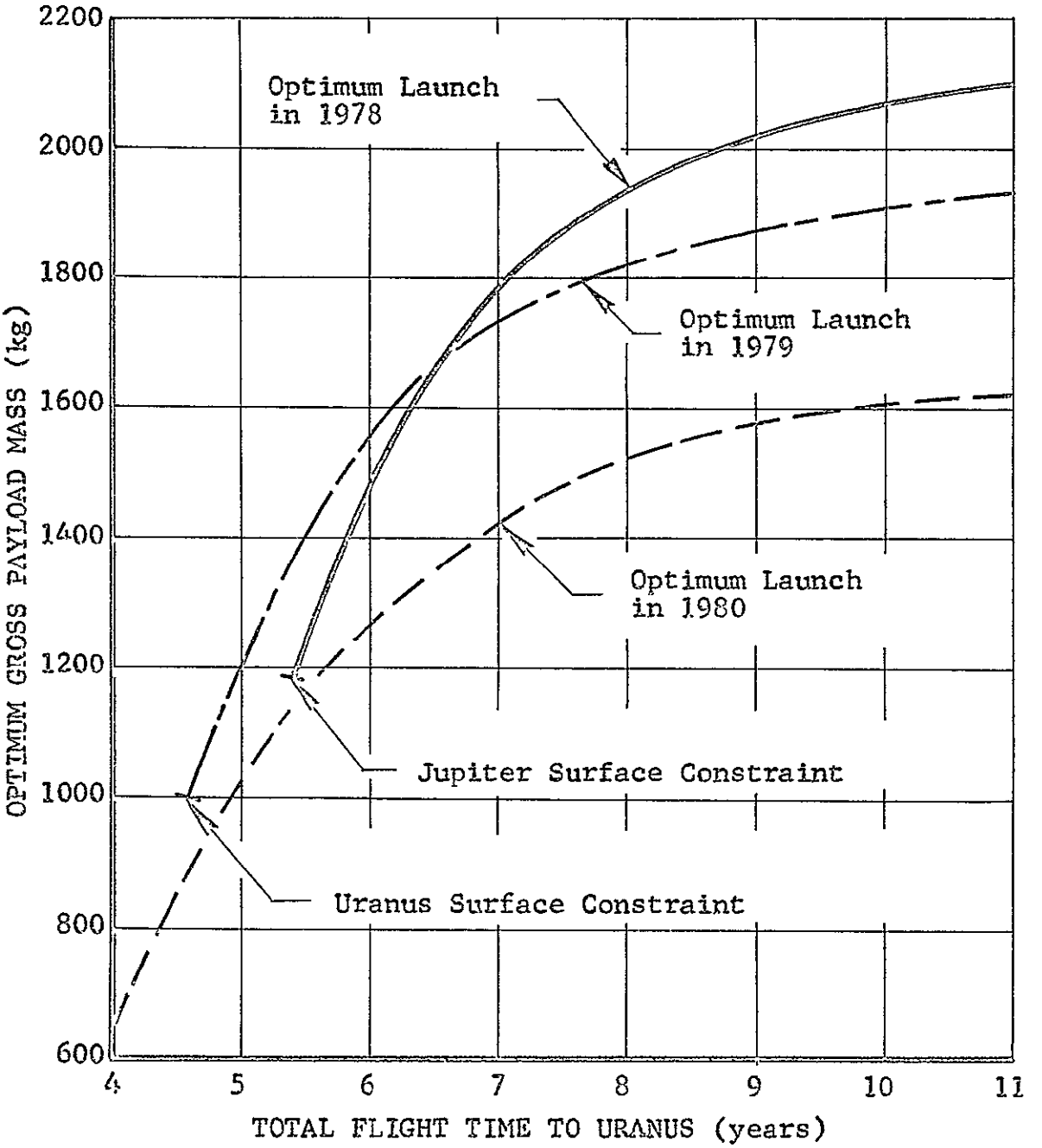

FIG. 30 - FLIGHT DURATION - PAYLOAD TRADEOFF FOR EARTH-JUPITER-URANUS MISSION. TITAN/CENTAUR DIRECT MODE.

trajectories of less than 4.6 years duration. 1979 is the best launch year for flights between 4.6 and 6.5 years in length; 1978 yields best payload for flight duration of greater than 6.5 years. Uranus opportunities via Jupiter are available about every 14 years.

SOLAR ELECTRIC GRAND TOUR MISSIONS

It was shown by Flandro (1,6) that earth-Jupiter-Saturn trajectories launched in the 1977-1978 opportunity may be continued after Saturn encounter to Uranus and finally to Neptune. This mission opportunity is repeated every 175 years. An unfortunate feature of the "grand tour" as this four-planet mission is often called results from the interaction of Saturn's ring system with the Saturn-Uranus trajectory leg. Trajectories which pass outside of the ring system require too long to reach Uranus and Neptune; those passing between the surface of Saturn and the rings might require unattainable guidance accuracy. In the latter regard, recent data seems to indicate that ring material may extend much closer to the planet than previously believed, thus making passage beneath the rings somewhat risky. It has thus been proposed that instead of a single "grand tour" mission that two be considered: (1) Earth-Jupiter-Saturn-Pluto and (2) Earth-Jupiter-Uranus-Neptune. By bypassing Saturn in the Uranus-Neptune mission the ring constraint obviously vanishes. Ring geometry is not so severe an effect in the earth-Jupiter-Saturn continuation to Pluto. Thus, with a pair of spacecraft launched in the 1977-1979 period, the entire center solar system can be explored utilizing launch vehicles already in advanced stages of development. Application of solar electric propulsion to the earth-Jupiter leg of the trajectory allows delivery of more than three times the gross payload which could be accommodated on a ballistic flight with the same basic launch vehicle.

EARTH-JUPITER-SATURN-PLUTO GRAND TOUR

Figure 31 shows the projection of a typical direct mode Pluto grand tour

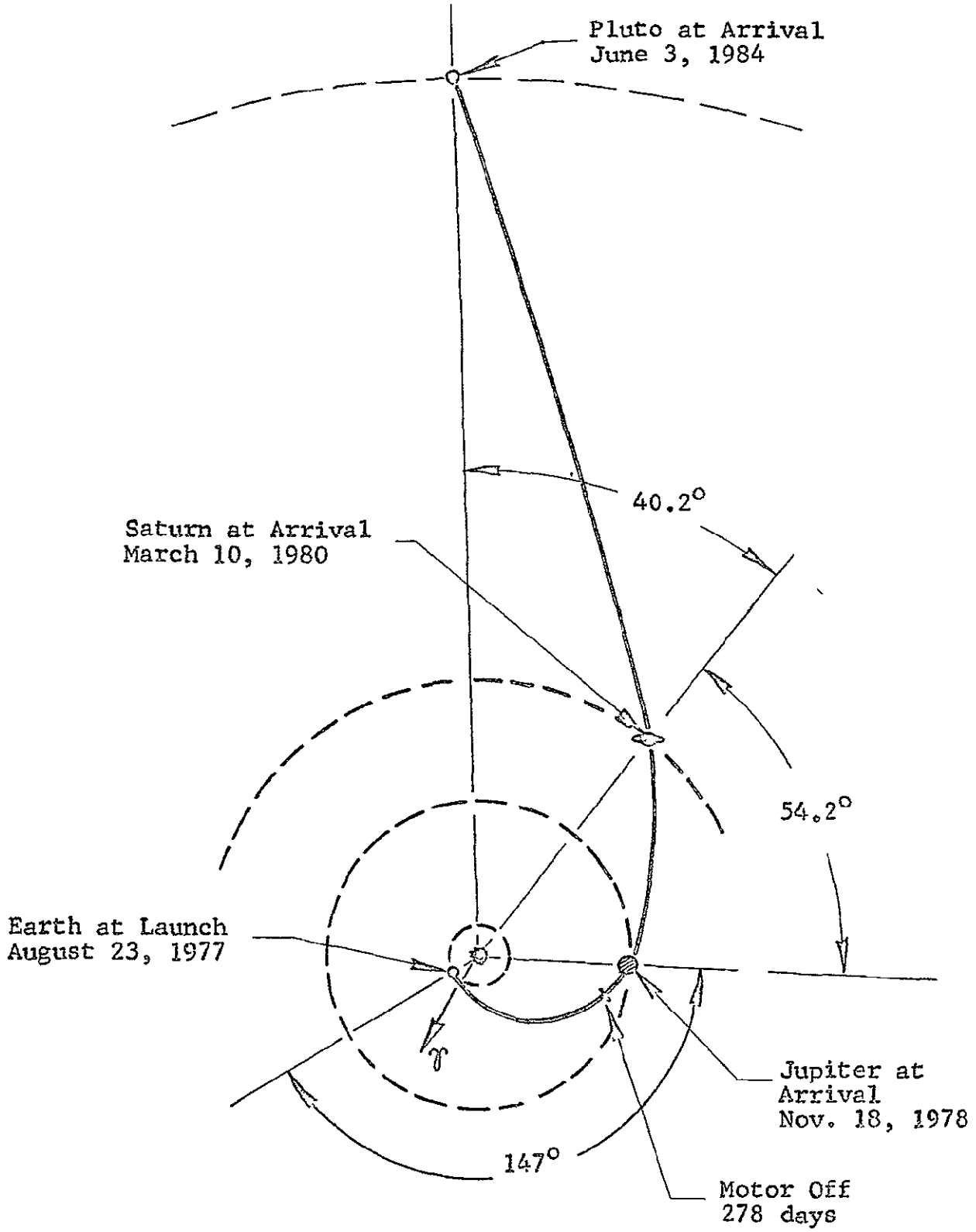

FIG. 31 - TYPICAL DIRECT MODE EARTH-JUPITER-SATURN-PLUTO "GRAND TOUR" FLIGHT PATH

in the ecliptic plane. As Figure 32 indicates, the required passage distances at Saturn for the trajectories of interest are sufficiently great to preclude problems due to the Saturn ring system. Details for the earth-Jupiter-Saturn portion of the mission profile were given in a previous section of the report. Optimum launch dates are the same as for the earth-Jupiter-Saturn missions. Figure 33 shows the payload-flight duration tradeoff for Titan 3X/Centaur booster. Note that launches in either 1977 or 1978 make possible delivery of payloads greater than 1000 Kg (2200 lb) in less than seven years with this launch vehicle. 1977 is the best launch year for flights of less than 9.3 years duration; 1976 launch gives higher payload for missions of greater than 9.3 years duration.

Figures 34 to 36 show curves of time of flight to Pluto versus launch date with payload as parameter for the 1976, 1977, and 1978 launch dates. These curves are for the Atlas SLV-3X/Centaur launches with direct flight mode. Indirect mode trajectories are represented in Figures 37 and 38 for the same boost vehicle system. Notice again the payload advantage exhibited by indirect mode trajectories as already discussed.

EARTH-JUPITER-URANUS-NEPTUNE GRAND TOUR

Figure 39 shows the flight path for a representative direct mode Neptune grand tour. Detailed data and optimum launch dates for the mission are discussed in the earth-Jupiter-Uranus section of the report. Figure 40 shows the required passage distance at Uranus for ballistic continuation to Neptune for the three possible launch years 1978, 1979, and 1980. All trajectories are type I, class I orbits representing minimum time of flight continuations. Figure 41 summarizes trajectory results for direct mode Neptune grand tours

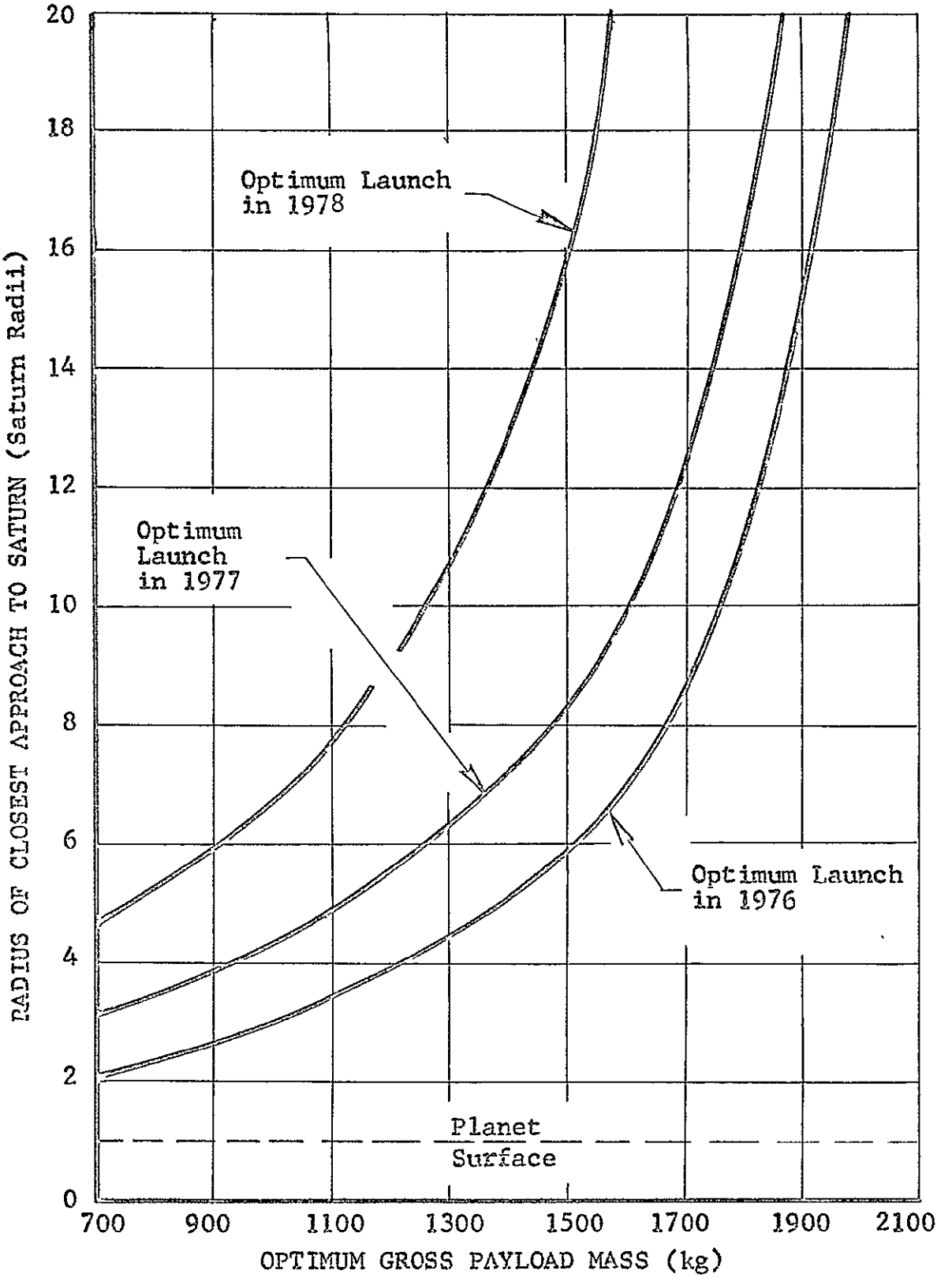

FIG. 32 - RADIUS OF CLOSEST APPROACH TO SATURN FOR EARTH-JUPITER-SATURN-PLUTO "GRAND TOUR" MISSIONS. TITAN/CENTAUR DIRECT.

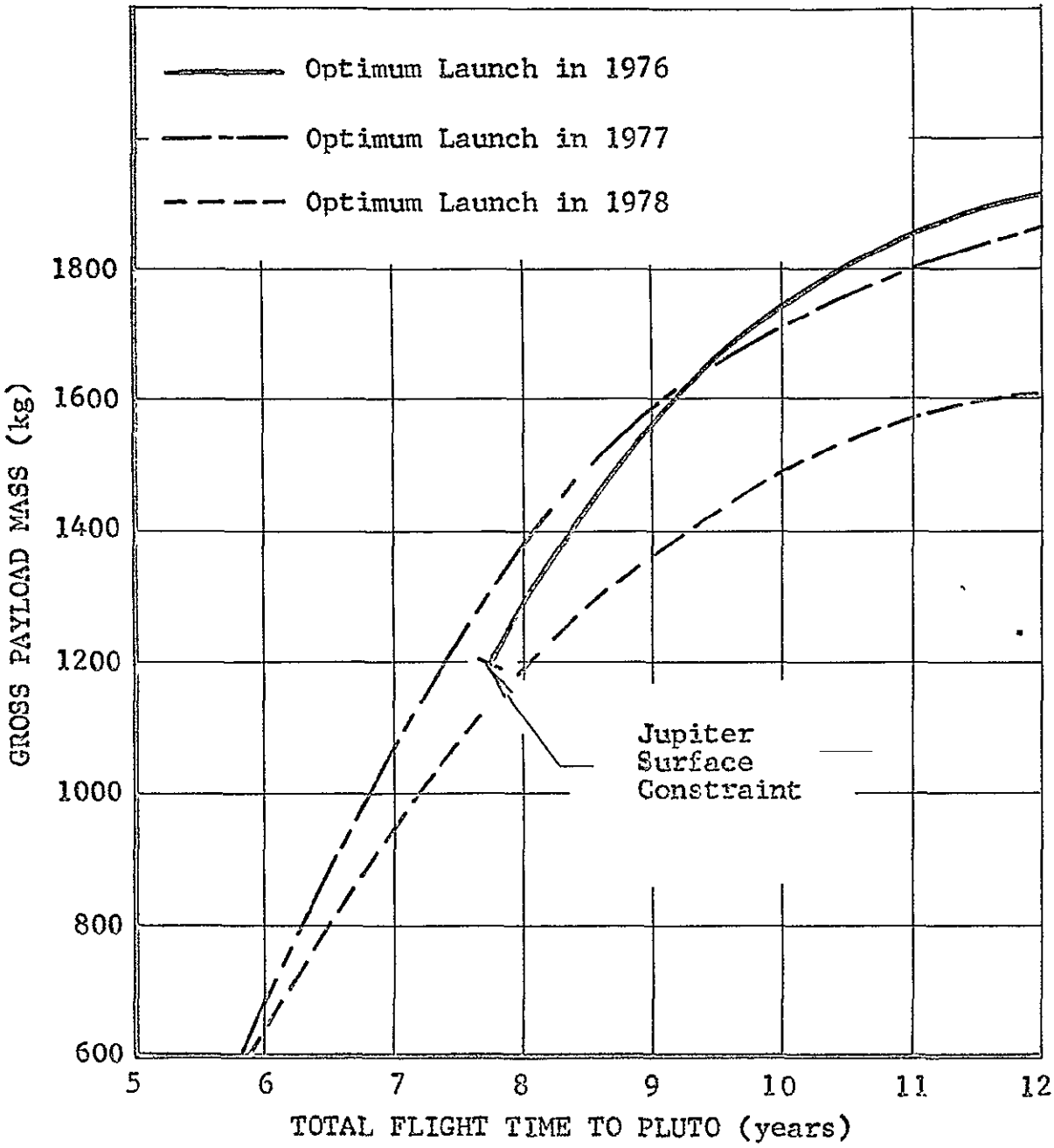

FIG. 33 - PAYLOAD - TRIP TIME TRADEOFF FOR EARTH-JUPITER-SATURN-PLUTO "GRAND TOUR" MISSION. TITAN/CENTAUR LAUNCH VEHICLE. DIRECT TRAJECTORY MODE.

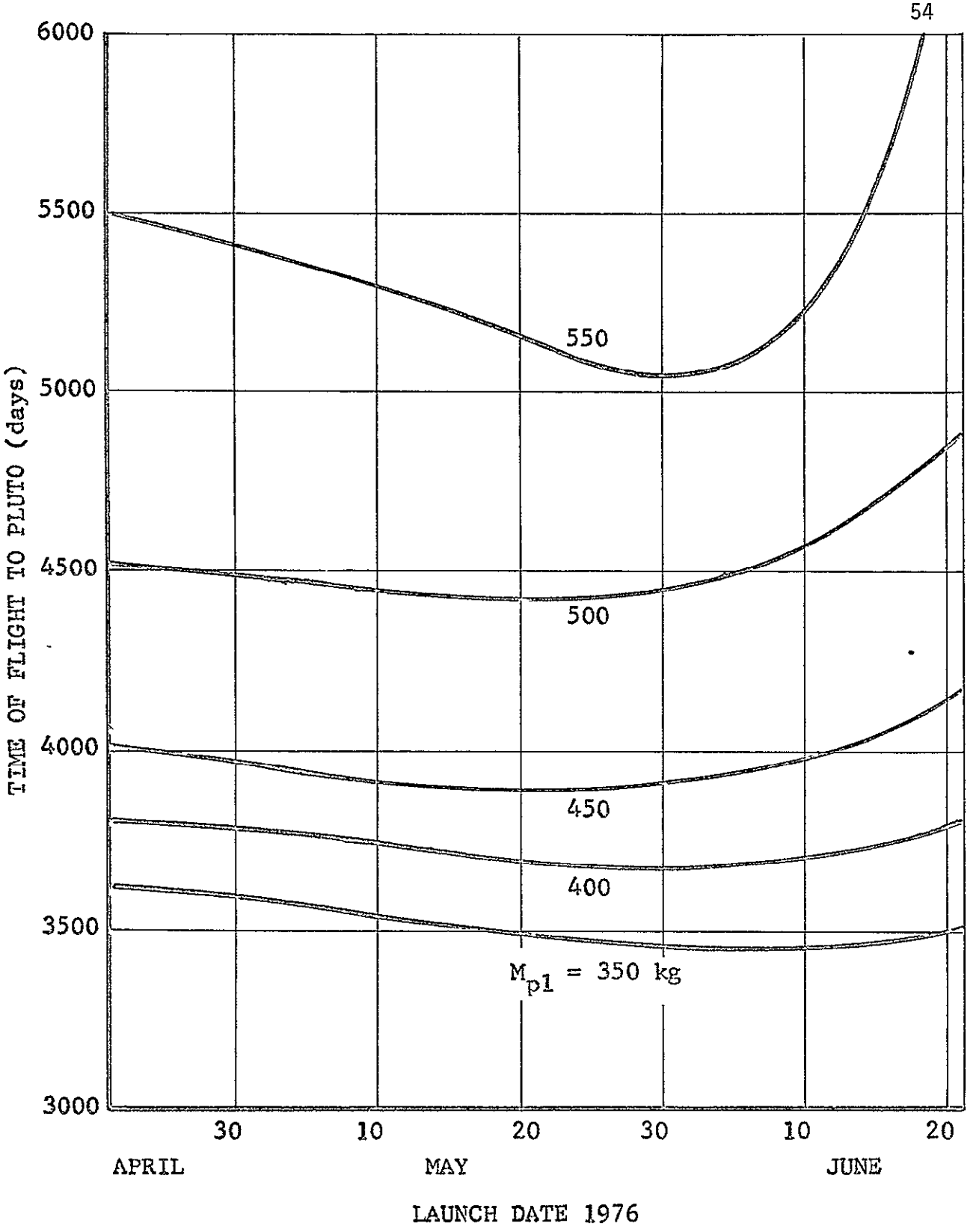

FIG. 34 - FLIGHT DURATION VS LAUNCH DATE FOR 1976 EARTH-JUPITER-SATURN-PLUTO "GRAND TOUR" MISSION. Atlas SLV3X/ Centaur LAUNCH VEHICLE. DIRECT MODE.

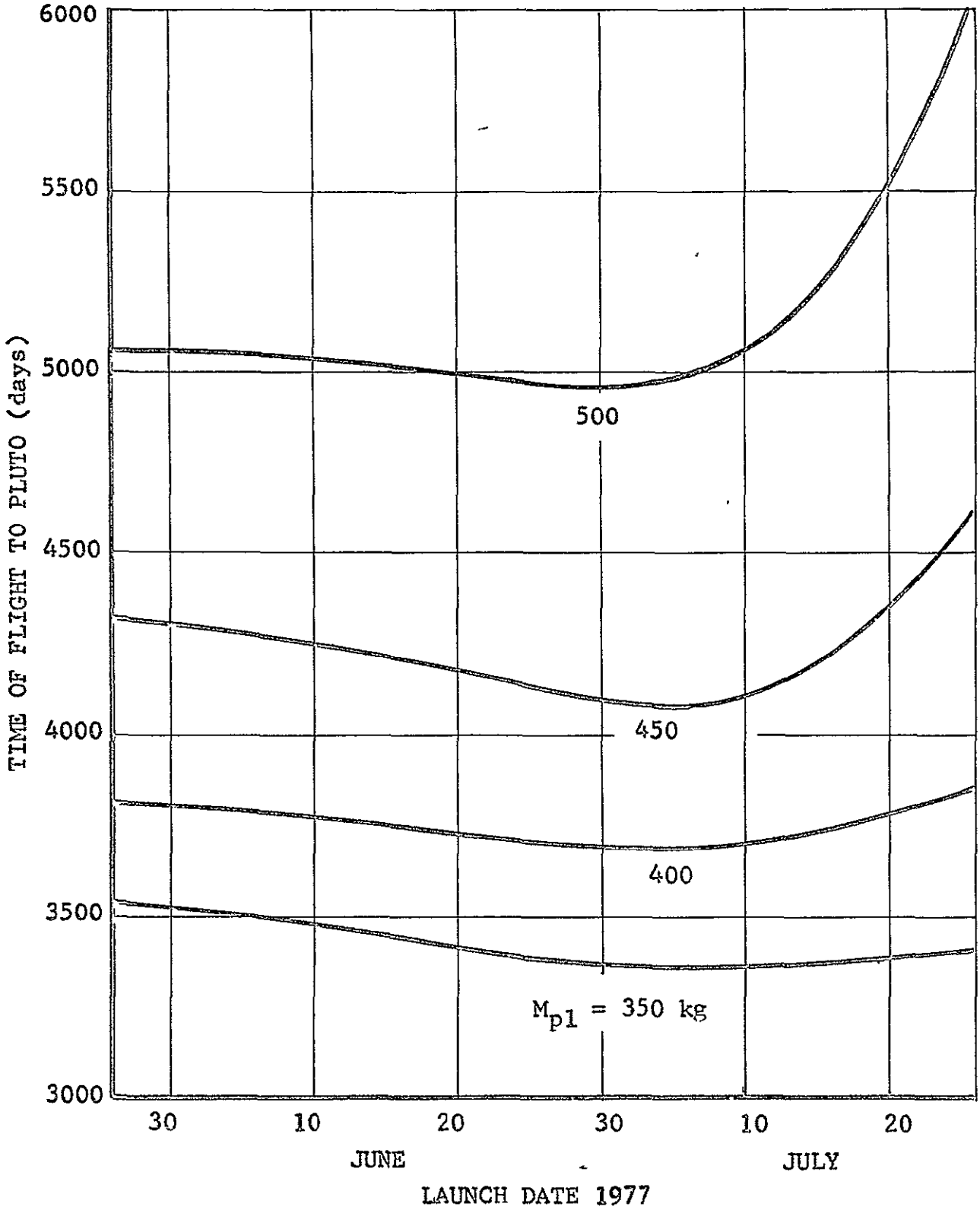

FIG. 35 - FLIGHT DURATION VS LAUNCH DATE FOR 1977 EARTH-JUPITER-SATURN-PLUTO "GRAND TOUR" MISSION. ATLAS SLV3X/ CENTAUR LAUNCH VEHICLE. DIRECT MODE.

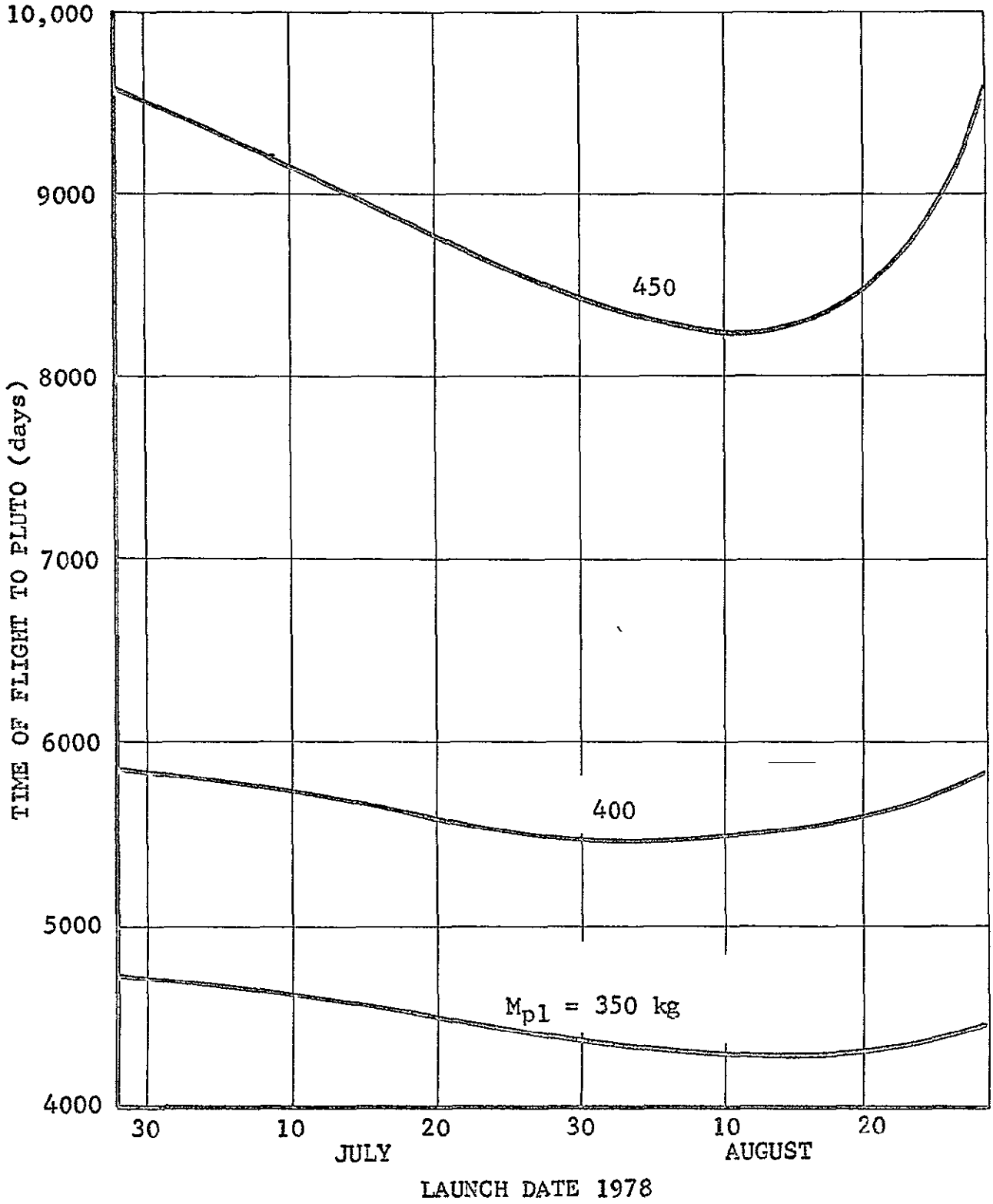

FIG. 36 - FLIGHT DURATION VS LAUNCH DATE FOR 1978 EARTH-JUPITER-SATURN-PLUTO "GRAND TOUR" MISSION. ATLAS SLV-3X/CENTAUR DIRECT MODE.

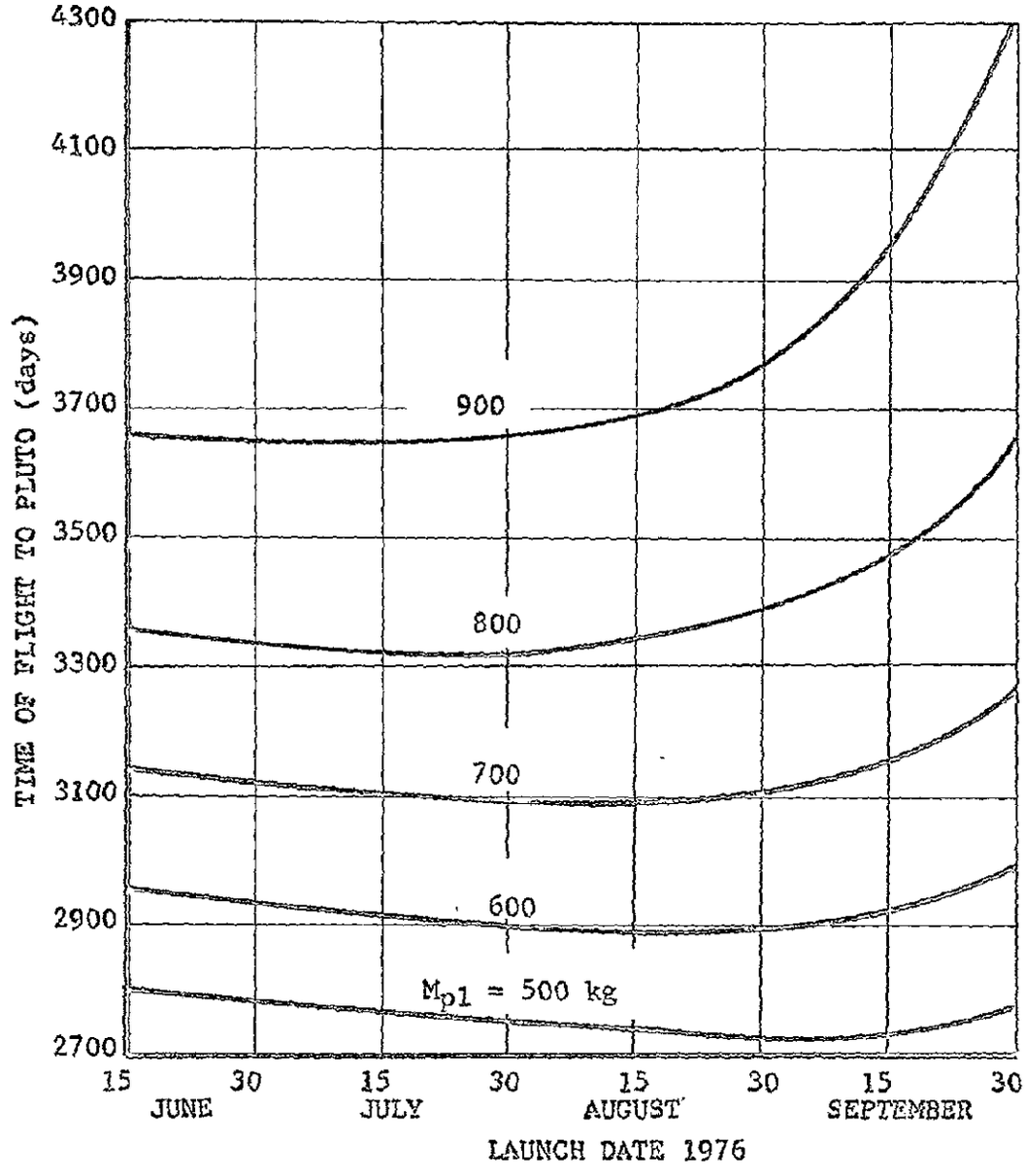

FIG. 37 - FLIGHT DURATION VS LAUNCH DATE FOR 1976 EARTH-JUPITER-SATURN-PLUTO "GRAND TOUR" MISSION, ATLAS SLV-3X/CENTAUR INDIRECT MODE.

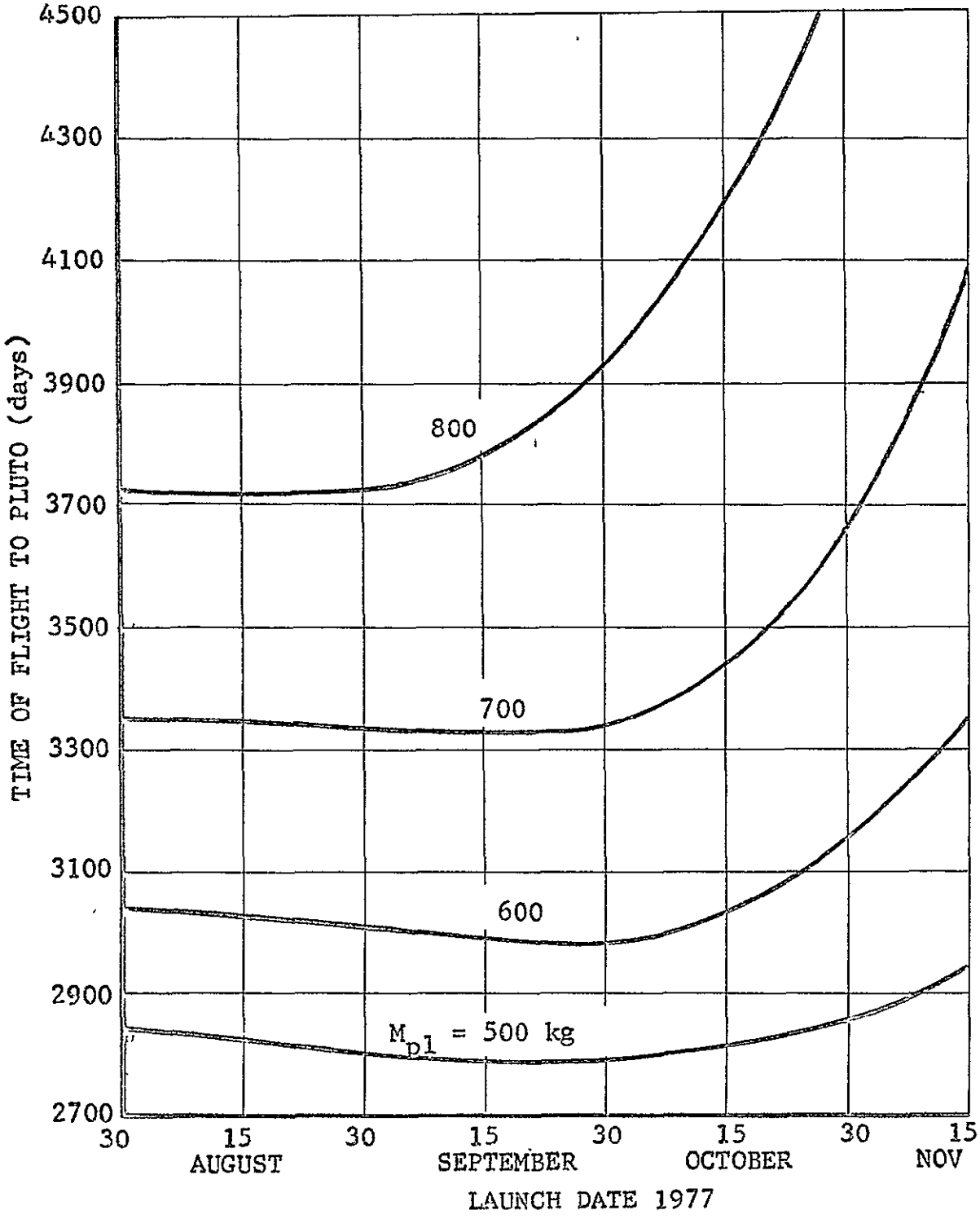

FIG. 38 - FLIGHT DURATION VS LAUNCH DATE FOR 1977 EARTH-JUPITER-SATURN-PLUTO "GRAND TOUR" MISSION. ATLAS SLV-3X/CENTAUR INDIRECT MODE.

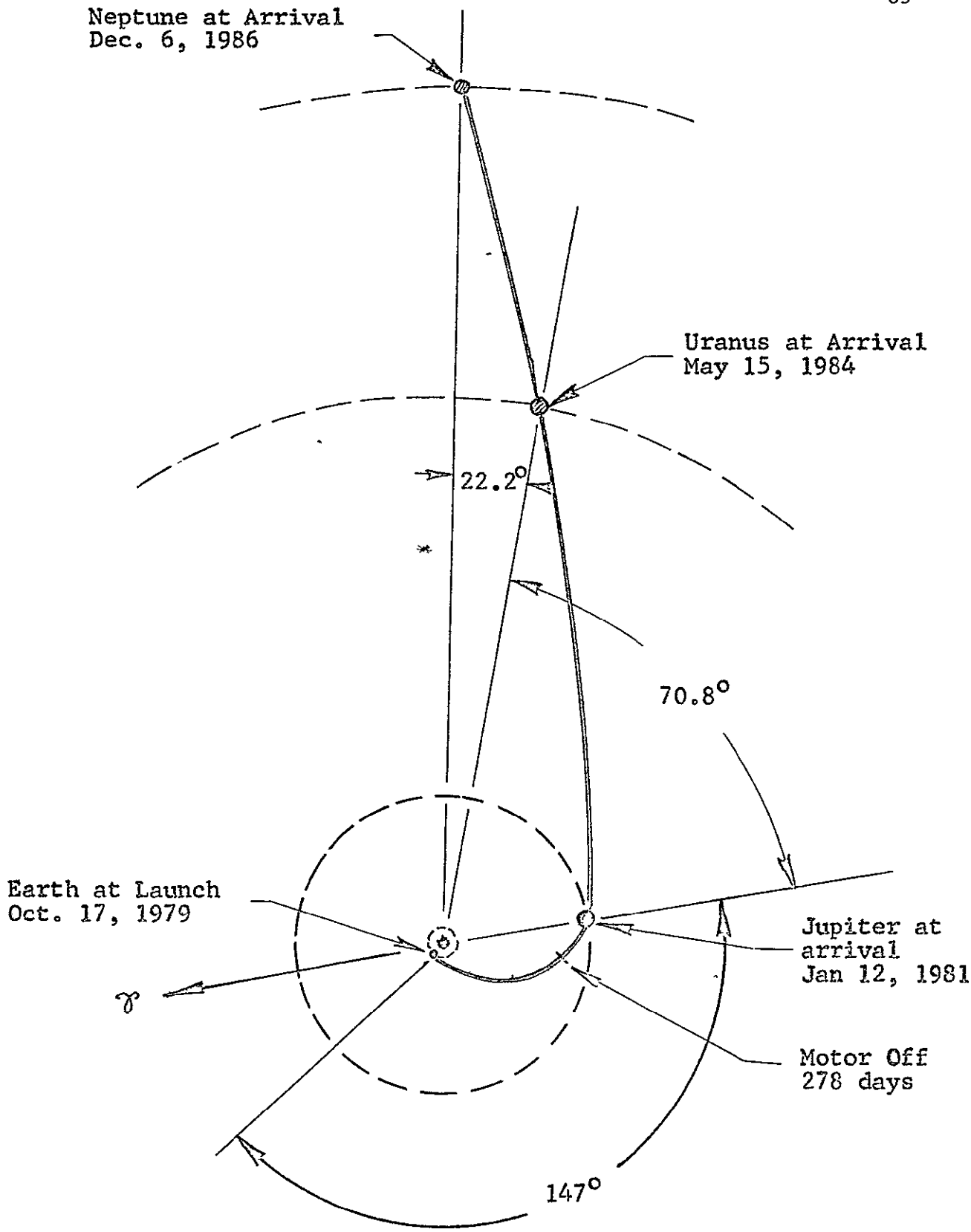

FIG. 39 - TYPICAL DIRECT MODE EARTH-JUPITER-URANUS-NEPTUNE "GRAND TOUR" FLIGHT PATH.

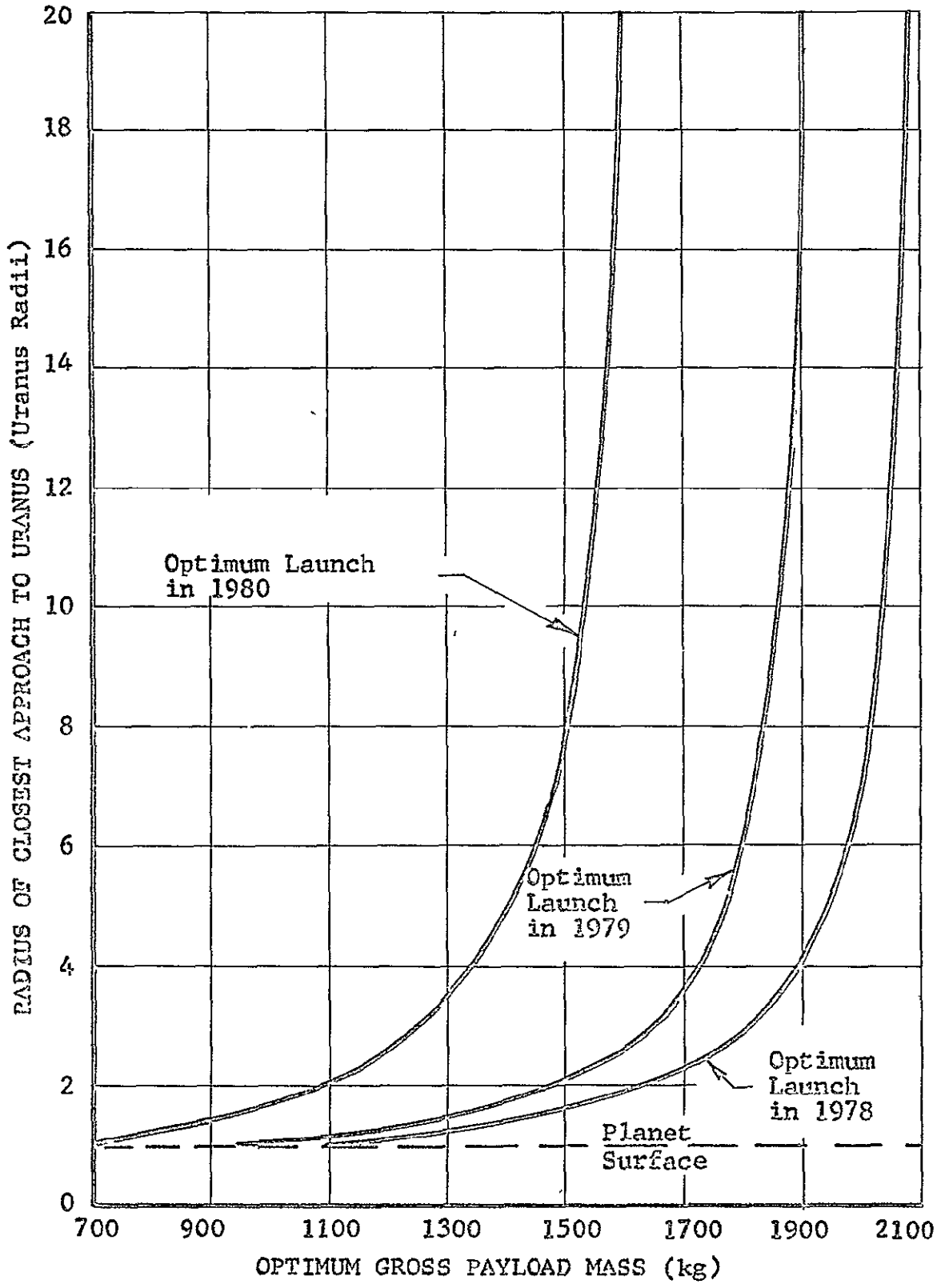

FIG. 40 - RADIUS OF CLOSEST APPROACH TO URANUS FOR EARTH-JUPITER-URANUS-NEPTUNE "GRAND TOUR" MISSIONS TITAN 3X/CENTAUR LAUNCH VEHICLE, DIRECT MODE.

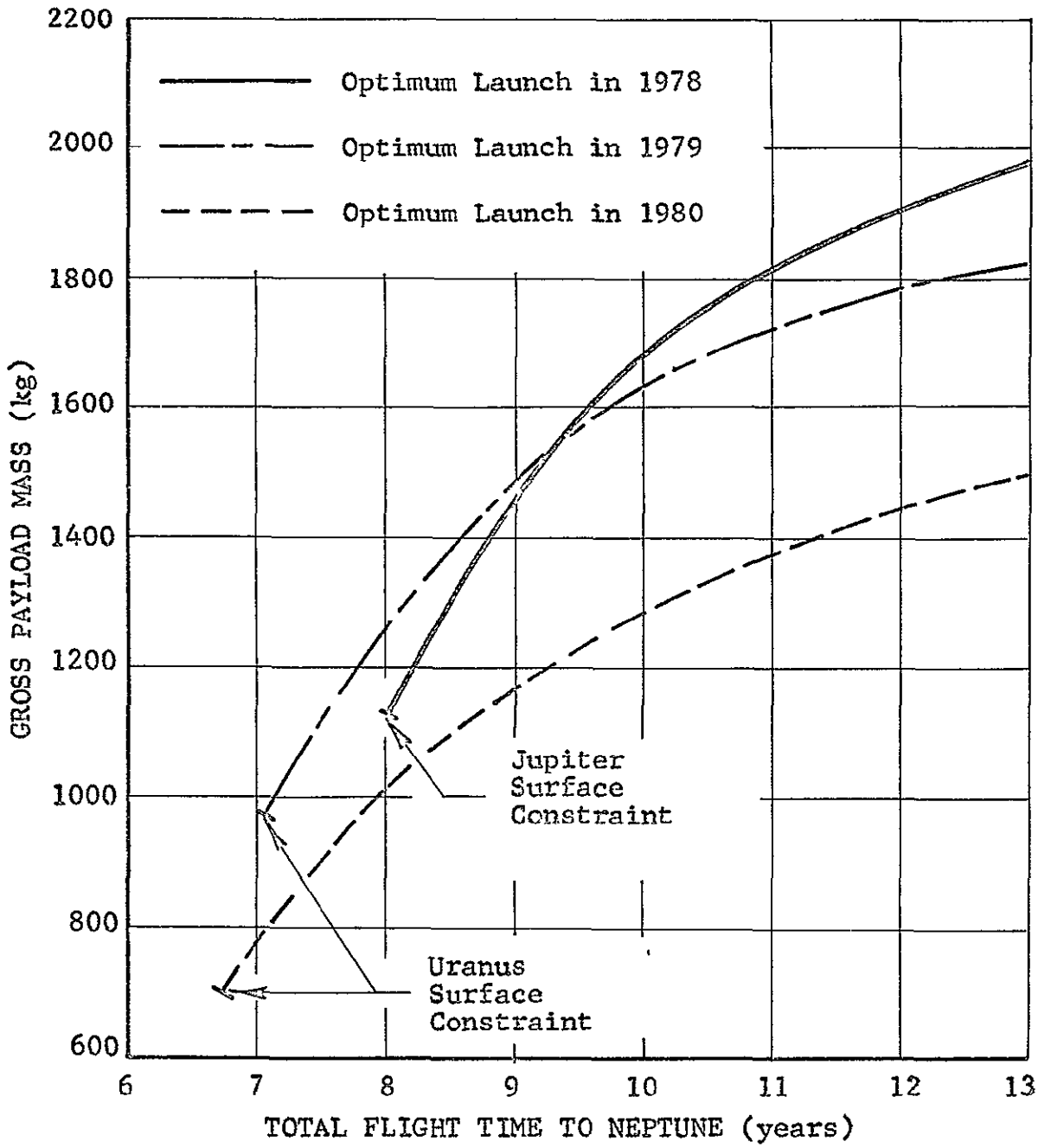

FIG. 41 - PAYLOAD - TRIP TIME TRADEOFF FOR EARTH-JUPITER-URANUS-NEPTUNE "GRAND TOUR" MISSION.
TITAN 3X/CENTAUR LAUNCH VEHICLE, DIRECT MODE.

utilizing the Titan/Centaur launch vehicle. For total flight duration of less than 9.3 years, the best launch year is 1979. However, there exists an Uranus surface constraint due to required deflection angle at Uranus for continuation to Neptune for the 1979 launches which precludes flights launched in that year of less than seven years duration. It is possible to launch in 1978 with flight time as low as 6.7 years at which point the Uranus surface constraint is interposed. For flight duration of greater than 9.3 years, the optimum launch year is 1978.

Plotted in Figures 42 and 43 are flight time versus launch date at earth for 1978 and 1979 Neptune grand tour missions utilizing the Atlas/Centaur launchers and direct solar electric trajectory mode. Figure 44 gives similar data for the 1978 indirect mode which year represents the best launch opportunity involving that mission mode.

The kinetic energy of the spacecraft at any time after Jupiter encounter in any of the trajectories discussed in the previous sections of the report exceeds that required for solar system escape; outer planet missions could well be continued after the final planetary encounters with Pluto or Neptune as galactic probes.

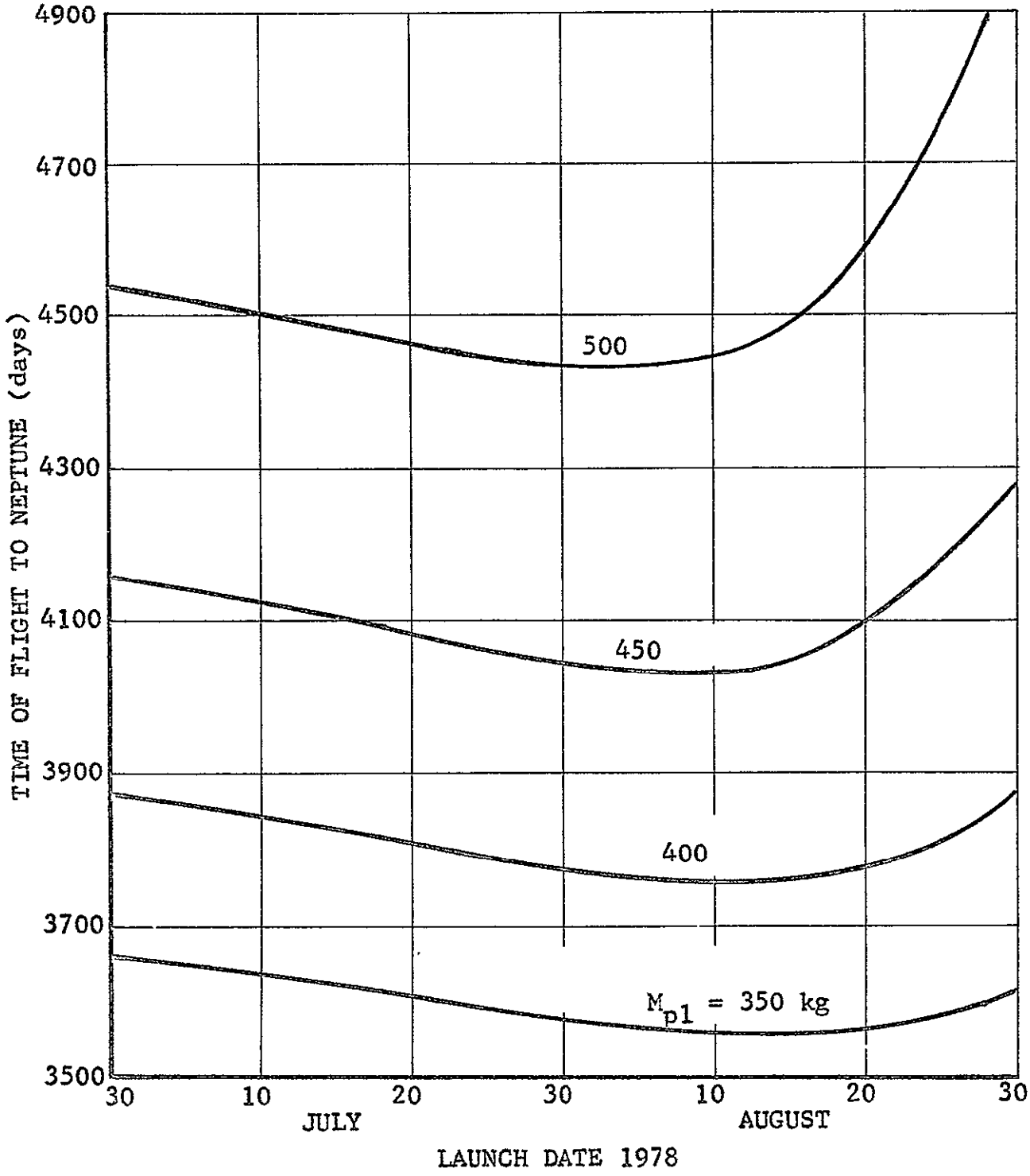

FIG. 42 - FLIGHT DURATION VS LAUNCH DATE FOR 1978 EARTH-JUPITER URANUS-NEPTUNE "GRAND TOUR" MISSION. ATLAS SLV-3X/ CENTAUR LAUNCH VEHICLE, DIRECT MODE.

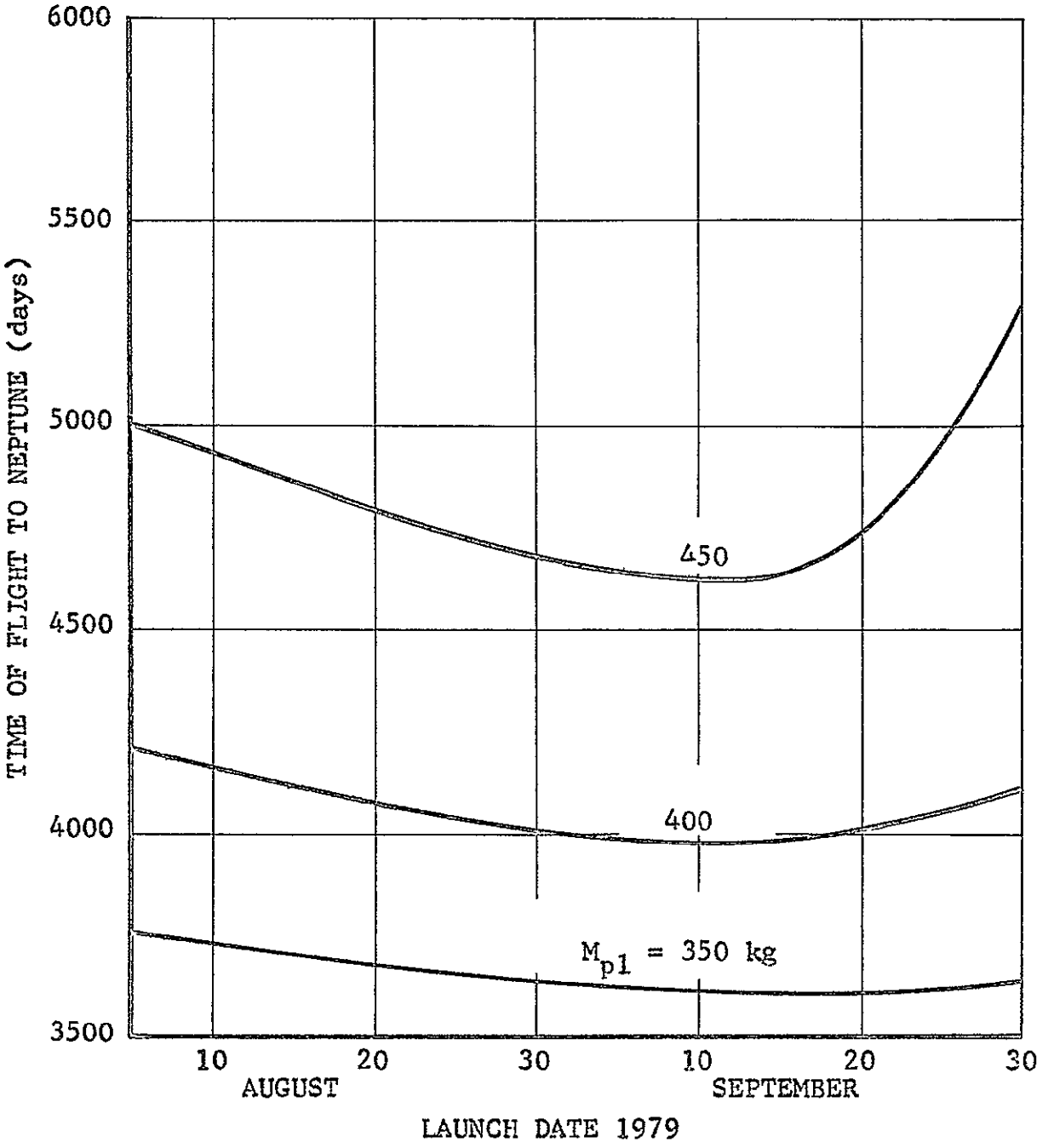

FIG. 43 - FLIGHT DURATION VS LAUNCH DATE FOR 1979 EARTH-JUPITER-URANUS-NEPTUNE "GRAND TOUR" MISSION. ATLAS SLV-3X/CENTAUR DIRECT MODE.

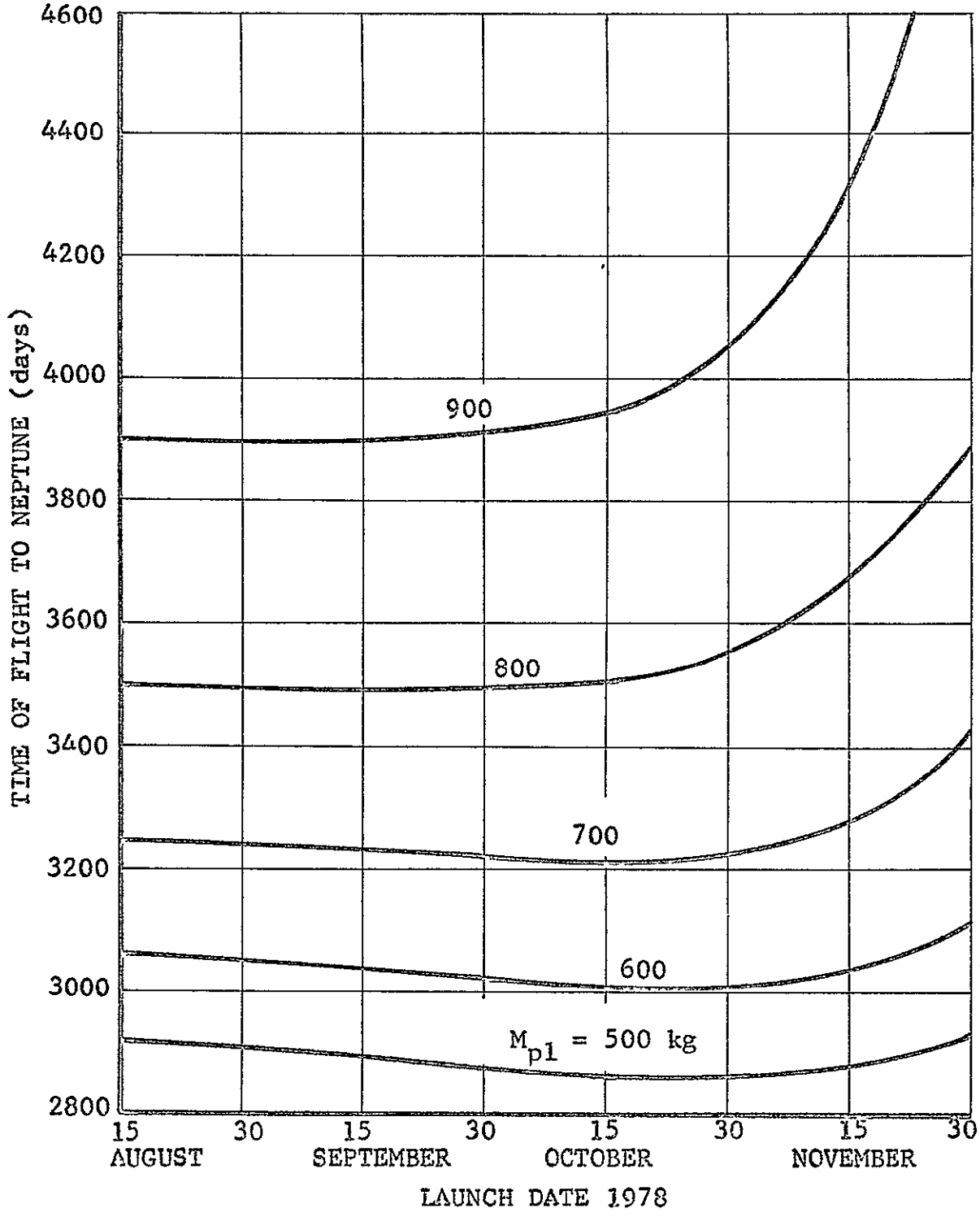

FIG. 44 - FLIGHT DURATION VS LAUNCH DATE FOR 1978 EARTH-JUPITER-URANUS-NEPTUNE "GRAND TOUR" MISSION. ATLAS SLV-3X/CENTAUR, INDIRECT MODE.

CONCLUSIONS

It has been shown that significant performance advantage results from application of optimized solar electric low thrust propulsion to the initial leg of Jupiter swingby missions to the outer planets. The indirect mode of solar electric flight with its initial close passage of the sun yields best payload performance at the expense of spacecraft design complications. Gross payload is typically tripled at the target by incorporation of electric propulsion.

Performance data for the mission designs considered herein are summarized in Figures 45 through 48. Optimum launch years, time of flight, and payload for each mission are represented for earth-Jupiter-Saturn, earth-Jupiter-Uranus, earth-Jupiter-Saturn-Pluto and earth-Jupiter-Uranus-Neptune flights. Notice again that the entire outer solar system is opened to unmanned exploration by the combined use of solar-electric propulsion and the intermediate planet swingby technique. Two spacecraft of more than 1000 Kg (2200 lb) payload launched in the 1977-1979 period could reach Saturn within 2.4 years, Uranus within 4.6 years, and Neptune and Pluto within seven years. Only launch vehicle systems which are already "off-the-shelf" items are required for this exploration.

The ultimate feasibility of complex space missions of the type described herein will depend on advances in guidance of low thrust vehicles, improved reliability of electric propulsion systems, and solution of spacecraft design problems posed by application of continuous propulsion. Solution of these problems will make possible the unmanned exploration of the entire solar system with launch vehicles of moderate size.

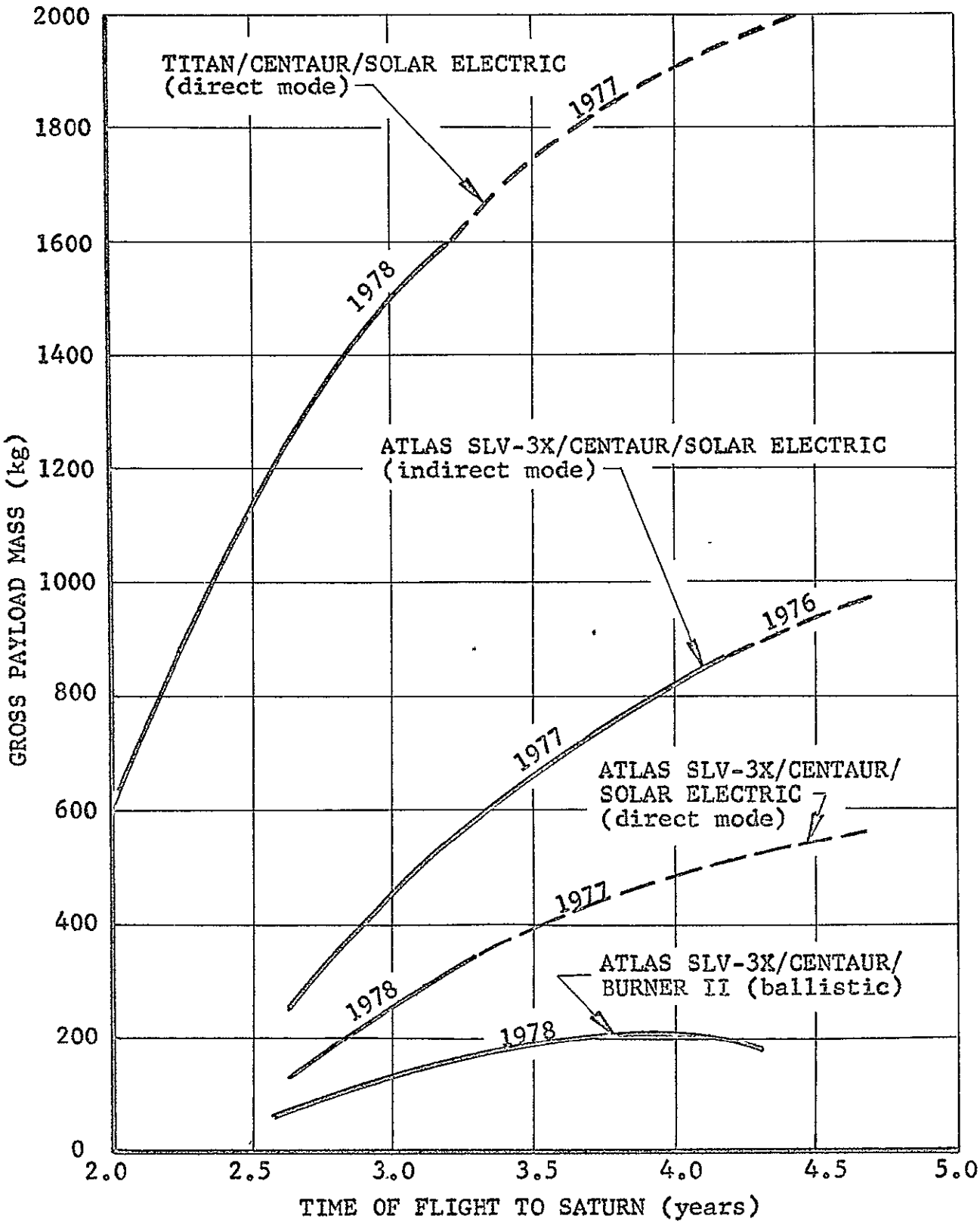

FIG. 45 - GROSS PAYLOAD VS TIME OF FLIGHT FOR OPTIMUM EARTH-JUPITER-SATURN SOLAR ELECTRIC MISSIONS

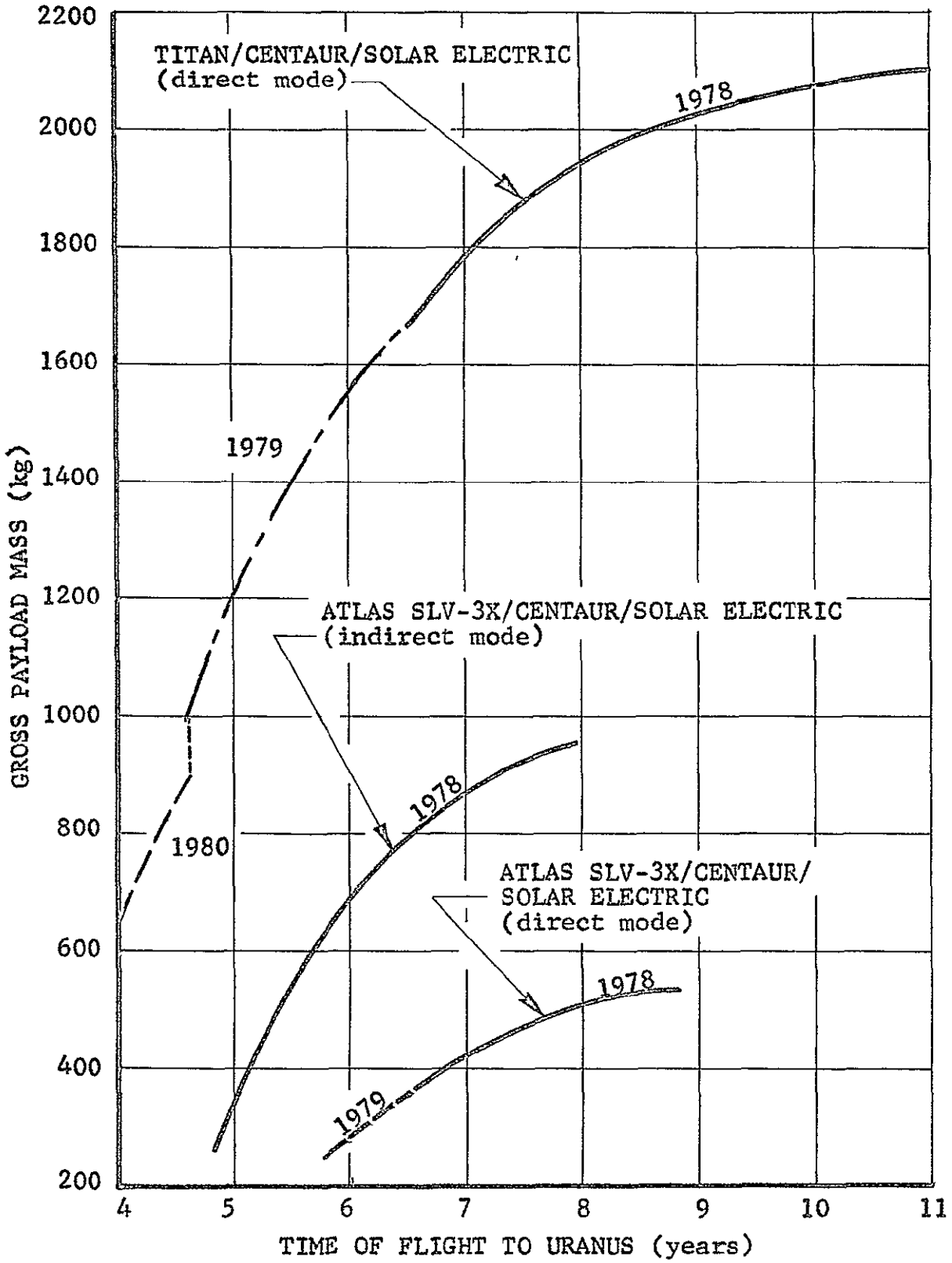

FIG. 46 - GROSS PAYLOAD VS TIME OF FLIGHT FOR OPTIMUM EARTH-JUPITER-URANUS SOLAR ELECTRIC MISSIONS

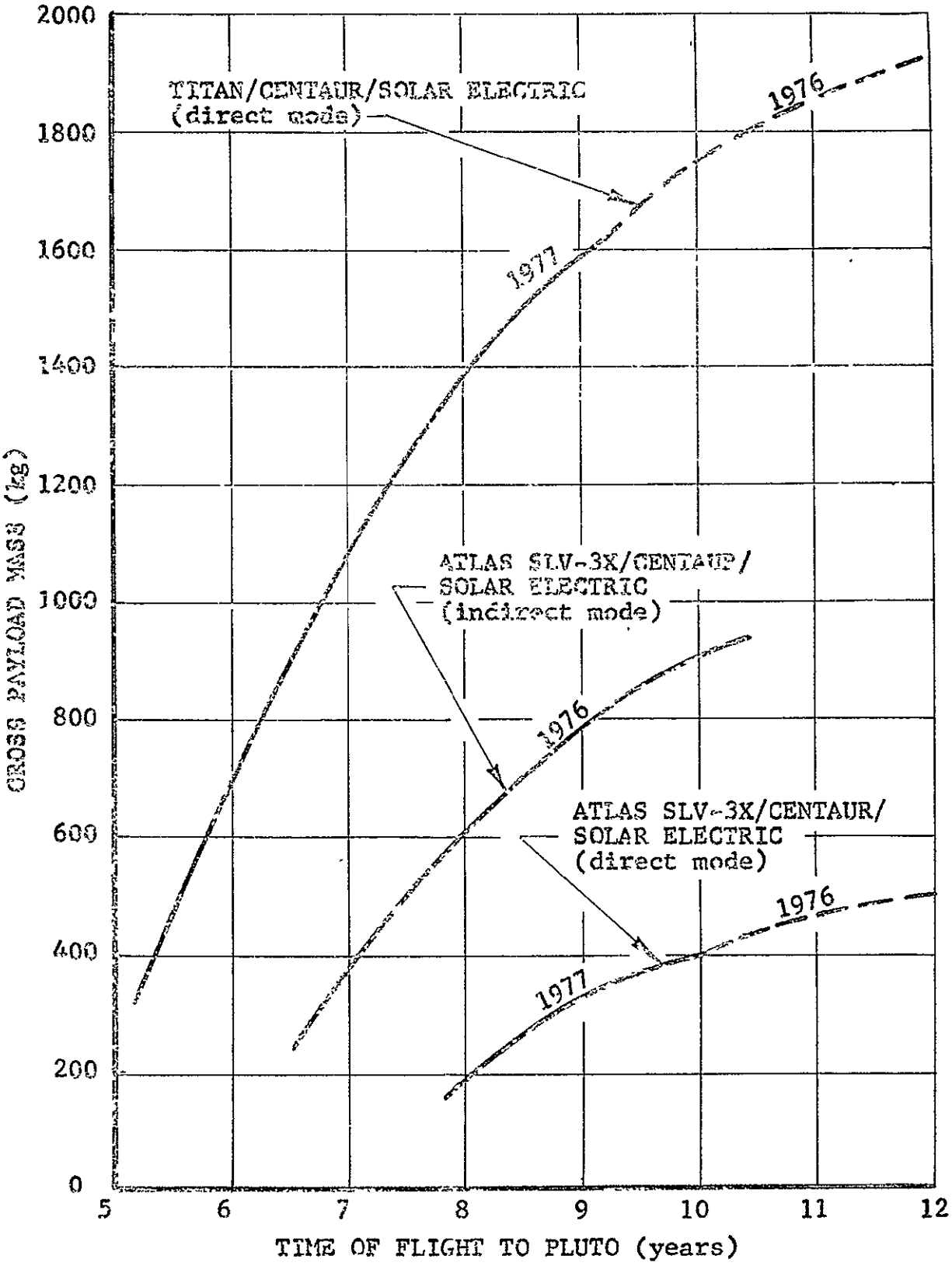

FIG. 47 - GROSS PAYLOAD VS TIME OF FLIGHT FOR OPTIMUM EARTH-JUPITER-SATURN-PLUTO SOLAR ELECTRIC "GRAND TOUR" MISSIONS.

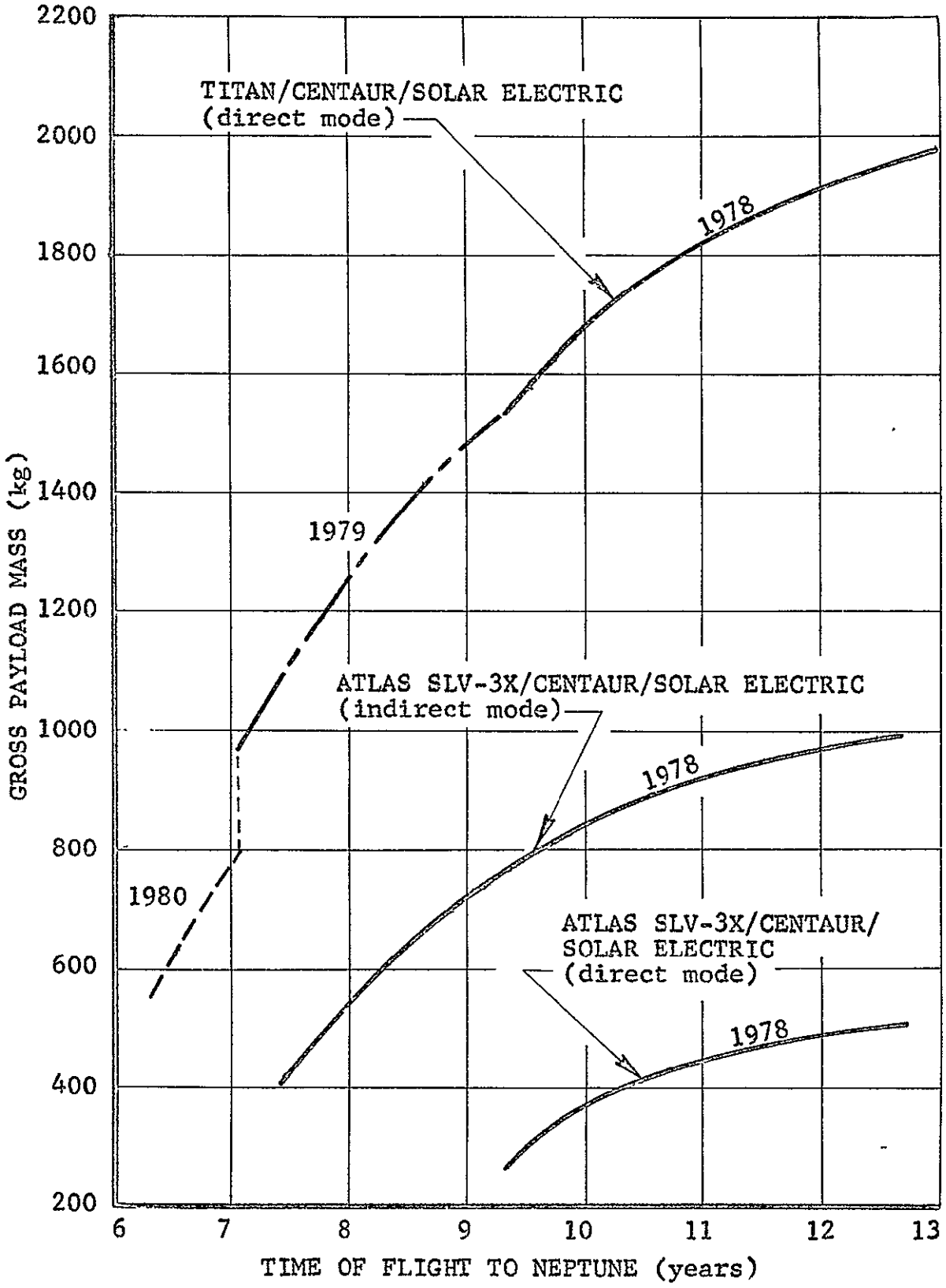

FIG. 48 - GROSS PAYLOAD VS TIME OF FLIGHT FOR OPTIMUM EARTH-JUPITER-URANUS-NEPTUNE SOLAR ELECTRIC "GRAND TOUR" MISSIONS.

APPENDIX 1

Basic Low Thrust Trajectory Data for Optimum Solar Electric Flight to Jupiter Utilizing Titan/Centaur Launch Vehicle

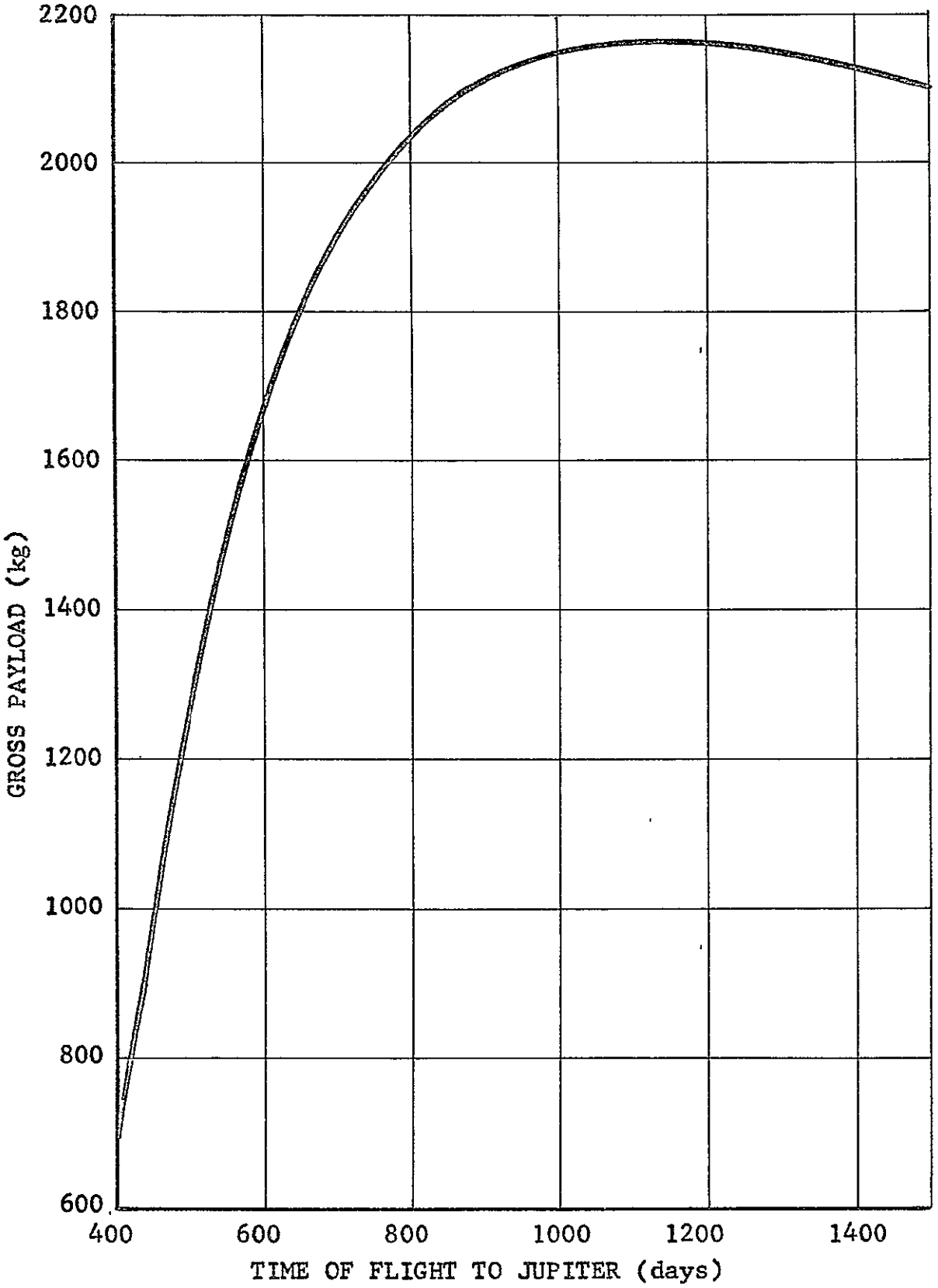

Fig. A.1 - GROSS PAYLOAD VS. TIME OF FLIGHT TO JUPITER
TITAN 3X(1205)/CENTAUR, DIRECT MODE.

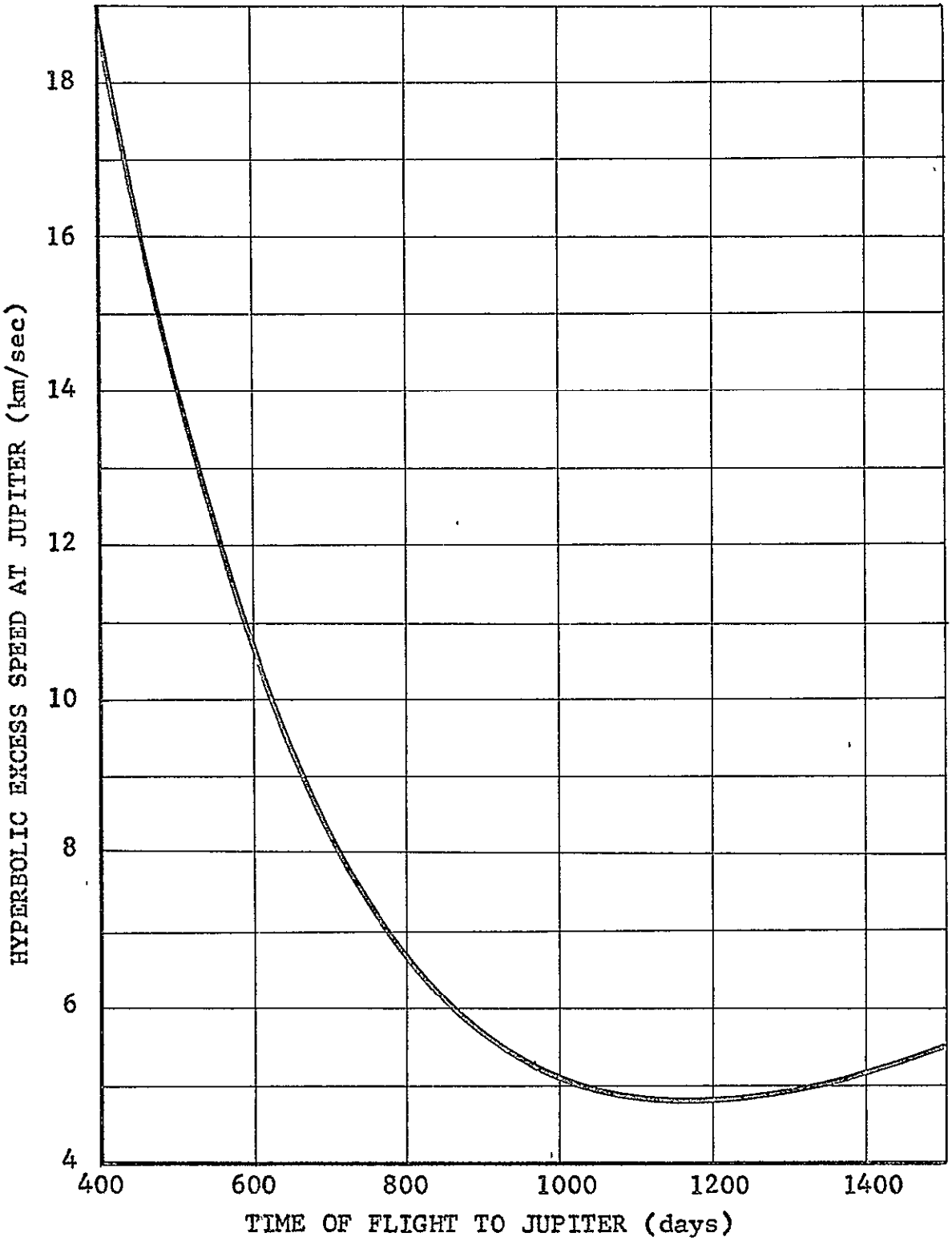

FIG. A.2 - HYPERBOLIC EXCESS SPEED AT JUPITER VS TIME OF FLIGHT TO JUPITER. TITAN/CENTAUR, DIRECT MODE

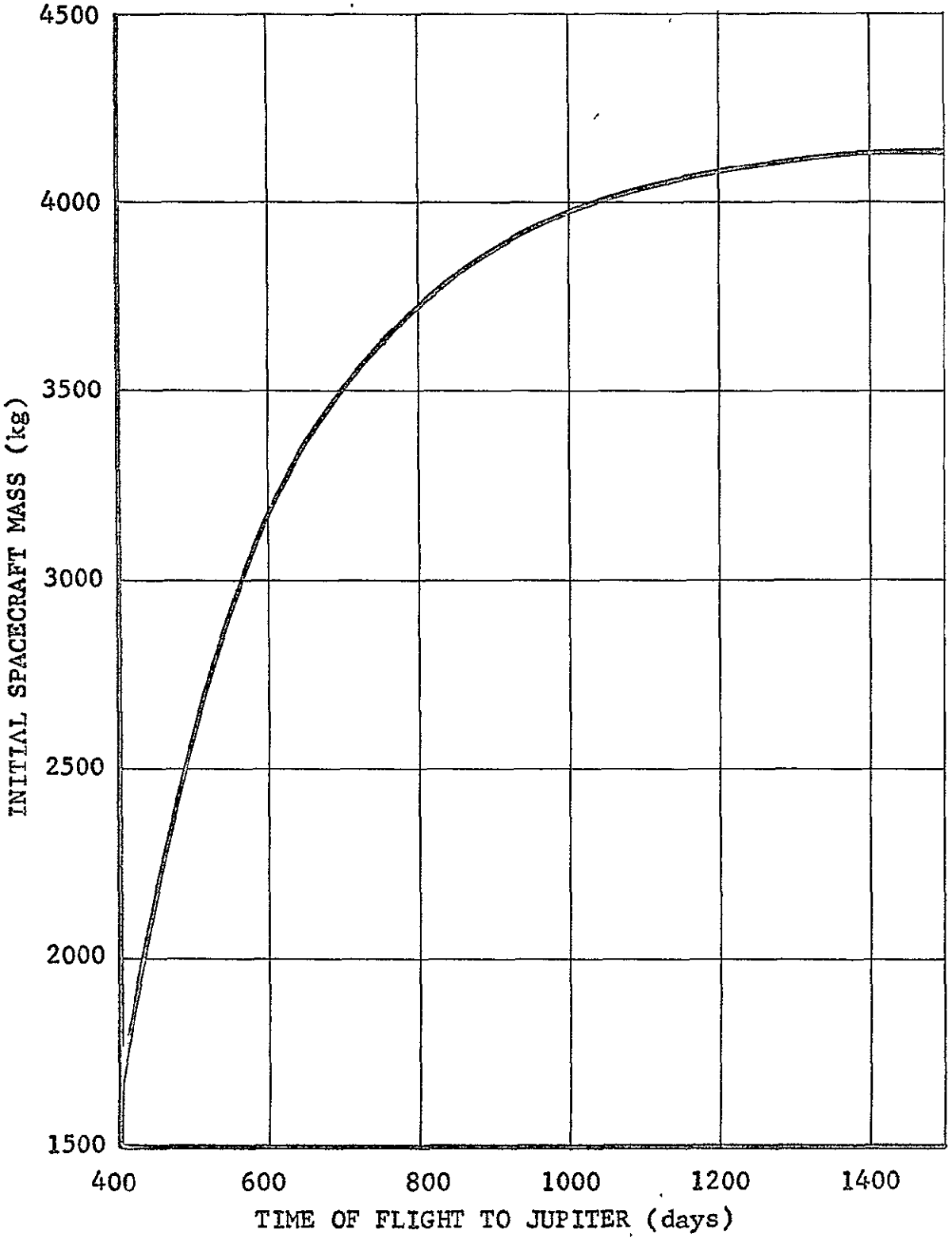

FIG. A.3 - INITIAL SPACECRAFT MASS VS TIME OF FLIGHT TO JUPITER. TITAN 3X/CENTAUR, DIRECT MODE.

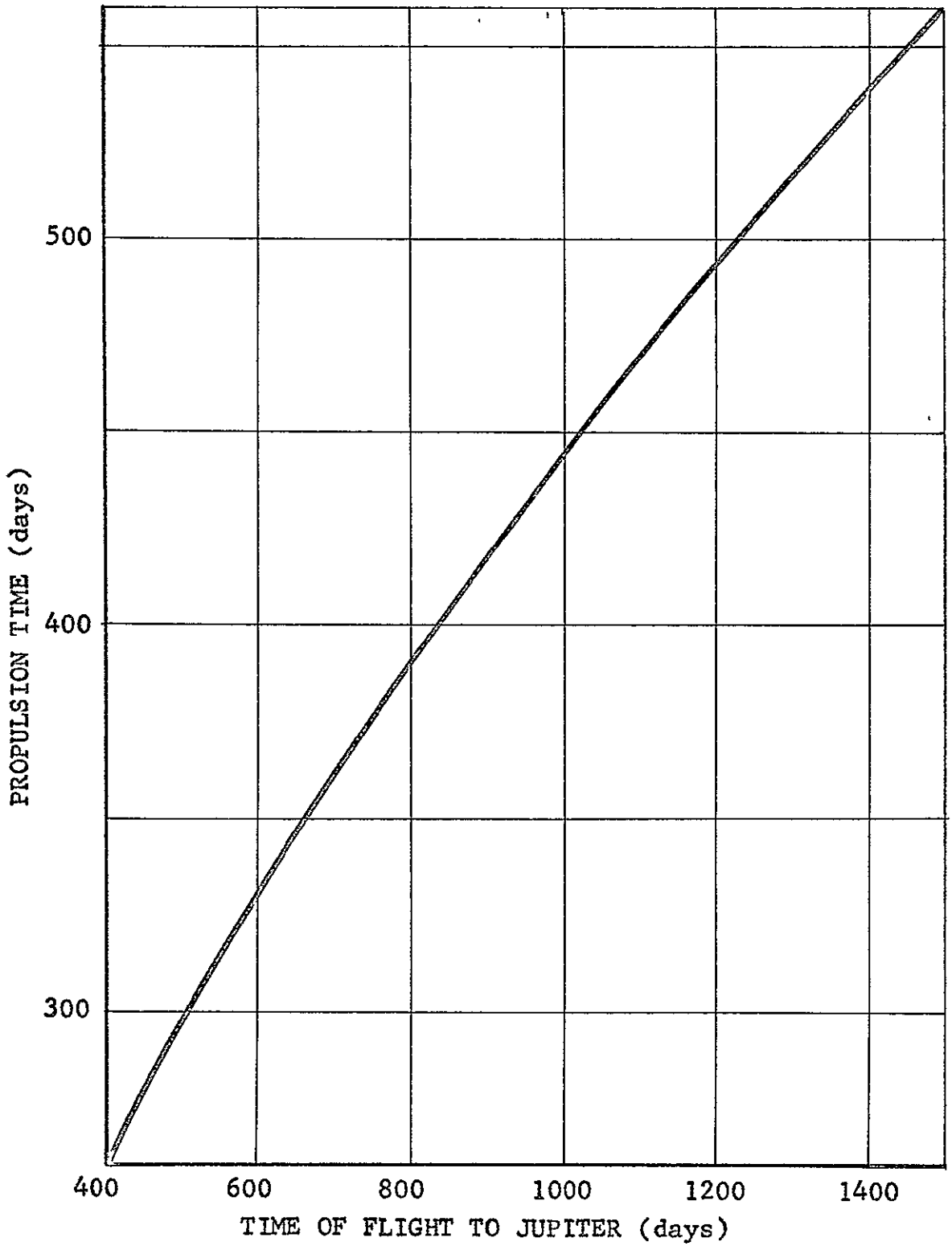

FIG. A.4 - TOTAL PROPULSION TIME VS TIME OF FLIGHT TO JUPITER. TITAN 3X(1205)/CENTAUR, DIRECT MODE.

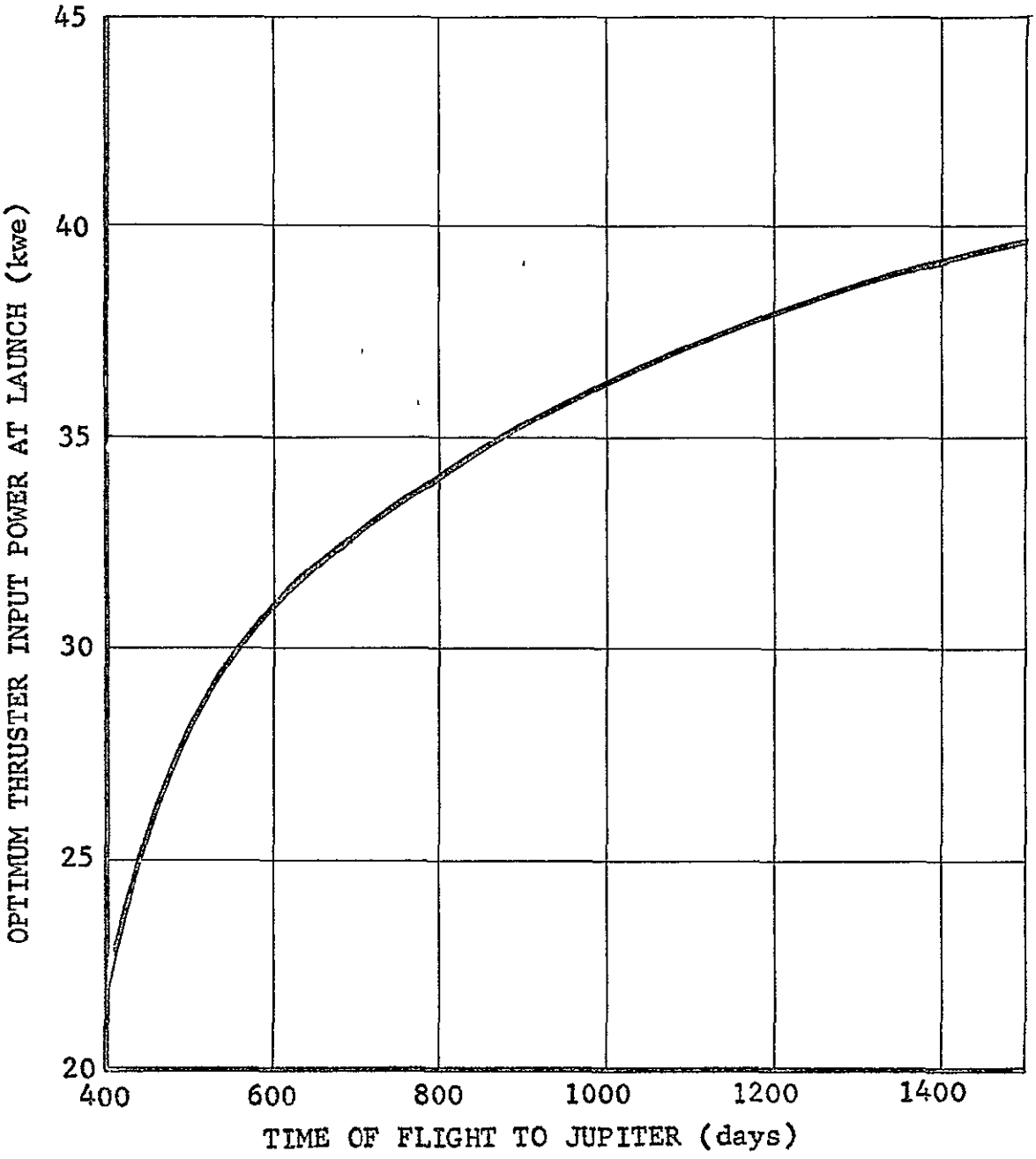

FIG. A.5 - OPTIMUM THRUSTER INPUT POWER AT LAUNCH VS TIME OF FLIGHT TO JUPITER. TITAN/CENTAUR DIRECT MODE.

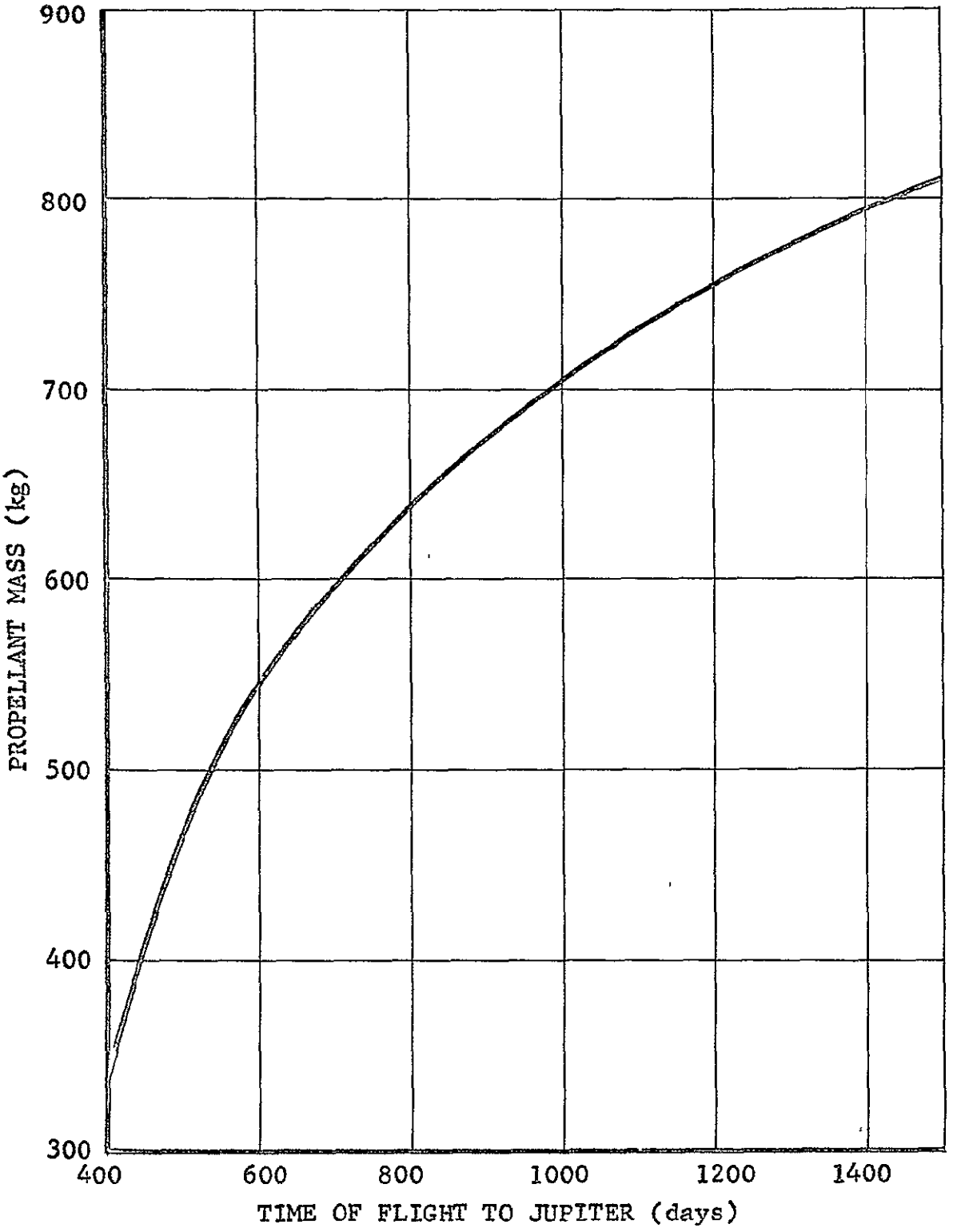

FIG. A.6 - PROPELLANT MASS VS TIME OF FLIGHT TO JUPITER
TITAN 3X(1205)/CENTAUR, DIRECT MODE.

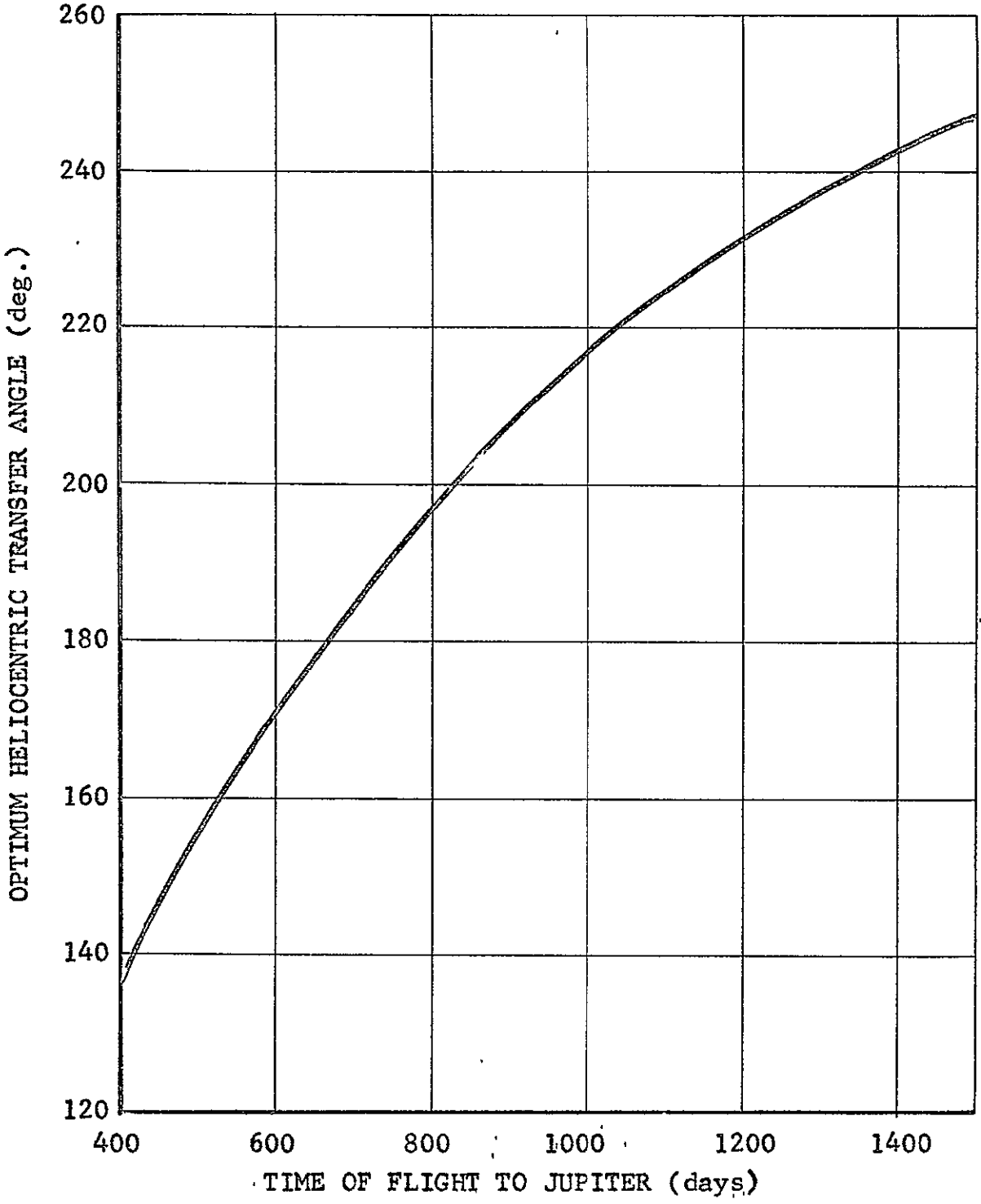

FIG. A.7 - OPTIMUM HELIOCENTRIC TRANSFER ANGLE VS TIME OF FLIGHT TO JUPITER. TITAN/CENTAUR DIRECT MODE.

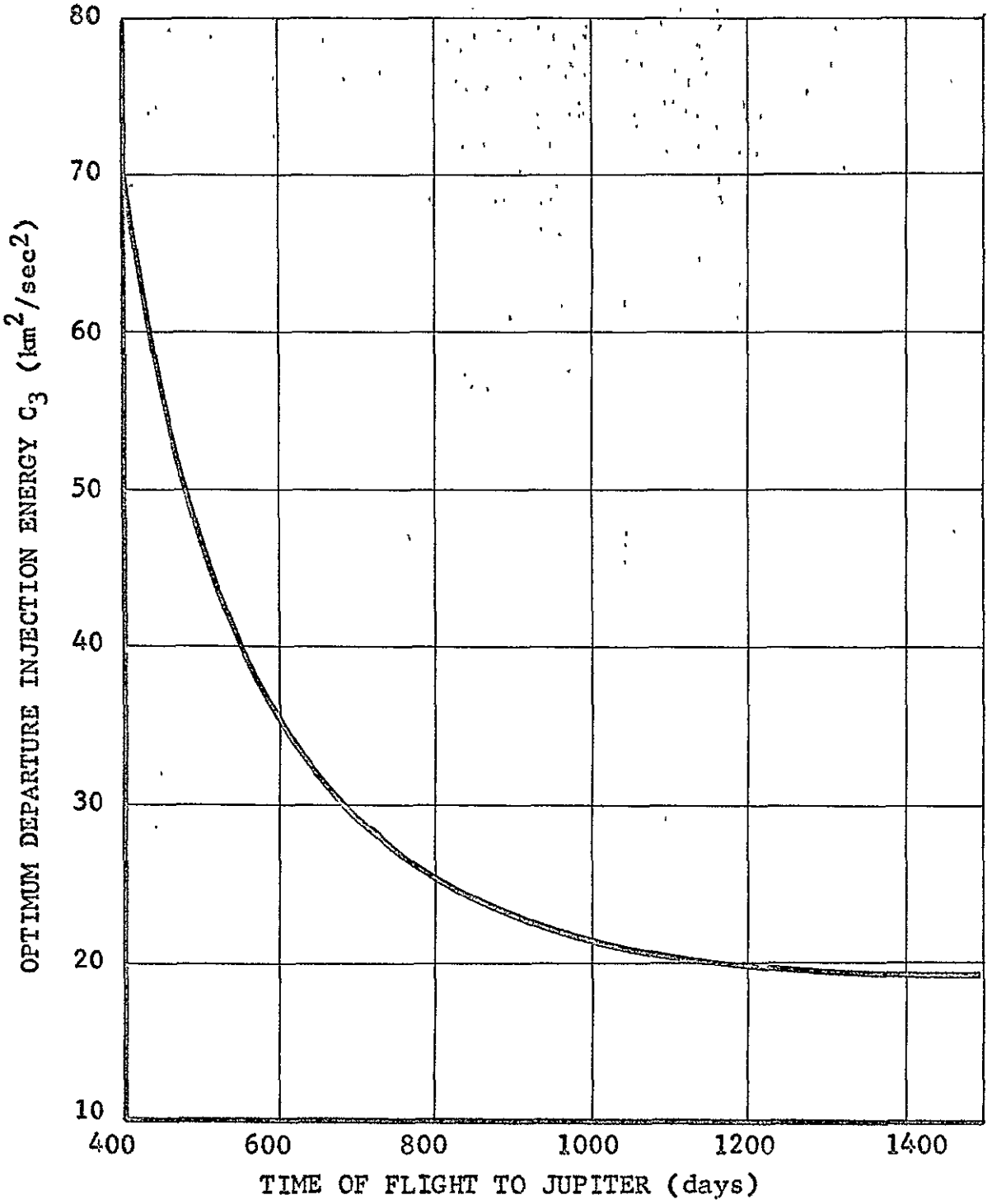

FIG. A.8 - OPTIMUM DEPARTURE INJECTION ENERGY VS TIME OF FLIGHT TO JUPITER. TITAN/CENTAUR, DIRECT MODE.

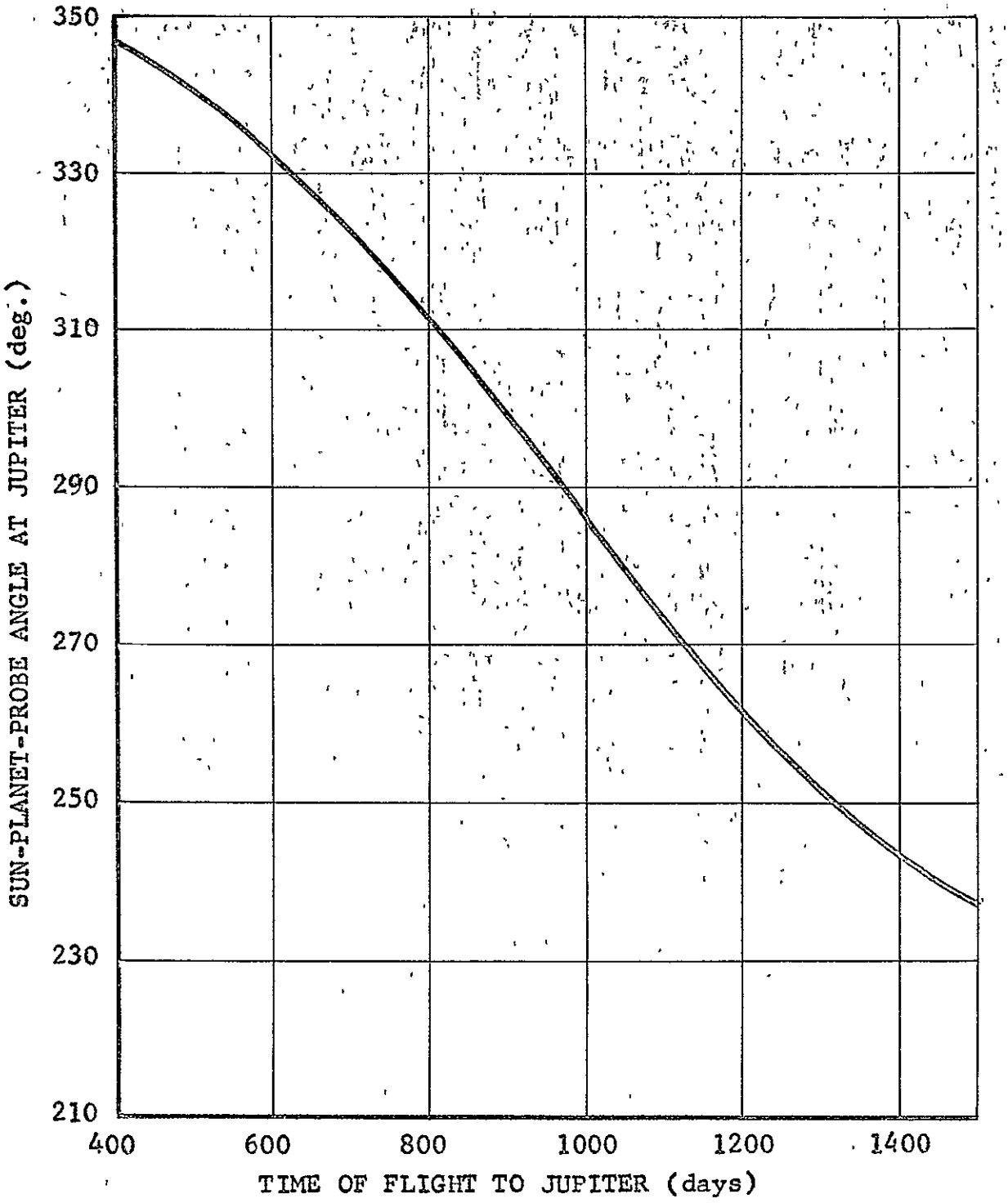

FIG. A.9 - SUN-PLANET-PROBE ANGLE AT JUPITER VS TIME OF FLIGHT TO JUPITER. TITAN 3X/CENTAUR, DIRECT MODE.

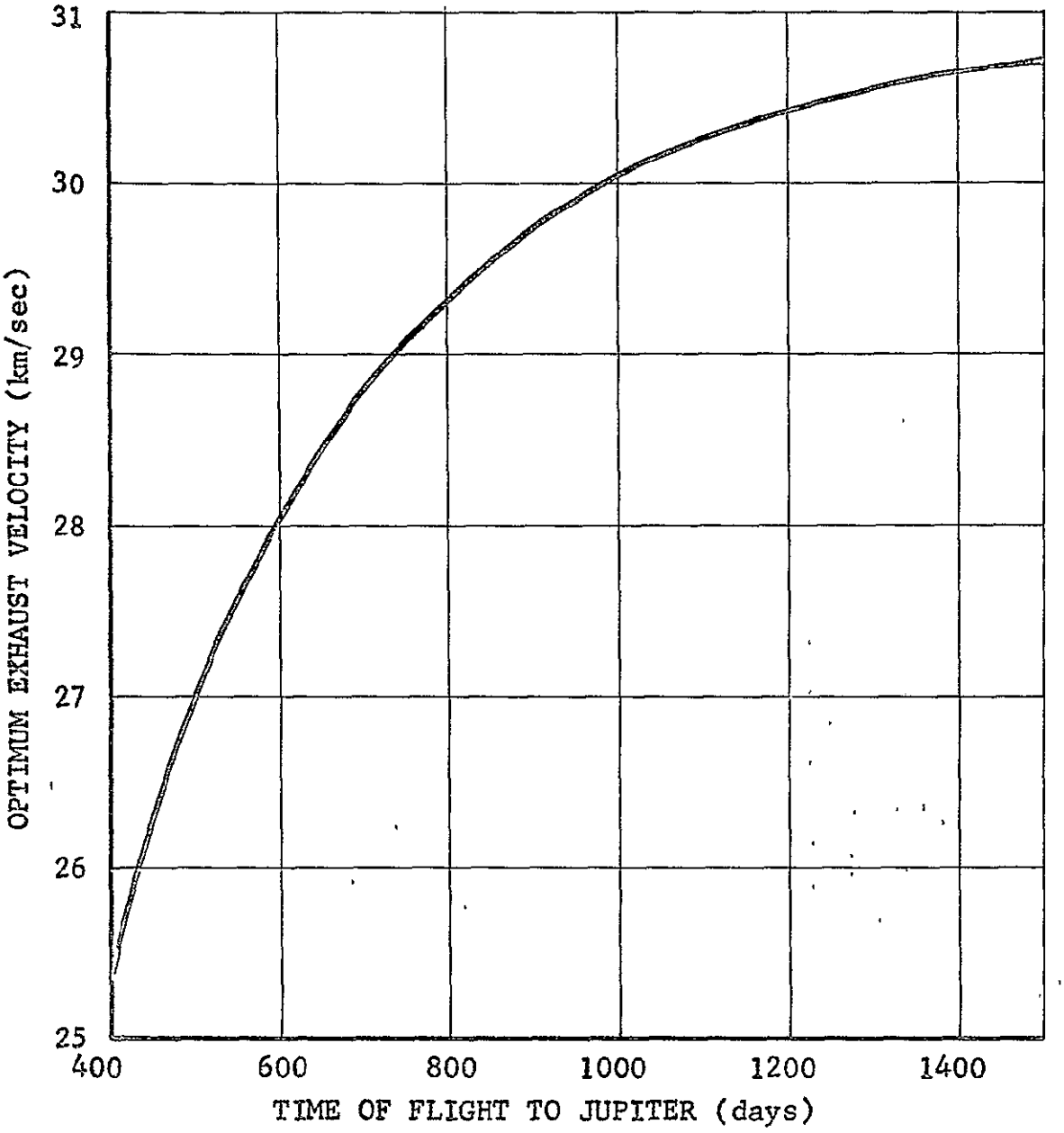

FIG. A.10 - OPTIMUM EXHAUST VELOCITY VS. TIME OF FLIGHT TO JUPITER. TITAN 3X/CENTAUR, DIRECT MODE.

LIST OF REFERENCES

1. Flandro, G. A., "Fast Reconnaissance Missions to the Outer Solar System Utilizing Energy Gained from the Gravitational Field of Jupiter." Astronautica Acta. 12:4, 329-337. 1966.

2. Flandro, G. A., "The Mechanics and Applications of the Planetary Swingby Technique for Optimization of Interplanetary Trajectories." Paper 68-4-1, American Astronautical Society. 1968.

3. Minovitch, M. A., "Determination and Characteristics of Ballistic Interplanetary Trajectories under the Influence of Multiple Planetary Attractions." Technical Report No. 32-464, Jet Propulsion Laboratory. 1963.

4. Sauer, C. G., "Trajectory Analysis and Optimization of a Low-Thrust Solar Electric Jupiter Flyby Mission." Paper 67-710, AIAA. 1967.

5. Flandro, G. A. and Barber, T. A., "Mission Analysis for Interplanetary Vehicles with Solar Electric Propulsion." Paper 67-708, AIAA. 1967.

6. Flandro, G. A., "Solar Electric Low-Thrust Missions to Jupiter with Swingby Continuation to the Outer Planets." Journal of Spacecraft and Rockets. 12:4, 329-337. 1966.

7. Dugan, D. W., "The Role of Staged Space Propulsion Systems in Interplanetary Missions." NASA Technical Note D-5593. 1969.

8. Friedlander, Alan, "Guidance Analysis of the Multiple Outer Planet (Grand Tour) Mission." Paper 68-109, American Astronautical Society. 1968.

9. Horsewood, J. L., "A Patched-Conic Low-Thrust Swingby Trajectory Optimization Program." Report No. 69-23, Analytical Mechanics Associates, Inc. November 1969.

10. Hohmann, W., Die Erreichbarkeit der Himmelskoerper. Munich: Oldenburg Publishing Corporation. 1925.

11. Barber, T. A., et al, "1975 Jupiter Flyby Mission Using a Solar Electric Spacecraft." Report ASD 760-18, Jet Propulsion Laboratory. March 1968.